HOST RESPONSE TO HSV-1 INFECTION: GENE EXPRESSION PROFILING TO INVESTIGATE MECHANISMS OF PATHOGENESIS AND DISEASE MARKERS

By
Amy Martinuk

A thesis
Submitted to the Faculty of Graduate Studies
in Partial Fulfillment of the Requirements
for the Degree of

Master of Science

Department of Medical Microbiology and Infectious Diseases
Faculty of Medicine
University of Manitoba
Winnipeg, Manitoba
Canada

THE UNIVERSITY OF MANITOBA

FACULTY OF GRADUATE STUDIES

*****

COPYRIGHT PERMISSION

HOST RESPONSE TO HSV-1 INFECTION: GENE EXPRESSION PROFILING TO INVESTIGATE MECHANISMS OF PATHOGENESIS AND DISEASE MARKERS

BY

Amy Martinuk

A Thesis/Practicum submitted to the Faculty of Graduate Studies of The University of Manitoba in partial fulfillment of the requirement of the degree

OF

MASTER OF SCIENCE

TABLE OF CONTENTS i

Acknowledgements

I would like to thank my supervisors Tim and Stephanie. Thanks for your patience, time and advice. Without it I would never have finished my thesis.

Thanks to my committee; Dr Embree, Dr Severini, and Dr Myal. Thanks for keeping me on track and for all advice given during my time here.

Elsie and Dan thanks for all your help, ideas and chats over the past three years. Without them my time here would not have been the same.

Thanks to my friends for distracting me and encouraging me. Thanks for making life in and out of Winnipeg fun. Thanks for the memories, chats and adventures along the way.

Laurie thanks for everything. Thanks for being the best friend anyone could ask for. Thanks for being my sounding board, my security blanket and my stress reliever. I think I might have gone crazy at times without you there to pull me back down to earth. Thanks for your love and unwavering support.

Finally and definitely not least thanks to my family. Thanks for all your love and support. Glenn thanks for always being there when I needed you and for some really great chats. Mom and dad thanks for always believing in me, for helping me out always, and for all the support and love you give me. Thanks especially for all the pep talks. I don't think I could have finished this without them.

LIST OF FIGURES

LIST OF TABLES

LIST OF ABBREVIATIONS

BCA	Bovine Carbonic Anhydrase
BMAP	Brain Molecular Anatomy Project
BSA	Bovine Serum Albumin
BSC	Biosafety cabinet
cDNA	complementary DNA
CMC	Carboxymethyl cellulose
CNS	Central Nervous System
CSF	Cerebral Spinal Fuid
CT	Computed Tomography
DAVID	Database for Annotation Visualization and Integrated Discovery
dH_2O	distilled water
DMSO	Dimethyl sulfoxide
DNA	Deoxyribonucleic acid
DO	Double Overlay
dpi	days post infection
dsDNA	double stranded DNA
EASE	Expression Analysis Systematic Explorer
EDGE	Extraction of Differential Gene Expression
EDTA	Ethylenediaminetetraacetic acid
EEG	Electroencephalogram
EST	Expressed Sequence Tag
FBS	Fetal Bovine Serum
FDR	False Discovery Rate
GAPDH	Glyceraldehydes-3-phosphate dehydrogenase
HBSS	Hanks Buffered Salt Solution
HCMV	Human Cytomegalovirus
HHV-6	Human Herpesvirus 6
HSE	Herpes Simplex Encephalitis
HSV-1	Herpes Simplex Virus 1
ICP	Infected Cell Protein
IE	Immediate Early
IFN	Interferon
IL	Interleukin
iNOS	inducible Nitric Oxide Synthase
Kb	Kilobase
LAT	Latency-Associated Transcript
MEM	Minimal Essential Medium
MHC	Major Histocompatibility Complex
MOI	Multiplicity of Infection
MRI	Magnetic Resonance Imaging
mRNA	messenger RNA
NML	National Microbiology Lab
ODP	Optimal Discovery Procedure
ORF	Open Reading Frame
PBS	Phosphate Buffered Saline
PCR	Polymerase Chain Reaction
pDNA	plasmid DNA
PKR	Protein Kinase
PRV	Pseudorabies virus
RNA	Ribonucleic acid
SAM	Significance Analysis of Microarrays
SDS	Sodium Dodecyl Sulfate
TLR	Toll-Like Receptor
UV	Ultraviolet
VP	Viral Protein
VZV	Varicella Zoster Virus

Abstract

Very little is known about how Herpes simplex encephalitis affects a host brain and the genes that could be targeted to develop therapies or rapid diagnostic methods. The question of whether HSV-1 infection affects host brain gene expression was addressed by using microarray transcript profiling of host gene expression in SJL mice. The hypothesis for this research was that genes, which respond in a characteristic way to virus infection and can be utilized as biomarkers. These responses can then be further investigated to reveal mechanisms of pathogenesis. Mice were inoculated intranasally with HSV-1 and examined viral replication and host gene expression in brain tissue; this route of infection delivers virus to the central nervous system (CNS) where it replicates for at least three weeks.

DNA was reverse transcribed and amplified by PCR, DNA extracted from SJL mouse brains, to confirm the mice were infected and to quantify the virus in the brains at each time point. Histology, immunohistochemistry and electron microscopy were also undertaken to look at the effects of HSV-1 infection on the mouse brain.

The expression of 16000 genes in the brain tissue of HSV-1 infected mice was analyzed using DNA microarrays. Microarrays with over half of the probe sequences on the arrays derived from CNS tissues were performed; this array was highly representative of gene expression in the brain. Labelled cDNA was

used from both HSV-1 and mock-infected mice at 3, 7, 14 and 21 days post-infection. Labeled cDNAs were hybridized to microarrays and the genes that were differentially expressed in infected, versus mock-infected, mouse brains were determined. To validate the microarray results protein arrays and semi-quantitative PCR analyses were performed for a selection of genes.

Significant changes in the expression of mouse neuronal genes were identified, including several with roles in immune response (Masp1), apoptosis (Bfar), CNS specific (Gap43), actin/microtubule (Tmod2) and cellular protein metabolim (Ier3). These studies demonstrate that HSV-1 infection can alter neuronal gene expression, and provide clues as to pathogenesis pathways.

Introduction

Herpes Simplex Virus 1 (HSV-1) is a member of the Herpesviridae family and is a human herpesvirus. The virus is widespread in the population. By age fifteen 50% of the population has antibodies to HSV-1 and 90% of adults show serological evidence of HSV-1 (Johnson 1998). It is the common cause of recurrent cold sores, ocular infection and non-genital cutaneous infections (Baringer 2000), as well as an increasing percent of primary genital infection. HSV-1 is also the principal cause of sporadic viral encephalitis. Primary infection with HSV-1 generally occurs during childhood from direct contact with infected droplets from nose or mouth secretions to a susceptible mucosal surface (Lin et al. 2001). The virus enters the body at mucosal surfaces and establishes infection locally. It can also travel to host sensory neurons and establish a lifelong latency. The incidence of herpes simplex encephalitis (HSE) is 1-4 per million each year (Lin et al. 2001;Sauerbrei et al. 2000;Schmutzhard 2001) which correlates to approximately 2000 cases per year in the United States alone (Chaudhuri and Kennedy 2002). Little is known about the factors that cause encephalitis and which genes could be targeted to develop therapies or rapid diagnostic methods.

1.1 HSV-1 Virions

Virions have an electron dense core, an icosahedral capsid, a layer of tegument and outer lipid envelope (Figure 1). In the core the DNA is packaged in the shape of a spool. The nucleocapsid is arranged in three layers. The outer layer

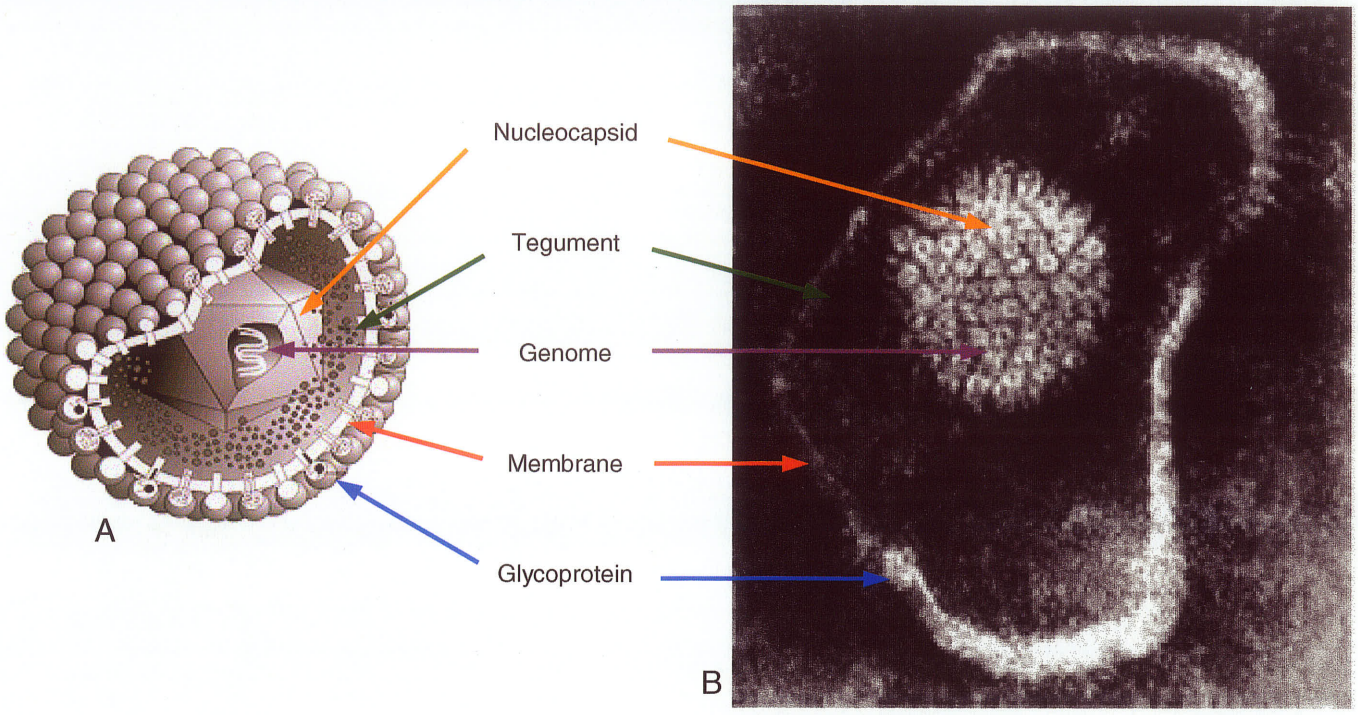

Figure 1. A: Graphic illustration of HSV-1. Modified from http://www.virology.net/Big_Virology/BVDNAherpes.html
B: Electron microscope image of HSV-1. Modified from http://www.cf.ac.uk/biosi/research/neuroscience/med.html

has a triangulation number of 16 while the center layer has a T=4 arrangement. The inner layer consists of the genomic DNA. The tegument that envelops the virions is largely unstructured. The outer lipid envelope is acquired from the host cell and has about 12 different viral glycoproteins embedded in it.

1.2 Lifecycle

HSV-1 enters cell by receptor-mediated endocytosis. It has a wide host range and can therefore infect many different species and cell types. Attachment of the virus to the host cell involves the interaction of glycoproteins. Glycoproteins B, C and D are important at this stage. Glycoprotein D is on the surface of the virion and stabilizes attachment (Kobelt et al. 2003;Scalan et al. 2003;Taylor et al. 2002). Possible receptors for glycoprotein D are HVEM and Nectin-1(Scalan et al. 2003). Glycoproteins B and C attach to heparin sulfate moieties on the host cell (Kobelt et al. 2003;Scalan et al. 2003;Taylor et al. 2002). After attachment, the virion envelope fuses with the plasma membrane and the nucleocapsid enters the cell (Figure 2). The tegument proteins are released and begin their activities immediately such as making the host cell environment less hostile and promoting α gene transcription. The nucleocapsid makes its way to the nucleus of the host cell. It is transported by microtubules (Taylor et al. 2002). Once at the nucleus, the nucleocapsid releases its viral DNA into the nucleus.

Replication of HSV-1 occurs in special structures in the nucleus called replication compartments (Taylor et al. 2002). When the viral DNA is in the host cell

Figure 2. Diagram of the replication cycle of HSV-1. The virion binds to the cell plasma membrane and fuses to it to release the capsid and tegument proteins into the cytoplasm. The capsid is transported to the nucleus and the viral DNA is released. The viral DNA cicularizes and is transcribed and translated into α, β and γ proteins. New capsids are formed and filled with viral DNA before budding. At this point one of two methods of egress occurs. Pathway A is the reenvelopment pathway where the envelope fuses with the outer nuclear membrane and a de-enveloped capsid is released into the cytoplasm. The capsid then buds into the Golgi apparatus to form an enveloped virion. Pathway B is the lumenal pathway where the virion buds through the outer nuclear membrane and is transported in a vesicle to the Golgi apparatus. The virion then passes through the Golgi apparatus to the exterior of the cell. Modified from figures 72-3 and 72-10 from Fields Virology.

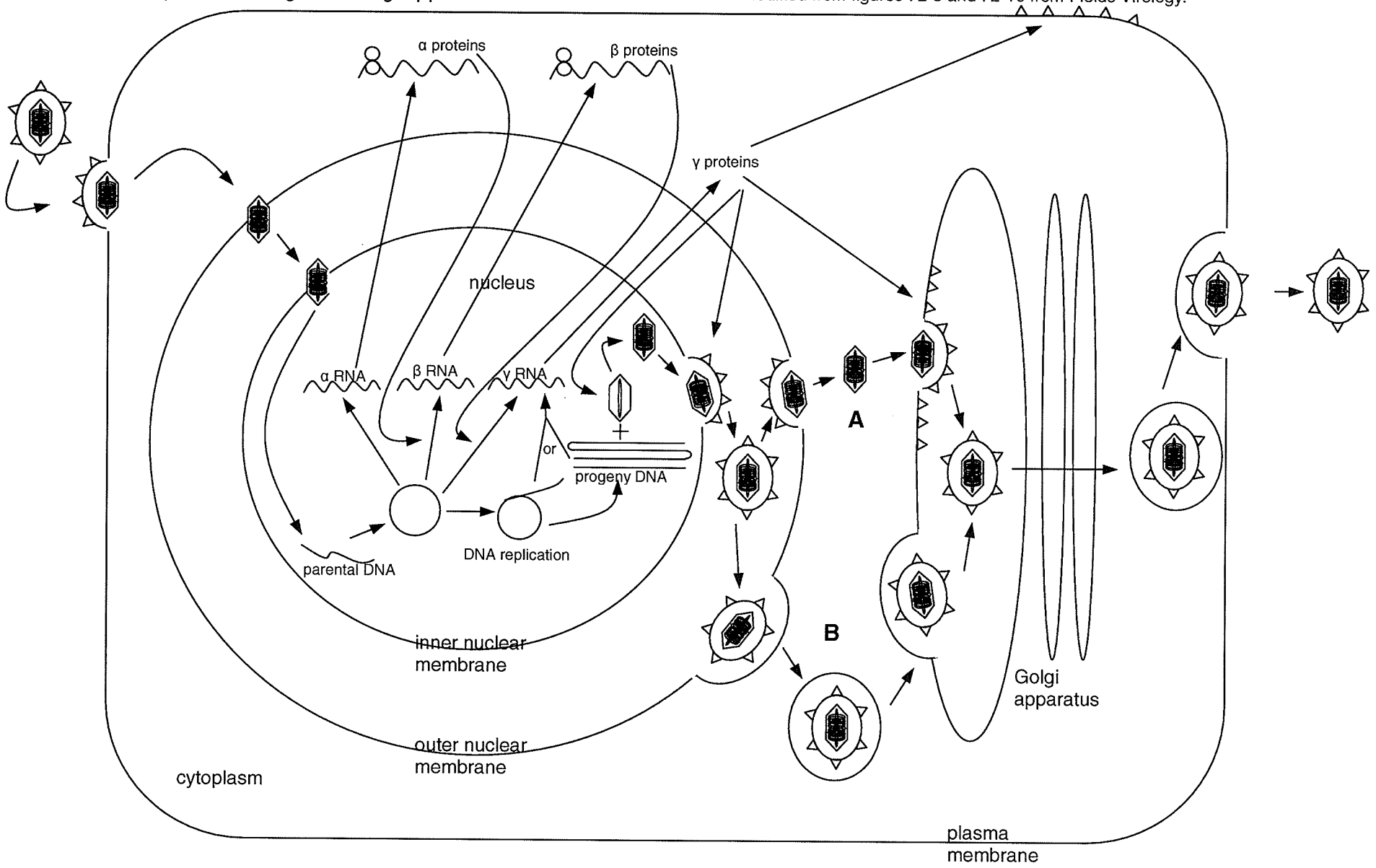

nucleus it is circularized and may replicate through rolling circle replication. This type of replication involves circularization of the viral DNA followed by initiation of replication and theta replication. Theta replication switches to rolling circle replication by some unknown mechanism and this generates long concatemers. These concatemeric DNA molecules are cleaved into genome length units at the virion assembly stage (Kobelt et al. 2003).

Nucleocapsids are made in the cytoplasm and transported back to the nucleus where genome length viral DNA is loaded into them. The mature capsid is composed of an outer shell comprised of VP5 arranged in pentons and hexons made of VP5 and VP23 (Taylor et al. 2002). Nucleocapsids bud through the inner nuclear membrane and acquire the tegument layer during this process.

Budding of the virus is still controversial. There are two proposed methods of egress but neither has been proven to date. The re-envelopment and lumenal pathways differ on how the virion is enveloped after it has acquired the tegument (Figure 2). In the reenvelopment pathway, the nucleocapsid fuses to the outer nuclear membrane and is deenveloped on its way into the cytoplasm. The nucleocapsid then buds into the trans-Golgi apparatus and is released by secretory vesicles. The lumenal pathway involves an enveloped nucleocapsid that passes through the endoplasmic reticulum to the trans-Golgi apparatus. In the trans-Golgi apparatus the viral glycoproteins undergo maturation and the virion is released from the cell by secretory vesicles.

1.3 Genome

The HSV-1 genome consists of two covalently linked regions that are designated as long or short. Each region is composed of unique sequences and large inverted repeats. There are three classes of genes in the HSV-1 genome. Those are α (immediate early), β (early) and γ (late). The α genes are found near the ends of the long and short strands while the β and γ genes are found scattered throughout the unique sequences of both long and short strands. The α genes are expressed very early in infection while β genes require the presence of functional ICP4 to be expressed and γ genes are only expressed after viral DNA synthesis has started.

1.4 Proteins/Genes of Interest

The replication cycle of HSV-1 commences with tegument proteins. The immediate early (IE) proteins are ICP4, ICP27, ICP0, ICP22 and ICP47. All of the IE proteins are nuclear phosphoproteins that act to regulate their own synthesis except ICP47 (Smiley 2004;Yang et al. 2003). The ICP4 and ICP27 proteins are essential for viral replication (Samaniego et al. 1998). ICP4 is also a major regulatory protein that is necessary for the transition from IE to early genes (Samaniego et al. 1998). The ICP27 protein impairs host mRNA splicing (Smiley 2004) and helps mediate expression of some early and most late genes (Pearson et al. 2004). The ICP0 protein is a major transcriptional activator that promotes viral mRNA translation and regulates the level of cellular proteins (Thompson et al. 2003). Promotion of late gene expression is dependent on

ICP22 (Samaniego et al. 1998). ICP47 may help the virus evade the immune system of the host by blocking the presentation of antigenic peptides to $CD8^+$ T cells (Goldsmith et al. 1998;Samaniego et al. 1998).

Another gene of interest when studying HSE is $\gamma_1$34.5. The $\gamma_1$34.5 gene has been implicated in HSV-1 neurovirulence. Mutants that fail to express the $\gamma_1$34.5 protein cannot cause encephalitis in mice because they are unable to replicate in the brain of animal models (Chou and Roizman 1992;Jing and He 2005). This gene produces a protein that is 263 amino acids in length (Chou et al. 1990;Chou and Roizman 1992). The protein has a large amino terminal domain, a linker region that consists of triplet repeats of Ala-Thr-Pro and a carboxyl terminal domain. The amino domain facilitates virus egress while the carboxyl domain functions to prevent the PKR response in virus infection (Jing and He 2005). PKR is a kinase that responds to limit viral infection. It works by inhibiting protein synthesis by phosphorylating the translation initiation factor eIF2. Activated PKR is sufficient to inhibit HSV-1. The linker region is thought to cause viral invasion from the peripheral nervous tissue to the CNS (Jing and He 2005). The $\gamma_1$34.5 protein also blocks the surface expression of MHC class II molecules in virus infected cells (Jing and He 2005).

1.5 Latency

A characteristic of human herpesviruses in general (eg HSV-1 and VZV) is the ability to become latent in infected cells. Latency occurs in the nuclei of nerve

cells only for primate alphaherpesviruses. Before latency can be established HSV-1 must infect an axonal nerve terminal and be conveyed by retrograde transport to the neuronal cell body (Kobelt et al. 2003). The nerves that become latently infected are the sensory ganglia that innervate the initially infected mucosal or epithelial cells (Kienzle et al. 2001). During latency the viral genome remains in the nucleus as circular episomal DNA (Johnson 1998;Kobelt et al. 2003;Millhouse and Wigdahl 2000; Simmons et al. 1992; Smiley 2004; Taylor et al. 2002). No viral progeny are made during latency and it is currently unknown how HSV-1 reactivates. Reactivation may occur due to unrelated stimuli such as emotional stress, fever, menstruation, immune suppression, surgery or even UV light (Kienzle et al. 2001;Turner and Jenkins 1997).

Latency-associated transcripts (LAT) are the only viral gene products that are expressed during latency. LATs are thought to have many different functions. They are nonpolyadenylated collinear RNAs (Kang et al. 2003) that are mostly expressed in latently infected cells. LATs have a role in blocking apoptosis (Bloom 2004; Kang et al. 2003), are involved in neurobiology (Millhouse and Wigdahl 2000), help to establish latency (Bloom 2004; Kang et al. 2003) and reactivation of the virus from latency (Kang et al. 2003) and also alter the transcriptional profile of the HSV-1 genome (Bloom 2004). It is not clear whether LATs are involved in the above-mentioned processes or if it is due to the environment of the neuron. There are several different LATs that have been observed in infected cells. The 8.3 Kb LAT is also known as the minor LAT

because it is only detected in low levels (Millhouse and Wigdahl 2000). The 2.0 Kb LAT is an intron of the 8.3 Kb LAT and can be expressed in both latent and acute infections (Millhouse and Wigdahl 2000). The third LAT is 1.5 Kb and it is formed from the 2.0 Kb LAT and can only be expressed latently (Millhouse and Wigdahl 2000). LATs are particularly unusual introns because they are stable. Their stability arises from an unusual splice junction that is not recognized by cellular degradation factors (Millhouse and Wigdahl 2000).

1.6 Cold Sores and Keratitis

HSV-1 is the cause of cold sores, eye infection and encephalitis. A cold sore, also known as a fever blister, is a virus filled sore that is usually situated on the lips, chin or cheeks. It causes pain, burning or itching before it bursts and crusts over. HSV-1 is highly contagious when cold sores are present. Epithelial cells that are in the vicinity of the mouth are the most common cells to become infected with HSV-1 (Figure 3). HSV-1 enters the sensory neuron that innervates these infected cells and the genome becomes latent to reactivate at a later date.

The eye infection caused by HSV-1 is known as keratitis. It is an inflammation in the corneal connective tissue and iris that can lead to corneal scarring and blindness. Keratitis caused by HSV-1 is the leading cause of blindness in industrialized countries (Millhouse and Wigdahl 2000).

Figure 3. Stages of HSV-1 infection of the host. HSV-1 is introduced onto a mucosal surface or break in the skin. It replicates in epithelial cells and then enters a sensory neuron. The virus then either replicates or becomes latent. The virus can reactivate to cause another infection. From this point the virus can also be transported to the CNS to cause HSE. Modified from figure 72-11 from Fields Virology.

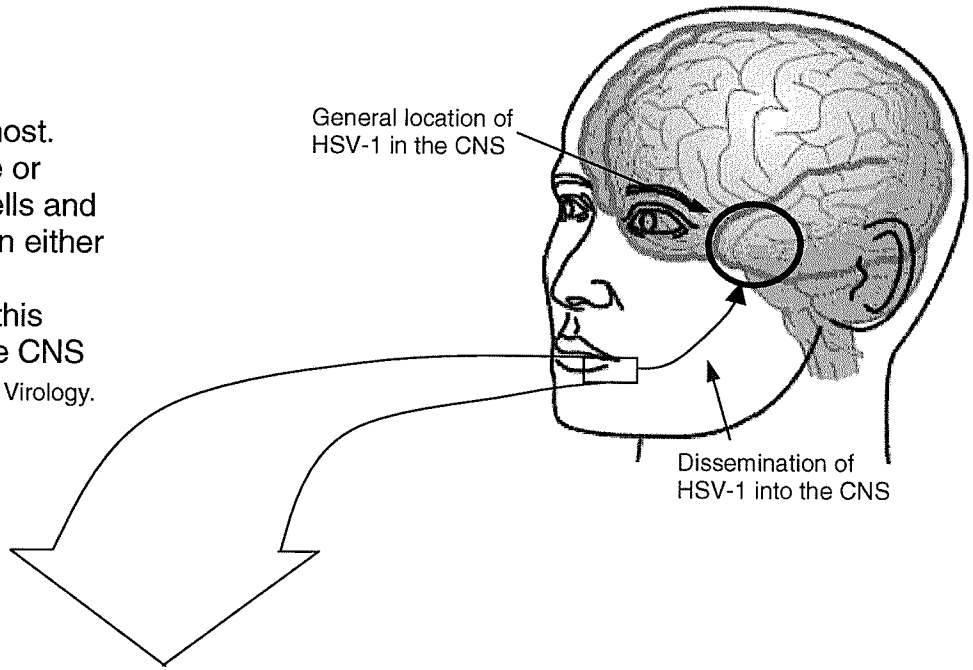

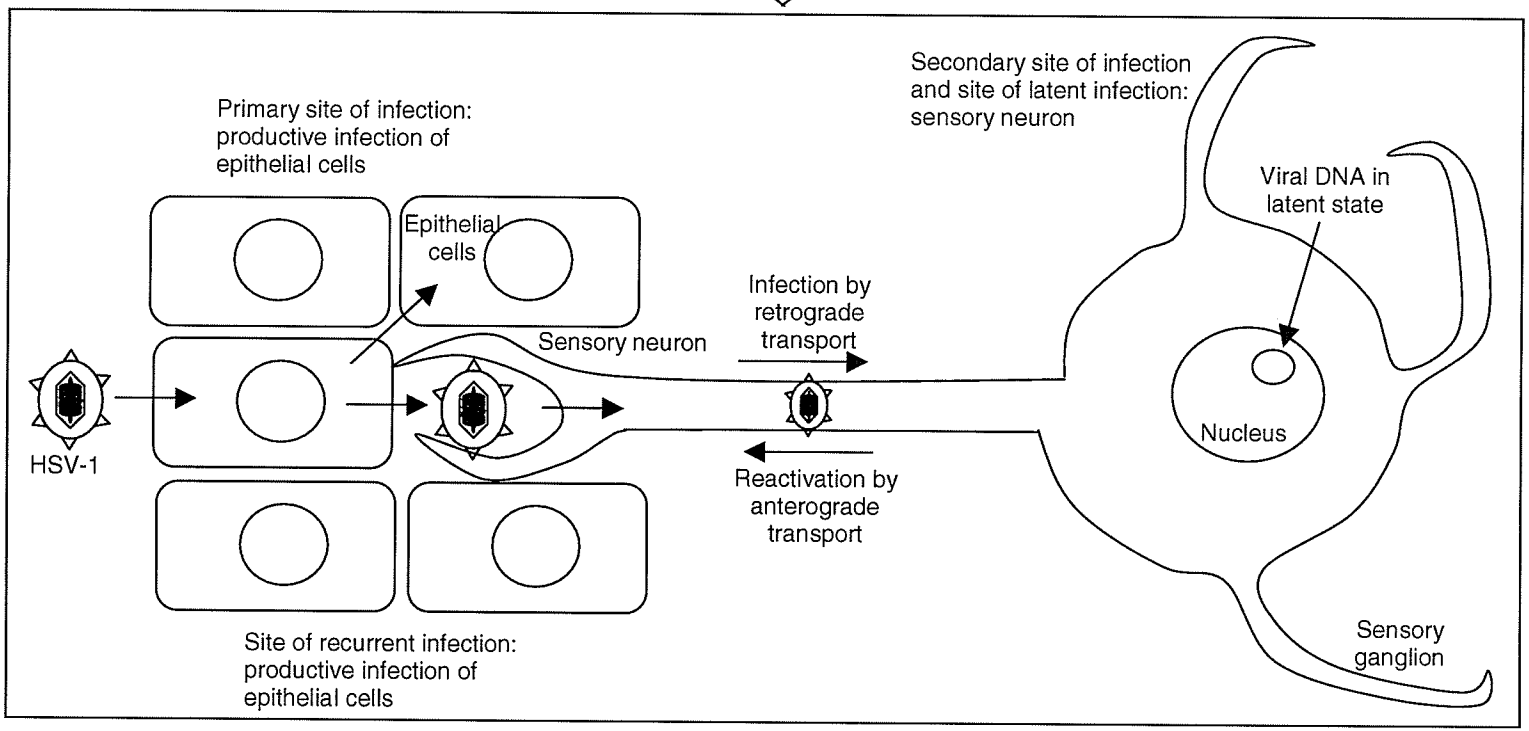

This page was intentionally left blank

1.7 Encephalitis

Encephalitis caused by HSV-1 occurs mainly in the subfrontal and medial temporal lobes of the cerebrum. There is acute inflammation and haemorrhage in those areas that is usually unilateral in distribution. One interesting fact to note is that selective vulnerability does not explain the localization of HSE. Virions are not localized to a specific subset of cells but rather can be found in both neurons and glia over the entire infected area (Davis and Johnson 1979). It is thought that HSE occurs in the frontal and temporal lobes because the virus usually enters the body via the olfactory tract and spreads along the base of the brain within the middle and anterior fossae to the temporal lobe (Johnson 1998;Kennedy and Chaudhuri 2002). The dissemination of HSV-1 in the CNS completely depends on the route of infection (Anglen et al. 2003).

Initial symptoms caused by HSE include fever and headache one to five days before focal encephalopathy (Skoldenberg 1996). Those symptoms are followed by confusion, behavioural changes, olfactory and gustatory hallucinations, seizures, speech difficulty, memory loss, episodes of terror, and slight paralysis (Baringer 2000;Ben Hur et al. 2003;Johnson 1998;Kienzle et al. 2001;Mahajan and Duggal 2002;Skoldenberg 1996;Whitley et al. 1977). Stupor and coma will follow in advanced cases. HSE usually has a sudden onset (Chaudhuri and Kenneday 2002) and brain damage may be irreversible within a few days (Whitley et al. 1977). There is not a seasonal distribution of HSE but there is a bimodal one with respect to age. Approximately 80% of HSE cases occur in

people under the age of 20 or over the age of 50 (Schmutzhard 2001;Johnson 1998). Both sexes are equally affected.

There are many problems that occur in survivors of HSE. Only 2.5% of those who recover end up regaining normal function (Whitley 1990). Some of the long term troubles associated with HSE are a detriment to learning and memory skills, general orientation struggles and perceptive-motor skill impairment (Liu et al. 2003;Skoldenberg 1996). Others might have severe debilitating sequelae including major motor and sensory deficits, aphasia, amnestic syndrome, and dysnomia (Johnson 1998;Raschilas et al. 2002). Complications can also arise including relapse, epilepsy, demyelination and chronic symptoms of ongoing disease (Lellouch-Tubiana et al. 2000).

It has been postulated that CNS damage may result from the immune response that occurs in the brain against the virally infected cells. HSV-1 may alter the blood brain barrier permeability due to inflammation and swelling of the brain and blood vessels (Bidanset et al. 2001). The blood brain barrier may continue to break down when subsequent inflammatory cells enter the CNS (Bishop and Hill 1991). The cytokines and prostaglandins produced during infection by inflammatory cells play a large role in the development of the clinical signs of HSE (Anglen et al 2003;Ben Hur et al. 2001;Ben Hur et al. 1996). It has also been observed that apoptosis is the main cause of death of cells in the CNS.

Immune interventions that can control HSV-1 neuropathology are those that restore or enhance T cell function (Bishop and Hill 1991). $CD8^+$ T cells also play a role in controlling the duration of HSV-1 replication in sensory ganglia and help to prevent the transmission of HSV-1 to the CNS (Goldsmith et al. 1998). Protection against neurotoxicity is also provided by iNOS inhibitors (Meyding-Lamade et al. 2003).

1.8 Diagnosis and Treatment of HSE

There have been many different diagnostic tests used to determine if the encephalitis in a patient is due to HSV-1. Rapid diagnosis is essential since mortality may be significantly decreased when antivirals are initiated soon after symptoms begin to occur. Cranial magnetic resonance imaging (MRI), neuroradiology, Computed Tomography (CT) scans, brain biopsies and Electroencephalogram (EEG) can all be used to diagnose HSE. Some of these methods are insensitive to the early stages of encephalitis because they are non-specific for HSE. The gold standard for HSE diagnosis is now a polymerase chain reaction (PCR) of cerebral spinal fluid (CSF). It can be used in conjunction with any of the above-mentioned methods. One reason that PCR of CSF is so valuable is because false negatives rarely occur. False negatives may occur is the CSF sample is obtained to early in the course of infection, if the sample is stored incorrectly, after acyclovir treatment or if there is a long delay in processing (Chaudhuri and Kennedy 2002).

Diagnosis of HSE can be difficult since there are many diseases that mimic it. Some of the more common diseases that imitate HSE include tuberculosis, brain abscess, brain tumor, cryptococcal infection, rickettsial and other herpesviruses (Skoldenberg 1996;Whitley 1990).

The recommended treatment of HSE is with acyclovir at 10 mg/kg three times a day for 14-21 days (Whitley and Kimberlin 1999). Some of the rare side effects of acyclovir are disorientation, hallucinations, tremors, ataxia, seizures and reversible renal dysfunction (Mahajan and Duggal 2002). Acyclovir is a nucleoside analogue that selectively inhibits HSV-1 specific DNA polymerase (Mahajan and Duggal 2002) and is non toxic to healthy cells which lack the tymidine kinase enzyme that is seen in HSV-1 infected cells (Kennedy and Chaudhuri 2002). Morbidity and mortality still exist despite Acyclovir use. There is a 20-30% mortality rate associated with Acyclovir (Chaudhuri and Kennedy 2002; Kennedy and Chaudhuri 2002). Some of the factors that affect the outcome of treatment are the patient's age, level of consciousness and duration of the disease (Skoldenberg 1996;Whitley 1990). In one study patients under the age of 30 had a mortality of 24% compared to those over 30 who had a mortality of 52%. Patients who were lethargic at the start of treatment had a mortality of 26% while those who were comatose or semicomatose had a mortality of 53% (Johnson 1998). The long-term evaluation of Acyclovir treatment showed that 38% of patients had normal or mild impairment, 9% had moderate sequelae and 53% were dead or were severely impaired after two years (Whitley 1990).

1.9 Vaccines

There have been several attempts to develop vaccines used to combat HSV-1 infection. These efforts are driven by economic and disease burden that this virus has on the world. The contribution of genital HSV to the HIV/AIDS pandemic is also increasing the pressure to produce and effective vaccine. The lifecycle of HSV-1 makes effective vaccines elusive to date. A successful vaccine candidate would need to protect against symptomatic HSV-1 and against acute infection and establishment of latency (Esiri 2001;Jones and Knipe 2003). Several vaccines showed promise in animal models, were immunogenic, but then failed to show effectiveness in clinical trials (Jones and Knipe 2003). This is probably due to the fact that HSV-1 has developed immune evasion mechanisms that are only effective in primates (Jones and Knipe 2003).

In order for a vaccine to work against HSV-1 infection it would need to induce both the cellular and humoral arms of the immune response (Cui et al. 2003;Erturk et al. 1992;Goel et al. 2003;Jones and Knipe 2003). This is in contrast to other successful vaccines. Polio vaccine, for instance, only needs to activate humoral immunity to successfully combat infection (Jones and Knipe 2003). The reason that both arms of the immune system need to be stimulated is because of the various stages of HSV-1 infection. Innate immunity comprising of natural killer cells and interferons is needed to limit replication at the site of entry (Jones and Knipe 2003). Clearance requires cell mediated immunity by CD4 T cells followed by CD8 T cells (Goel et al. 2003;Jones and Knipe 2003).

Antibodies have been shown to contain the spread of virus in the blood and from peripheral nerves to the CNS (Erturk et al. 1992;Jones and Knipe 2003).

Subunit vaccines generally fail to induce cell mediated immunity and have not been successful to date (Jones and Knipe 2003). It has been shown, however, that glycoprotein D contains an epitope at its N terminus that produces a protective response in both B and T cells. This epitope is recognized by both humans and mice and elicits a neutralizing antibody (Goel et al. 2003). Unfortunately glycoprotein D also contains an epitope that suppresses immune responses (Goel et al. 2003). Live attenuated vaccines have shown limited immunogenicity and are now being developed for gene therapy in the CNS (Jones and Knipe 2003). Live attenuated vaccines have a low immunogenicity since the wild type virus itself remains hidden from the immune system during the course of a natural infection. New strategies for HSV-1 vaccines include DNA vaccines, peptide vaccines along with strategies to increase innate immunity and develop novel delivery systems to increase cell mediated immunity (Jones and Knipe 2003).

Glycoprotein D subunit vaccines are capable of inducing a protective Th1 response in mice. It can limit the spread of disease and promote survival from lethal challenge. Unfortunately no antibody is detected in the mouse prior to challenge and the mechanism of protection is unknown (Goel et al. 2003). This vaccine has yet to be tested in clinical trials. Vaccines using mixed HSV-1

glycoproteins reduced detectable HSV-1 in the brains of mice (Esiri 2001). However, to be effective in preventing acute HSE from a latent brain infection the vaccine must be administered before latent infection is naturally acquired (Esiri 2001). Naked plasmid DNA (pDNA) vaccine that has been transfected intravascularly has been shown to be effective in protecting mice from HSV-1 infection (Cui et al. 2003). Replication defective mutants for ICP8 or ICP27 are effective at eliciting an immune response and protect against challenge but they can establish latency and are replication competent (Augustinova et al. 2004). All of the vaccine candidates mentioned above have shown promise in mice but have yet to be tested in humans. Safety and efficacy in eliciting effective immune responses are the major criteria in developing an HSV-1 vaccine.

1.10 Microarrays

Microarrays (Figure 4) are a flexible method used for analyzing large numbers of nucleic acid fragments in parallel. A better picture of the interactions found among the genes can be gained simultaneously when a whole genome is arranged on a single chip. Microarrays provide a method for matching known and unknown DNA samples, based on base-pairing hybridization rules, using an automated process to identify the expression levels of the unknowns. By reversing the Northern blot principle so that the labelled moiety is derived from the mRNA sample and the immobilized fractions are the known sequences, microarrays can determine expression levels of thousands of genes simultaneously in a single experiment. Microarrays provide a powerful tool for

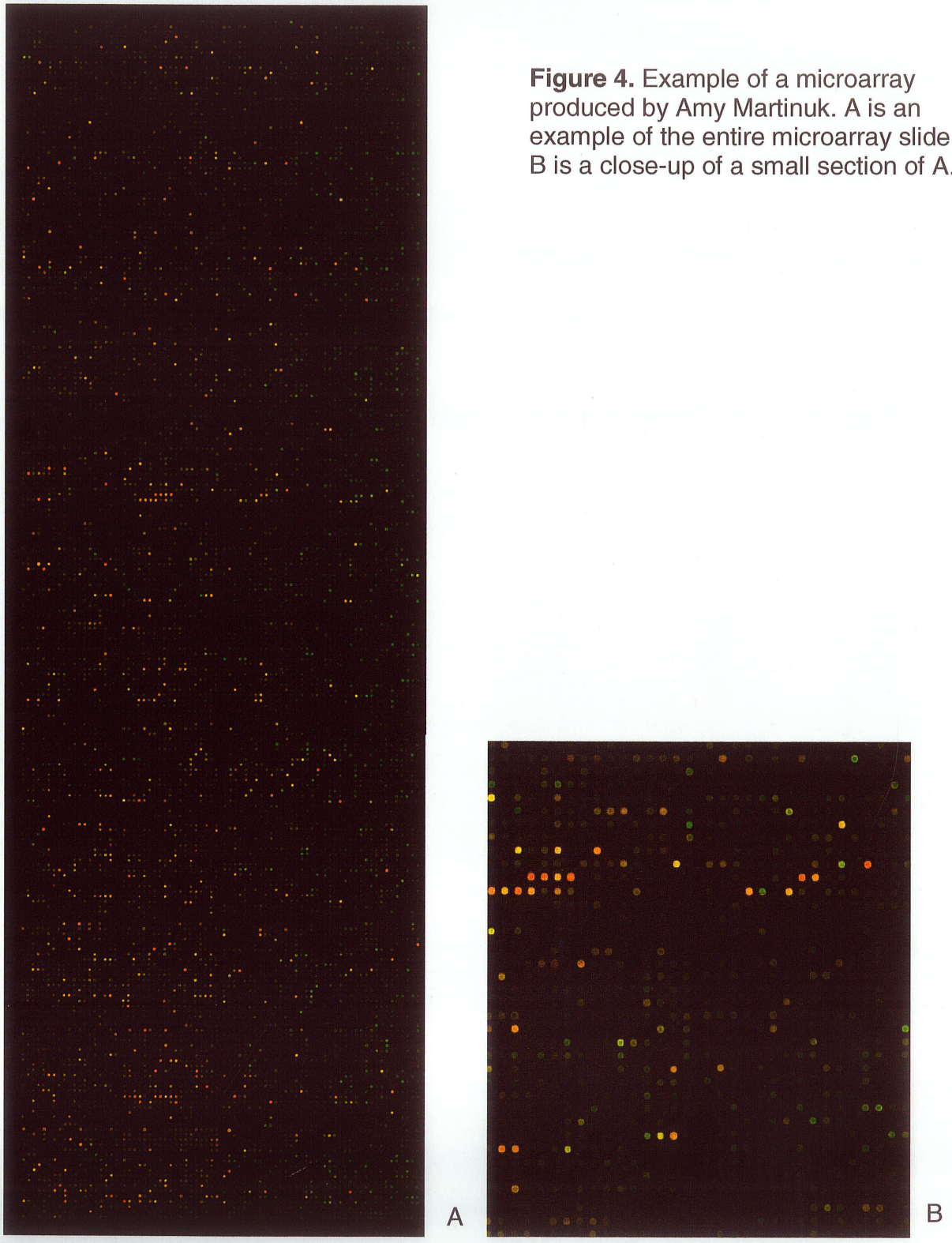

A B

Figure 4. Example of a microarray produced by Amy Martinuk. A is an example of the entire microarray slide and B is a close-up of a small section of A.

studying complex phenomena such as pathogenesis (DeRisi et al. 1996). Microarrays can recognize alterations in the expression of genes that can lead to further investigation of the genetic basis of pathogenesis and disease of specific types of cells. The results of microarrays can provide a broad view of the diverse biological systems that are changed in a model system; they focus the attention on a specific gene, gene product or pathway that may be of particular importance (DeRisi et al. 1996).

The greatest advantage of a microarray experiment is that multiple mRNAs can be measured at one time. Microarrays have the advantage when compared to Northern blot or nuclease protection assays as these two procedures are serial and involve measuring a single mRNA at a time (Lockhart et al. 1996). They are also difficult to automate. Two disadvantages attributed to microarrays are the inability to generate quantitative results and frequent false positives (Lockhart et al. 1996). Gene expression microarrays generate the relative intensities of the signals that will reflect the relative abundance of the particular transcripts in the two samples tested.

The production of a microarray begins with the selection of probes. Arrays used for higher eukaryotes are typically based on the expressed sequence tag (EST) portions of the genome while yeast and prokaryotic arrays use probes that are generated from gene-specific sites (Duggan et al. 1999). For this project, specific genes and ESTs were used in combination. Out of a total of 16171

genes, 11 136 clones represented ESTs derived from 5471 unique known genes and 5665 not yet characterized mRNAs, and from part of a library that was created as part of the Brain Molecular Anatomy Project (BMAP) (Booth et al. 2004). All of the probes utilized came from the Brain Microarray Project and thus the probes were those found mostly in the central nervous system.

Several previous studies have used microarrays to monitor host gene expression of herpes viruses. It has been shown by Mayne et al that Human Herpesvirus 6 (HHV-6) can induce the gene expression and protein production of several proinflammatory molecules, most specifically IL-18 and CD4, while downregulating chemokine receptors and members of the amyloid beta processing pathway, IL-10 and IL-14 (Mayne et al. 2001). During Varicella Zoster Virus (VZV) infection in primary T cells and skin xenographs caspase 8 was shown to be downregulated (Jones and Arvin 2003). Human Cytomegalovirus (HCMV) infection led to 1425 mRNAs being up or down regulated in the host, including 25 anti-apoptotic genes and 97 genes involved in cell cycle regulation and oncogenesis (Browne et al. 2001).

During an HSV-1 infection in the eye, 3800 out of 12488 genes were shown to be upregulated by Zheng et al. Among these genes 10 were associated with T cells, 11 with macrophages, 11 related to immunoglobulin and B cells, 53 cytokine genes, 16 MHC and eight chemokine genes (Zheng et al. 2003). A comparison of PRV and HSV-1 infection of rat embryonic fibroblasts showed that

host transcriptional changes occurred late after infection. HSV-1 infection affected the expression of genes involved in cell adhesion, immunity, channels, transporters and growth factors (Ray and Enquist 2004). Genes belonging to the following classes were also affected; IFN and IL related, oxidative stress genes and PI3K/Akt genes (Ray and Enquist 2004). HSV-1 has also been shown to completely suppress host cellular protein synthesis (Smiley 2004). The present study will undertake a comprehensive approach by using an *in vivo* mouse model and microarray analysis of genes.

1.11 Hypothesis

The hypothesis tested in this project is that genes in mouse brain tissue are over or under expressed in a disease-specific fashion to HSV-1 infection. The hypothesis that various infectious agents (eg prion diseases) cause type-specific responses has been tested by comparing data from other research. Identification of such disease markers will allow further study to verify mechanism of disease and identify possible targets for therapy.

1.12 Objectives

The objective of the study is to identify neuronally expressed genes that respond to HSV-1 and to quantify their expression during the course of infection in a mouse model of herpes simplex encephalitis (HSE). This will be accomplished by examining genes that are up or down regulated in an infected mouse brain when compared to a mock-infected individual.

Identification of the genes, which respond to HSV-1 infection, will help future research to do the following:

(1) Identification of markers of infection which will be useful for developing diagnostic tests able to characterize similar or new disease agents by classification methods rather than carrying out exhaustive multiple diagnostic tests to exclude possible agents.

(2) Analysis of the genomic response to infection to detect possible mechanisms and pathways involved in pathogenesis and to develop an understanding of tissue and cell tropisms of herpesvirus in the brain.

(3) Identification of possible gene targets for therapeutic intervention through antivirals or vaccines, or to identify other possible treatments employing drug therapies that may counteract specific pathogenesis pathways.

(4) Comparison with other disease agents (e.g. prions) to develop a disease classification system based on gene expression profiles (for example to detect a class of infection such as viral encephalitis)

Materials and Methods

2.1 Cells and Viruses

Vero cells (American Type Culture Collection) were cultured in minimal essential medium (MEM) (National Microbiology Lab (NML) media department) that was supplemented with 5% fetal bovine serum (Gibco), 1% glutamine (Gibco), 1% penicillin-streptomycin (Gibco) and 2% $NaHCO_3$ (sodium bicarbonate)(Gibco). Cells were maintained in a 250 cm^2 flask (Corning). Cultures were split twice a week as follows: old medium was discarded and cells were rinsed first with Hanks buffered salt solution (HBSS) (NML media department), then with trypsin-EDTA HBSS (1:9). The cells were then incubated at 37°C with trypsin-EDTA (Gibco) HBSS (In house media department) for 1-2 min. The side of the flask was tapped firmly to facilitate the detachment of the cells. Once dislodged, 7 mL of growth medium (as described above) was added to the flask to inactivate the trypsin. Cells were gently pipetted up and down to disrupt clumps before being aliquoted into new 250 mL flasks.

2.1.1 Virus Stock Preparation

Vero cells grown in a 150 cm^2 flask (Corning) were stained with trypan blue (Gibco) and counted using a hemacytometer. The cells were inoculated when they reached a concentration of $1.9x10^9$ cells/flask. HSV-1 virus strain F stock (21-03-02) with a virus titre of $2.8x10^9$ pfu/mL was used. The desired pfu/mL was $2.0x10^7$ for a 0.1 multiplicity of infection (MOI) of 7.1µL/flask. Approximately 10 µL of stock HSV-1 was added to 2 mL of 2% MEM medium per flask. The

medium of ten flasks was emptied and 2 mL of virus dilution was added. The flask was rocked side to side to completely cover the monolayer of cells. The infected flask was incubated for 1 hour at 37°C. After the hour 38 mL of MEM was added and incubated for 24-48 hours.

When the cells began detaching, the medium was aspirated and 5 mL of cold PBS (NML media department) was added. The cells were scraped into the PBS and the PBS from all flasks was pooled. The flasks were then rinsed with the same 10 mL of cold PBS. The cells were spun down to pellet the cells for 5 minutes at 2000 rcf with gentle deceleration. The pellet was resuspended in 10 mL of cold PBS (1 mL per flask used). The cells were then quick frozen/thawed 3 times in an acetone/dry ice bath to lyse the cells and release the virus. An acetone/dry ice bath was used to freeze the cells and a 42°C waterbath was used to thaw them. The cells were spun down at 5000 rcf and the supernatant was removed. The pellet was made into 150 µL aliquots and stored at -80°C.

2.2 Plaque assay

Virus infectivity was tested using two types of plaque assays. Vero cells were plated onto petri dishes (Corning) to form monolayers. Once the monolayer was formed 200 µL of each dilution of the virus stock (diluted in MEM supplemented with 5% fetal bovine serum, 1% glutamine, 1% penicillin-streptomycin and 2% $NaHCO_3$) was added to the cell monolayer. Adsorption of the inoculum was carried out at 37°C for 1 hour. After adsorption, infected cells were overlayed

with one of two mediums. The first medium was composed of 50 mL of 2X MEM (4.70 g MEM (Gibco) and 250 mL dH_2O (Gibco)) supplemented with 2% FBS, 5 mL of glutamine, 10 mL of $NaHCO_3$ and 5 mL of penicillin-streptomycin and 75 mL of 1.5% agar (3.75 g agar (Sigma) and 250 mL dH_2O). The plaque assays were then incubated at 37˚C until plaques were visible.

The second medium was composed of 3% carboxymethyl cellulose (CMC) (7.5 g CMC (Sigma) and 250 mL dH_2O) used in a 1:1 ratio with 2X MEM supplemented with 2% fbs, 5 mL of glutamine, 10 mL of $NaHCO_3$ and 5 mL of penicillin-streptomycin. The 2X MEM and 3% CMC were mixed for at least 3 hours before plating and the plaque assays were then incubated at 37˚C until plaques were visible.

Cells were fixed with 10% formalin (Fisher Scientific) and stained with crystal violet (Sigma). Viral plaques were counted and viral titres were calculated.

2.3 Biological Material

The Canadian Science Centre for Human and Animal Health Animal Care Committee approved all procedures involving live animals. SJL mice (ordered from Charles River Canada) and were allowed to acclimatize to the lab for 1 week. Number of mice per cage varied between 6-12. Mice were given Alpha-Dri bedding (Shepherd's Specialty Papers), as a form of environmental enrichment. Water bottles were changed every other day and food hoppers were

changed weekly. It was ensured that water and food levels were full daily. Cage changes occurred once a week and a handful of food was placed in the bottom of the cage as a form of foraging environmental enrichment for the mice.

Set up for intranasal inoculation involved placing bench paper inside the biosafety cabinet (BSC), setting up a biohazard bag along with pipettes, pipette tips and inoculum. SJL mice were inoculated intranasally with 10 µL of 10^3 pfu HSV-1 in each nostril. Mock-infected control mice were inoculated intranasally with 10 µL of PBS in each nostril. Mice were removed from the cage one at a time and anaesthetized with isoflurane. After the mouse was anaesthetized it was removed from the anaesthetic and held upright with the ventral side of the mouse facing the handler and the head tilted up. The pipette tip was placed at the nostril opening and the droplet of inoculum was dispensed with the animal's inspiration. Once the full dose had been administered the animal was kept in an upright position for a few seconds to allow the inoculum to reach the innermost passages. The mouse was then placed back in its cage and monitored until it recovered.

Mice were examined for clinical signs of disease daily from day 10 until day 21. The following clinical signs were looked for: appearance (ruffled or normal coat), posture (hunched or normal), weight (greater than or equal to 15% or normal), respiration (laboured or normal), behaviour (hyper-excitability/depression or normal) and neurological signs (presence or absence of signs such as seizures

or circling). A grade of 0 or 1 was given for each clinical sign. A grade of 0 indicated normal and a grade of 1 indicated atypical characteristic. The clinical score was determined by adding up the individual scores with 0 being normal and 6 being the worst clinical score. If an animal had a clinical score of 2 or more then decision to continue scoring or euthanise the mouse would be decided. The decision was to be decided based on the exact symptoms of the mouse in question.

The mice were sacrificed initially at 7 days post infection and then in a second experiment at 3, 7, 14 and 21 days post infection (dpi). The incubation periods represent early (3dpi), middle (7 and 14 dpi) and late (21 dpi) infection periods. All mice were sacrificed via cervical dislocation. Briefly, mice were removed one at a time from their cage by the tail and placed on a rough flat surface in the BSC. The mouse was allowed to grasp the surface and with the tail held firmly the body was slightly stretched out. The handle of a scalpel was placed lightly over the neck at the base of the skull. Downward pressure was applied in one quick movement and at the same time the tail was pulled backwards in a slightly upwards-angled motion. Mice were not anaesthetized prior to cervical dislocation as this would affect the results generated by the microarray experiments.

Mouse brain tissue was stored at -80˚C in RNAlater solution (Ambion) until all experimental time points were completed.

2.4 Array Construction

Arrays were constructed using cDNA derived from clones isolated from the brain of adult mice (strain c57BL/6) (Research Genetics). The 11136 clones represented ESTs from some 5471 unique known genes and 5665 as-yet-uncharacterized mRNAs and form part of a library that was created as part of BMAP. Each insert from this BMAP 3'EST library was amplified by PCR. Purification of cDNA was carried out using Millipore multiwell purification plates and lyophilized PCR products were resuspended in 1X Micro-spotting Solution Plus (TeleChem) at a concentration of 0.25-0.75 μg/μL. DNA was spotted onto CMT-GAPS-coated glass slides (Corning) by using Stealth-micro-spotting pins (TeleChem) (Figure 5).

2.5 Trizol Extraction

Each mouse brain was homogenized in 3 mL of Trizol Reagent (Invitrogen). The homogenate was centrifuged at 8800 g for 10 minutes at 4˚C. The resulting pellet contained proteins and polysaccharides while the supernatant contained the RNA. The supernatant was transferred to a fresh 15 mL tube and 0.6 mL of chloroform (Fisher Scientific) was added. The samples were shaken for 15 seconds and incubated at room temperature for 2 minutes before being centrifuged at 8800 g for 15 minutes at 4˚C. The mixture separated into 3 phases: a phenol-chloroform phase, an interphase and a colourless upper aqueous phase. The RNA was in the upper aqueous phase. The aqueous phase was transferred to a fresh 15 mL tube and RNA was precipitated with

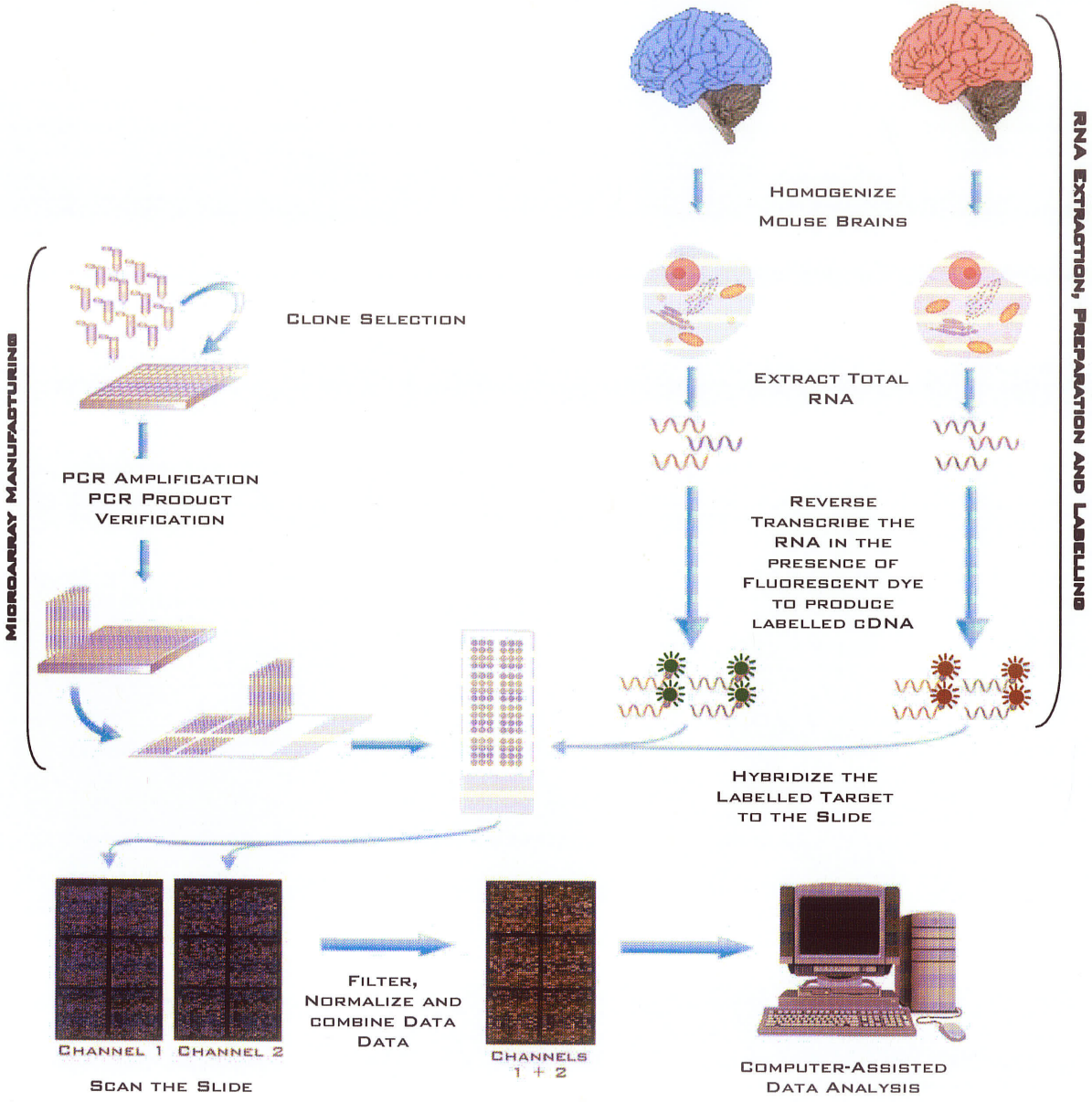

Figure 5. The steps involved in a microarray experiment. HSV-1 and mock-infected mouse brains are homogenized and total RNA is extracted. RNA is reverse transcribed and labeled with Cy3 or Cy5 dye. Microarray slides are hybridized with the labeled product and scanned at 555nm and 647nm. The images are then filtered, normalized and analyzed for results to be obtained.
Modified from **MacGregor, P. F. and Squire, J. A.** 2002. Application of Microarrays to the Analysis of Gene Expression in Cancer. Clinical Chemistry. **48**:1170-1177.

isopropyl alcohol (Fisher Scientific). Isopropyl alcohol (1.5 mL) was added and the mixture was shaken gently and incubated for no more than 1 hour at -80˚C. The mixture was then centrifuged at 9000 g for 10 minutes at 4˚C. The supernatant was removed and the RNA pellet was washed using 3 mL of 75% ethanol (Fisher Scientific). The sample was vortexed and centrifuged again at 7500 g for 5 minutes at 4˚C then the ethanol was removed and the pellet was dried.

2.6 RNA Clean-up

The following were added to the RNA pellet: 0.5 mL of RNase-free water (Gibco), 2.0 mL of RLT buffer (Qiagen) supplemented with 0.2 µL of beta mercaptoethanol (Sigma) and 1.4 mL of 100% ethanol (Fisher Scientific). The mixture was shaken and applied to an RNeasy midi column (Qiagen) and centrifuged for 5 minutes at 4000 g. Buffer RPE (2.5 mL) (Qiagen) was added to the column and it was centrifuged for 2 minutes at 4000 g. Another 2.5 mL of Buffer RPE was added to the column and it was centrifuged for 5 minutes at 4000 g. To elute, the RNeasy column a new 15 mL tube and 150 µL of RNase-free water was added. The RNeasy column containing RNase-free water was left for 1 minute at room temperature before being centrifuged at 4000 g for 3 minutes.

2.7 RNeasy Lipid Tissue Extraction

Before thawing, each mouse brain was homogenized in 5 mL of QIAzol Lysis Reagent (Qiagen) in a 15 mL tube. The brain and QIAzol Lysis Reagent mixture was left at room temperature for 5 minutes and then centrifuged at 8800 g for 10 minutes at 4˚C. The clear middle layer was placed into a fresh 15 mL tube and 1 mL of chloroform was added. This mixture was vortexed for 15 seconds and left at room temperature for 2 minutes before being centrifuged at 5000 g for 15 minutes at 4˚C. The upper aqueous phase was transferred to a new collection tube and 2-3 mL (1 volume) of 70% ethanol (Fisher Scientific) was added. A 4 mL aliquot of this mixture was placed in an RNeasy Midi Spin column (Qiagen) in a 15 mL tube and centrifuged for 5 minutes at 4000 g. This step was repeated for the remaining mixture. A 4 mL aliquot of Buffer RW1 (Qiagen) was added and centrifuged for 5 minutes at 4000 g. A 2.5 mL aliquot of Buffer RPE was added twice. Between each addition of Buffer RPE (Qiagen) the column was spun at 4000 g for 2 and 5 minutes respectively. The RNeasy Midi Spin column was placed in a new collection tube (Qiagen) and at least 100 µL of RNase-free water (Gibco) was added directly to the column for elution. The column containing RNase-free water was left to stand for 1 minute at room temperature and then centrifuged for 3 minutes at 4000 g. The elution step was repeated with a second volume of RNase-free water.

2.8 Generation of Labelled cDNA Targets

2.8.1 Aminoallyl Labeling: Reverse Transcription Reaction

A 10 µg amount of total RNA with a concentration of approximately 2 µg/µL was added to 2 µL of Oligo-dt primer (Invitrogen) (0.5 µg/µL) and topped up to 18.5 µL with RNase-free water (Gibco). This mixture was incubated at 70˚C for 10 minutes using the thermocycler. Immediately after the 10 minutes the mixture was snap frozen for 30 seconds on ice. The following was made up in a master mix depending on the number of reactions being done: 6 µL of 5X first strand buffer (Invitrogen), 3 µL of 0.1M DTT (Invitrogen), 0.6 µL of 50X dNTP mix (Invitrogen) and 2 µL of Superscript II RT (Invitrogen) (200 U/µL). A 11.6 µL aliquot was added to each tube and then the mixture was incubated at 42˚C overnight.

2.8.2 Indirect Labelling of Target cDNA

2.8.2.1 Hydrolysis of RNA Template

The cDNA template was hydrolyzed with 10 µL of 0.5 M EDTA (Ambion) then 10 µL of 1 M NaOH (Fisher Scientific). The mixture was then incubated at 65˚C for 15 minutes in the thermocycler. 10 µL of 1 M HCl (Fisher Scientific) was added to neutralize the pH.

2.8.2.2 cDNA Purification

Unincorporated aa-dUTP and free amines were removed from the reaction by using the Micron YM-30 Cleanup Method. Before using the columns, 100 µL of

RNase-free water (Gibco) was placed in the columns and centrifuged for 3 minutes at 15300 rcf to clear the excess tris in the column. After clearing the excess Tris the Micron sample reservoir (Micon) was placed in a collection microfuge tube (Micon). A 375 µL aliquot of RNase-free water was added to the hydrolyzed cDNA template before it was added to the Micron sample reservoir. The sample was centrifuged for 8 minutes at 15300 rcf. To wash the column, 450 µL of RNase-free water was added to the sample reservoir and centrifuged for 8 minutes at 15300 rcf. The wash step was repeated. The sample reservoir was placed inverted in a new collection microfuge tube and centrifuged for 2 minutes at 15300 rcf to collect the purified sample. The cDNA was analyzed using the NanoDrop Spectrophotometer and then the sample was dried in the SpeedVac for approximately 15 minutes.

2.8.2.3 Coupling aa-cDNA to Cy Dye Esters

The cDNA was resuspended in 4.5 µL of 0.1 M sodium carbonate buffer (Merck) (Na_2CO_3, pH 9.0, made fresh every month). One lyophilized aliquot of mono-reactive Cy3 (Alexa Fluor® 555, Molecular Probes) or Cy5 (Alexa Fluor® 647, Molecular Probes) dye (4.5 µL) was added to the cDNA. The Cy3 and Cy5 dyes were resuspended in DMSO (Sigma), then aliquotted and stored at -80°C. The tubes were kept in the dark and incubated for 1 hour at room temperature. The labeling reaction was stopped with 35 µL of 100 mM sodium acetate (Ambion) (NAOAc, pH 5.2).

2.8.2.4 Reaction Purifictation: Removal of uncoupled dye

Uncoupled Cy dye was removed from the labeled cDNA using the Qiagen PCR Purification kit. A 250 µL (5X reaction volume) aliquot of Buffer PB (Qiagen) was added to the cDNA sample and transferred to a QIAquick spin column (Qiagen) in a collection tube and centrifuged for 1 minute at 17900 rcf. To wash the column, 750 µL of Buffer PE (Qiagen) was added and centrifuged for 1 minute at 17900 rcf. The collection tube was emptied and centrifuged once more for 1 minute at 17900 rcf. The QIAquick spin column was placed in a 1.5 mL microfuge tube and 30 µL of Buffer EB (Qiagen) was added to the center of the column. This was incubated at room temperature for 1 minute and then centrifuged at 17900 rcf for 1 minute. The elution step was repeated. The labeled cDNA was analyzed using the NanoDrop and then the sample was dried in the SpeedVac.

2.9 Array Hybridization

2.9.1 Prehybridization

Prehybridization buffer (5X SSC (Ambion), 0.1% SDS (Ambion), 1% BSA (Sigma)) was prepared fresh and pre-heated to 42˚C. The printed slides were incubated for a minimum of 45 minutes. The slides were washed just prior to hybridization for optimal hybridization efficiency. Dipping 5 times in dH_2O (Gibco) in a 50 mL tube and then dipping once into isopropanol (Fisher Scientific) in a 50 mL tube washed the slides. They were dried using the slide spinner. The

appearance of the slides was noted and the wash steps were repeated if necessary.

2.9.2 Labeled Probe Hybridization

The labeled cDNA was resuspended in 30 µL of DIG Easy Hib hybridization buffer (Roche) and then the mixture was pooled to have 1 Cy3 and 1 Cy5 sample hybridized together. A 1 µL aliquot of COT1-DNA (Invitrogen) (20 µg/µL) and 1 µL of Poly(A)-DNA (ResGen) (20 µg/µL) were added to block non-specific hybridization. To denature, the probe mixture was heated to 95˚C for 3 minutes and then snap cooled on ice for 30 seconds. It was then centrifuged for 1 minute at 17900 rcf and kept at room temperature.

A lifter slip (Fisher Scientific) was placed over top of the printed grid on a prehybridized slide. The labeled cDNA was applied to the array near the end with the label. It was pipetted slowly under the lifter slip and capillary action wicked the probe solution under the lifter slip uniformly over the microarray. The hybridized slide and lifter slip were placed in a hybridization chamber. A 4 mL aliquot of DIG Easy Hib hybridization buffer was added to maintain humidity. The hybridization chamber was sealed and incubated overnight at 42˚C.

2.9.3 Post Hybridization Wash

The hybridization chamber was taken apart and the hybridized slides and lifter slips were placed in low stringency wash buffer (1X SSC (Ambion), 0.2% SDS

(Ambion)) to remove the lifter slips. The slides were washed for 4 minutes in the low stringency wash buffer on a shaker. They were then washed in high stringency buffer (0.1X SSC, 0.2% SDS) for 4 minutes with agitation. The slides were then placed in 0.1X SSC and washed with agitation for 4 minutes. The slides were then spun dry in the array dryer for 10 seconds. If the slide did not dry it was soaked in water and spun dry again. The slides were stored in a light tight slide box prior to being scanned.

2.10 Slide Scanning and Image Acquisition

Hybridized arrays were scanned using the Agilent scanner. The scanner was warmed up for approximately 20 minutes and the carousel was loaded with the microarray slides in the dark. Each slide was placed in a slide holder with the barcode at the top. The slides were scanned from behind to protect the microarray. The Aligent scanner uses an autofocus to detect the plane of the glass. This allows for optimal fluorescence to be detected. The scan region, channel intensity and resolution can all be made specific to the microarray being scanned. The channel intensity was left at 100% and the resolution was set at 10 µm. After the slides were scanned the Aligent software automatically scales the images from the red and green channels. This produces an image with the same signal intensity.

2.10.1 Array-Pro Analysis

The gray scale raw images were imported into Array-Pro (Media Cybernetics) and the Cy3 and Cy5 images were assigned a green or red colour respectively. The images were optimized to improve visualization of spots. The spacial calibration found under the file menu was set to "none". The 2 images were grouped under "ImGroup1" and labeled "Cy3" and "Cy5" accordingly. The Cy3 grid must always be first and worked on before the Cy5 grid. Grids were found using the wizard in the program. Under the analysis menu the data table was created with the following headings in this order: grid, row, column, raw intensity Cy3, raw intensity Cy5, background Cy3, background Cy5, spot position X Cy3, spot position X Cy3, spot position Y Cy5, spot position Y Cy5, diameter (max) Cy3, diameter (max) Cy5. The data table was saved to file for import into Gene Traffic Duo.

2.10.2 GeneTraffic Duo Analysis

A new project was created and all necessary information was imputed into GeneTraffic Duo (Iobion). For each microarray experiment, two Tiff images and the data table (from Array Pro) were imported. The array layout file also needed to be uploaded into this program. Once the project has been defined the data was loaded by attaching the array layout, 2 Tiff files and data table to the correct hybridization. The data was normalized as lowess (sub-grid, non-flagged) and then exported as Microsoft Excel files.

2.10.4 Quadratic Regression Analysis

The quadratic regression analysis is used for gene discovery and pattern recognition for non-cyclic short time-course microarray experiments. It was developed by Liu *et al* (BMC Bioinformatics). The macro that is required for this analysis was downloaded from the following website; http://www.mc.uky.edu/UKMicroArray/bioinformatics.htm. The log R^2 ratio data outputted by the Gene Traffic Duo was then inputted on the working sheet. In the first row the names of the genes were placed and the time points, in numerical form, were placed in the order that they were obtained. The program then generated all of the necessary data tables.

2.10.5 SAM Plot Analysis

The Significance Analysis of Microarrays (SAM) (Stanford University) correlates expression data using a set of gene-specific t-tests. Each gene is given a score based on its change in gene expression compared to the standard deviation of repeated measurements for that gene. Genes that have a score higher than the threshold are considered significant.

2.10.6 EASE Analysis

Expression Analysis Systematic Explorer (EASE) software was used to identify over-represented categories of genes, to examine potential relationships between the expression of genes and their biological function. The EASE software can be found at; http://david.niaid.nih.gov/david/ease.htm.

2.11 Antibody Arrays

2.11.1 Protein Extraction and Labelling

Before starting the protein extraction, the following were chilled to 4˚C; mortar and pestle, microcentrifuge tubes and 15 mL conical centrifuge tubes. Frozen brain (100-200 mg) was transferred to the pre-chilled mortar and covered with 0.25-0.5 g of alumina (Sigma). The pestle was used to grind the brain until a paste was formed. A 2 mL aliquot of pre-chilled Extraction/Labelling Buffer (BD Biosciences) was added and mixed into the paste using the pestle. The second 1 mL of Extraction/Labelling Buffer was used to get the paste off of the pestle and back into the mortar. The extract was transferred to a 2 mL microcentrifuge tube and centrifuged at 10000 g for 30 minutes at 4˚C. The supernatant was transferred to a pre-chilled 15 mL conical centrifuge tube (Figure 6).

2.11.1.1 Protein Assay Determination

The protein concentration was measured using Pierce's BCA Protein Assay Reagent Kit. The Working Reagent (Pierce) was prepared by adding 50 mL of BCA Reagent A (Pierce) with 1 mL of BCA Reagent B (Pierce) in a 50 mL conical tube. The Diluted Albumin Standards (Pierce) were prepared as shown in Table 1.

Each standard (25 µL) was pipetted in triplicate into a microplate well. Each unknown sample was pipetted neat, in a 1:10 dilution and a 1:100 dilution, also in triplicate. A 200 µL aliquot of Working Reagent was added to each well and the

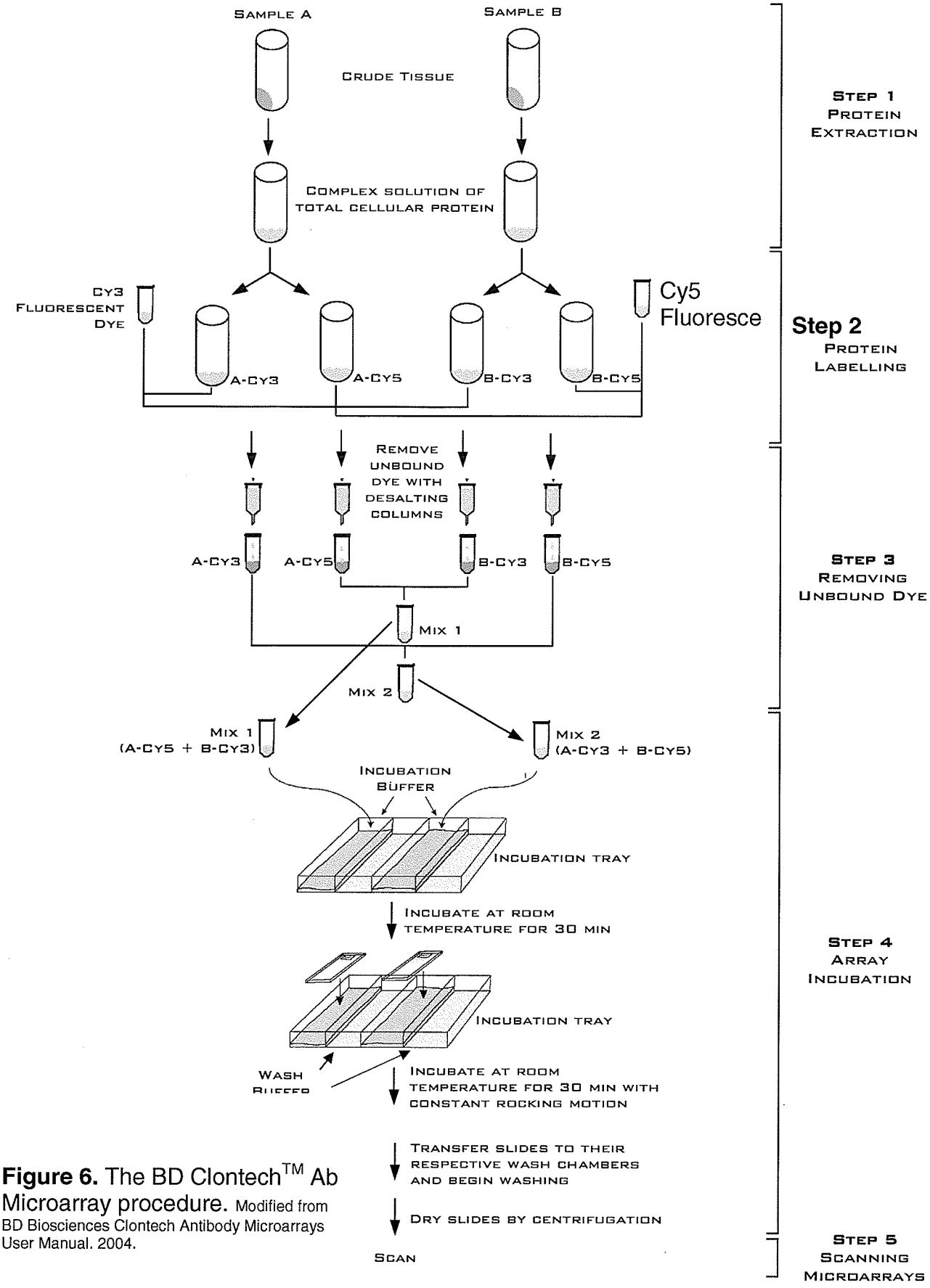

Figure 6. The BD Clontech™ Ab Microarray procedure. Modified from BD Biosciences Clontech Antibody Microarrays User Manual. 2004.

Table 1. The preparation of the Diluted Albumin (BSA) Standards used in the protein assay of the antibody array preparation.

Vial	Volume of Working Reagent (µL)	Volume and Source of BSA (µL)	Final BSA Concentration (µg/mL)
A	0	150 of Stock	2000
B	62.5	187.5 of Stock	1500
C	187.5	162.5 of Stock	1000
D	87.5	87.5 of Vial B	750
E	187.5	187.5 of Vial C	500
F	162.5	162.5 of Vial E	250
G	162.5	162.5 of Vial F	125
H	200	50 of Vial G	25
I	200	0	0

plate was mixed thoroughly by hand. The plate was covered in incubated at 37°C for 30 minutes. The absorbance was measured at 562 nm on a plate reader.

Each sample was diluted to 1.2 mg protein/mL by adding the appropriate volume of Extraction/Labeling Buffer.

2.11.2 Protein Labeling with Fluorescent Dye

The Cy3 and Cy5 dyes were each dissolved in 110 µL of Extraction/Labeling Buffer and centrifuged at moderate speed for 10 seconds to recover liquid in the bottom of the tube. A 50 µL aliquot of Cy3 dye (Amersham Biosciences) was added to 2 tubes and 50 µL of Cy5 dye (Amersham Biosciences) was added to 2 tubes. Infected protein sample (450 µL) was added to both a Cy3 and a Cy5 tube. The same was done for the control protein sample. The 4 tubes were inverted 3 times to mix the contents and centrifuged at moderate speed for 10 seconds to recover the liquid at the bottom of the tube. The tubes were incubated on ice for 90 minutes and inverted every 20 minutes. A 4 µL aliquot of Blocking Buffer (BD Biosciences) was added to each tube. The tubes were once again incubated on ice for 30 minutes and inverted every 10 minutes.

2.11.3 Removal of Unbound Dye (Desalting)

Preparation of the Desalting columns (Amersham Biosciences) was done during the 30 minute Blocking Buffer incubation. Four Desalting columns were used

and labeled in the following manner; Control-Cy3, Control-Cy5, Infected-Cy3 and Infected-Cy5. 1X Desalting Buffer (100 mL) was prepared by diluting the 10X Desalting Buffer (BD Biosciences) with Milli-Q-grade water. Each column was equilibrated with 3 x 5 mL of 1X Desalting Buffer. The Cy3 and Cy5 labeled protein samples were added to the corresponding column and allowed to pass. A 2 mL aliquot of 1X Desalting Buffer was added to the column. Microcentrifuge tubes (2 mL) were placed under the corresponding columns to collect the flow through and applying 2 mL of 1X Desalting Buffer to each column eluted the protein sample.

2.11.4 Antibody Array Incubation

Incubation Buffer (45 mL) was prepared by mixing 4.5 mL of Background Reducer (BD Biosciences) with 40.5 mL of Stock Incubation Buffer (BD Biosciences). A 5 mL aliquot of Incubation Buffer was added to the two incubation wells in the incubation chamber. Two 1.5 mL microcentrifuge tubes were labeled Slide 1 Mix and Slide 2 Mix. Slide 1 Mix combined 500 µL of Control-Cy5 and 500 µL of Infected-Cy3. Slide 2 Mix combined 500 µL of Control-Cy3 and 500 µL of Infected-Cy5. Each Slide Mix (200 µL) was added to the appropriate wash well in the incubation chamber. The tray was incubated for 30 minutes at room temperature with gentle rocking.

Meanwhile, the antibody microarrays (BD Biosciences) were prepared by washing the slides as follows. The Storage vial was decanted from the green-

capped Storage Vial. A 30 mL aliquot of Stock Incubation Buffer was added and the vial was capped and inverted slowly 10 times. The Stock Incubation Buffer was decanted and 20 mL of Incubation Buffer was added. Just before use the Incubation Buffer was decanted.

One slide was assigned to Slide 1 Mix and the other to the Slide 2 Mix. The slides were placed printed side up in the wells containing the Incubation Buffer/Slide Mix. The slides were incubated at room temperature for 30 minutes with gentle rocking. Every 10 minutes a micropipette was used to pry up one end of the slide to assist the exchange of liquid on all sides of the slide. Incubation Buffer (5 mL) was added to the wash wells in the incubation chamber and the slides were transferred to their respective wash wells and incubated at room temperature for 5 minutes with gentle rocking. The buffer was removed from the wash wells and 5 mL of Wash Buffer 1 (BD Biosciences) was added to each well. This was incubated for 5 minutes at room temperature with gentle rocking. This was repeated for Wash Buffers 2 to 7 (BD Biosciences).

The slides were dried using the slide dryer and were stored in a light tight slide box prior to being scanned.

2.11.5 Slide Scanning and Image Acquisition

Hybridized arrays were scanned using the Agilent scanner and analyzed in the same manner as the microarray slides.

2.12 DNA extraction

2.12.1 Tissue Preparation

Brains were separated into quarters and only one quarter was used per extraction. The brain was homogenized in 500 µL of PBS (In house media department) in a 50 mL conical tube. The buffer and brain fragments were transferred to a 1.5 mL eppendorf tube.

2.12.2 Sample Digestion

Proteinase K was added (12.5 µL of 20 µg/µL) (Invitrogen) for a final concentration of 500 µg/µL then add 50 µL of 10% SDS (Ambion) for a final concentration of 1%. The mixture was incubated overnight at 37˚C with gentle rotation.

2.12.3 Phenol/Chloroform Extraction

A volume of phenol (Invitrogen) (500 µL) equal to the volume of the sample was added then rotated for 10 minutes at room temperature. The mixture was centrifuged at 14000 rpm for 10 minutes at 4˚C. The upper aqueous phase was transferred to a new tube and a volume of phenol/chloroform (1:1) equal to the volume of the sample was added. The mixture was rotated for 10 minutes at room temperature then centrifuged at 14000 rpm for 10 minutes at 4˚C. the upper aqueous phase was transferred to a new tube and a volume of chloroform (Fisher Scientific) equal to the volume of the sample was added. The mixture was rotated for 10 minutes at room temperature then centrifuged at 14000 rpm

for 10 minutes at 4˚C. The upper aqueous phase was transferred to a new tube. An aliquot of 50 µL of Sodium Acetate (Ambion) (NaAc, 3.0 M) was added for a final concentration of 0.3 M and a volume of ice-cold 100% ethanol (Fisher Scientific) equal to 2.5X the volume of the aqueous phase (1250 µL) was added. It was mixed gently and incubated on ice for 10 minutes then centrifuged at 14000 for 20 minutes at 4˚C. The supernatant was discarded and 100-300 µL of water was added depending on the size of the pellet. The pellet was allowed to dissolve at room temperature for 30 minutes by shaking gently every 10 minutes.

2.13 PCR

PCR was performed to amplify segments of viral ORF something from DNA extracted from HSV-1 infected mouse brains. The reactions were set up in 40 µL volumes with 21.9 µL of dH_2O (Gibco), 5 µL 10X PCR Buffer (Applied Biosystems), 5 µL 25 mM $MgCl_2$ (Applied Biosystems), 4 µL 2.5 mM dNTP (Invitrogen), 1.8 µL of 20 µM primer #1 (Invitrogen), 1.8 µL of 20 µM primer #2 (Invitrogen) and 0.5 µL of AmpliTaq Gold (Applied Biosystems). To this 10 µL of template DNA was added. Reactions lacking template DNA were also set up with each primer pair. The reactions were amplified in a Thermo Cycler and were run with the following conditions: initial denaturation at 95˚C for 8 minutes, 3 cycles of 95˚C for 1 minute, 60˚C for 1 minute and 72˚C for 1 minute. This was followed by 37 cycles of 95˚C for 1 minute, 55˚C for 45 seconds and 72˚C for 1 minute. A final extension at 72˚C lasted for 7 minutes. The quality of the PCR reaction was determined using a 5% agarose gel made with 2.5 g of UltraPure

Agarose (Invitrogen), 2.5 g of NuSieve GTG Agarose (Cambrex), 100 mL of 1XTBE (NML media department) and 5 µL of EtBr (Fisher Biotech). A 10 µL aliquot of PCR product and 5 µL of blue juice (Invitrogen) were used for each reaction. The gel was run for 60 minutes at 90 volts.

2.13.1 Gel Purification

Some PCR reactions contained more than one band, thus the correct band (550 base pairs) was gel purified. The rest of the 40 µL PCR reaction (30 µL) was loaded into a 5% agarose gel (same as in section 2.13). The band of the appropriate size was cut out with a scalpel and the DNA was extracted using the QIAquick PCR Purification Kit. Three volumes of Buffer QG (Qiagen) was added to 1 volume of gel (100 mg ~ 100 µL). The samples were incubated at 50°C until the gel slice was completely dissolved. One gel volume of isopropanol (Fisher Scientific) was added to the sample and it was mixed. A QIAquick spin column (Qiagen) was placed in a 2 mL collection tube and the sample was applied. It was centrifuged for 1 minute at 13000 g. A 0.75 mL aliquot of Buffer PE (Qiagen) was added to the column and it was centrifuged for 1 minute at 13000 g twice. The QIAquick column was then placed into a clean 1.5 mL microcentrifuge tube and the DNA was eluted by adding 30 µL of Buffer EB (Qiagen). The column was incubated at room temperature for 1 minute and then centrifuged for 1 minute at 13000 g.

2.14 Digestion

Each digestion reaction was carried out in a separate tube and a control was used that contained no enzyme. Each tube contained 10 µL of PCR product, 2 µL of buffer (BioLabs), 1 µL of enzyme, 7 µL of water (Gibco) and 0.2 µL of BSA (BioLabs) as required. The digestion was undertaken for 1 hour at the appropriate temperature. *Bst*U1 (BioLabs) and *Bam*H1 (BioLabs) were the enzymes used. The quality of the digestion reaction was determined using a 5% agarose gel made with 2.5 g of UltraPure Agarose (Invitrogen), 2.5 g of NuSieve GTG Agarose (Cambrex), 100 mL of 1XTBE (NML media department) and 5 µL of EtBr (Fisher Biotech). An aliquot of blue juice (Invitrogen) (5 µL) and the sample was loaded onto the gel for each reaction. The gel was run for 60 minutes at 90 volts.

2.15 Sequencing

The PCR product was added to the tube (Millipore) and centrifuged for 15 minutes at 2300 g. The column was flipped over and 30 µL of nuclease free water (Gibco) was added. The column was centrifuged for 3 minutes at 3300 g. The nanodrop spectrophotometer was used to measure the amount of dsDNA. The product was diluted to 50 ng/µL in water and the primers were diluted to 1 µM. The sample was then sent to the NML DNA core for sequencing.

2.16 Electron Microscopy

2.16.1 Specimen Processing

Immediately upon dissection of the brain from the mouse it was cut up into specimens (1 mm^3 cubes) with a scalpel and placed in 2% gluteraldehyde (Marivac) in phosphate buffer. The specimens were stored at 4°C. The gluteraldehyde was removed and the tissue was washed in 2 mL of 0.1 M phosphate buffer (NML media department, pH 7.2-7.4) for 20 minutes. This step and all subsequent steps were accompanied with agitation on an orbital shaker, unless otherwise stated. The previous step was repeated with fresh phosphate buffer. The specimen was then fixed in 1% OsO_4 (Electron Microscopy Sciences) for 1 hour at room temperature. The specimen was washed again in 2 mL of phosphate buffer for 10 minutes. That wash step was repeated two more times. The specimen was dehydrated in ethanol, using the following dilution series; 50%, 50%, 70%, 70%, 95%, and 95% ethanol (Fisher Scientific), 10 minutes for each step. The specimen was then placed in 100% ethanol for 20 minutes, followed by a second dehydration step in fresh 100% ethanol for 20 minutes. The specimen was then suspended in 2 mL of propylene oxide (Electron Microscopy Sciences) for 20 minutes, this step was repeated with fresh propylene oxide for another 20 minutes. The specimen was then placed in 2 mL of a propylene oxide: EMbed-812/DER 73 resin (Electron Microscopy Sciences) mixture (1:1 ratio) for 1 hour at room temperature. Finally the specimen was placed in 2 mL of pure EMbed-812/DER 73 resin and mixed in with a 10 µL pipette tip. This mixture sat overnight and then one specimen was placed into

each gel capsule. The brain fragments were added first so that they were near the bottom and then the gel capsule was filled with pure resin before being capped and baked at 65˚C for 3-4 days.

2.16.1.1 Preparation of EMbed-812/DER 73 Resin

Resin was prepared by adding 9.12 g of DER 73 epoxy resin (Electron Microscopy Sciences), 2.16 g of EmBed 812 (Electron Microscopy Sciences) and 11.08 g of Nadic Methyl Anhydride (Electron Microscopy Sciences) (NMA) together in a 50 mL polypropylene tube. The mixture was stirred using a glass rod being careful not to create bubbles. The mixture should look clear before 280 µL of DMP-30 (Electron Microscopy Sciences) (the accelerator) was added. The mixture was stirred for another 5 min until the colour had changed to amber. The resin was placed in a disposable syringe for easy airtight storage and dispensation.

2.16.2 Sectioning

The resin capsule was trimmed using the Leica EM Trim specimen block trimmer to approximately a 1 mm^2 area around the brain sample embedded inside of it. Resin sections were then cut using a Leica Ultracut UCT Ultramicrotome to a thickness of about 100-120 nm. The sections were floated off of the glass knife and into a water bath before several sections were picked up on a copper grid (Electron Microscopy Sciences). The grids were left to air dry before being examined under the electron microscope.

2.16.3 Uranyl Acetate and Lead Citrate Staining

The following amounts of autoclaved milli-Q water were placed in three 15 mL tubes: 10 mL, 13 mL and 13 mL. The tubes were capped but not tightly and boiled for 5 minutes and then cooled on ice until they reached room temperature to remove the carbon dioxide. An aliquot of 100 µL of 10 M NaOH (Fisher Scientific) and 10 mL of prepared milli-Q water were combined and then 0.03 g of lead citrate (Marivac) was added. The mixture was shaken to dissolve the lead citrate and then let sit for 5 minutes. The lead citrate was made into aliquots of 1 mL each and placed in 1.5 mL Ependorf microcentrifuge tubes. The tubes were spun at maximum in a desktop centrifuge for 10 minutes.

A staining dish for the lead citrate was prepared by placing wet filter paper in a petri dish and then covering it with a piece of parafilm and several pellets of NaOH. The lid was placed on the dish and let sit while the uranyl acetate staining took place.

Aqueous uranyl acetate (2%) (Marivac) was prepared using milli-Q water. A second piece of parafilm was used for uranyl acetate staining and several drops of uranyl acetate were placed on the parafilm. One drop was used for each grid. The grids were left in the uranyl acetate for 5 minutes and then the excess stain was wicked off of the grid and tweezers. The grid was then washed by gently dipping it into three 1.5 mL ependorf microcentrifuge tubes filled with prepared milli-Q water. The grid and tweezers were wicked dry with filter paper and left to

air-dry. The same procedure was used to uranyl acetate stain the opposite side of the grid. The grid was once again let air dry for 5 minutes. Several drops of lead citrate were placed in the petri dish that had been left sitting with NaOH pellets in it. Each grid was then placed in the lead citrate so that both the top and bottom were covered, they were left to stain for 10 minutes in the covered petri dish. Breathing on the sample was avoided since the carbon dioxide from the experimenter's breath can cause a precipitate. The excess fluid was wicked off of the grid and tweezers. The grid was then washed 3 times with milli-Q water and then let air-dry.

2.16.4 Electron Microscope Imaging

The copper grid that contained the resin sections was put into the FEI Tecnai 20 transmission electron microscope, and the magnification was set to 19000x. The grids were scanned for evidence of HSV-1 infection. HSV-1 virions are 120 nm in diameter and particles that were round and of this size were photographed.

2.17 Hematoxylin and Eosin slides

2.17.1 Fixation

Fixation was carried out right after removal of the brain from the mouse to prevent autolysis. Brains were placed in 10% buffered formalin (Fisher Scientific). Formalin was used because of its ability to fix tissue by forming cross-linkages in the proteins, particularly between lysine residues. In this process, antigenicity is largely retained.

2.17.2 Tissue Processing

Each brain was cut into 3 sections using a scalpel. All sections were cut sagittally. One cut was made through the left side of the brain approximately one third of the way in. The second cut was made in the same place on the right side of the brain. Once cut each brain was placed into a separate labeled cassette (Fisher Scientific).

The cassettes containing the brains were processed as follows. The cassettes were placed in formalin for 2 hours, then in the following series of alcohols for 75 minutes each: 70% ethanol, 80% ethanol, 95% ethanol, and 100% ethanol (3 times). This dehydrated the tissues. The cassettes were then placed in 3 different containers of xylene for the 30, 45 and 45 minutes respectively. The cassettes were then placed in wax for 75 minutes, 1 hour and 1 hour each in a different receptacle. The tissues were then removed from the cassettes and put into paraffin blocks.

2.17.3 Sectioning

A microtome was used to cut sections of the embedded tissues. The sections were cut at 4 microns. Once the sections were cut they were floated on a water bath to remove wrinkles and picked up on a glass microscope slide (Fisher Scientific). The slides were allowed to dry before processing continued.

2.17.4 Staining

Water-soluble dyes cannot penetrate tissues embedded in paraffin, so the embedding process must be reversed. This was done by deparaffinizing the slides by running them through xylenes to alcohols to water. First slides were heated to 60˚C for 30 minutes to melt the wax and adhere the tissue section to the slide. They were then placed in xylene (Surgipath Canada Inc.) for 5 minutes. From there the slides were placed into xylene, 100% ethanol (Surgipath Canada Inc.), 90% ethanol and 70% ethanol for 2 minutes each. The slides were then washed in water.

Slides were placed in hematoxylin (Surgipath Canada Inc.) to stain the nucleic acids of the nucleus. They were left in this stain for 5 minutes, washed in water, then differentiated in 1% acid alcohol (1% hydrochloric acid in 70% methanol, made in house) until only the nuclei were stained. They were then washed in water and the nuclei were blued by immersion in Scotts Tap Water Substitute (Surgipath Canada Inc.) for 30 seconds. The slides were again washed in water, and stained with eosin (Surgipath Canada Inc.) for 3 minutes, which has an affinity for the cytoplasmic components of the cell. The slides were finally washed in water, dehydrated in a graded series of alcohols, cleared in xylene and mounted with Micromount (Surgipath Canada Inc.), a hydrophobic mounting media.

2.18 Immunohistochemistry

2.18.1 Deparafine-rehydrate

Slides were pre-warmed to room temperature and place in xylene for 3 minutes. Drip the excess xylene on a paper towel and repeat 2 more times. Slides were washed in 95% ethanol for 3 minutes and excess was blotted on a paper towel. The process was the same in 95% ethanol, 70% ethanol and 50% ethanol, followed by a final wash in distilled water for 30 seconds to 1 minute.

2.18.2 Block/Primary and secondary antibodies

Blocking solution was added on top of the sections using a transfer pipette and incubated at room temperature for 10 minutes. The excess blocking solution was blotted and the primary antibody was then added. The slide was incubated at room temperature for 30 minutes in a humid chamber. The avidin-biotin-alkaline phosphatase reagent was prepared during the last 3 minutes of the primary antibody incubation. The slides were washed gently with PBS from a squirting bottle but be sure to avoid squirting PBS directly onto the sections. The slides were transferred to a standard rack and then washed in PBS. The slides were washed in PBS-0.05% Tween 20 for 10 minutes and then washed in PBS for several dips. Excess blocking agent was removed by blotting and the secondary antibody was added. The slides were incubated at room temperature for 30 minutes. They were washed gently with PBS from the squirting bottle, transferred to the standard rack and washed for several dips in PBS. The slides

were then washed in PBS-0.05% Tween 20 for 10 minutes and again washed in PBS for several dips again. The slides were removed from the PBS.

2.19 Real Time PCR

Expression of messenger RNA from 20 genes (10 down- and 10 up-regulated) was tested. The endogenous controls tested were glyceraldehydes-3-phosphate dehydrogenase (GAPDH) and β-actin, GAPDH was chosen based on the analysis of its relatively constant expression throughout different dilutions and state of pathogenesis of the samples. The calibration control was the RNA extracted from the control mice. For each gene, the RNA from 3 different mice from each time point was used. Each reaction was carried out 3 times to ensure statistical significance. For each gene, one set of TaqMan probes and primers was tested. The probes contained a 6-carboxy-fluorescein phosphoramidite (FAM dye) label at the 5' end of the gene and a minor groove binder and nonfluorescent quencher at the 3' end. This allowed the probe to hybridize across exon junctions. The assays were supplied with primers and probe concentrations of 900 nM and 250 nM respectively.

The volume of components needed to prepare the 2X RT master mix was calculated. Each reaction required 10 µL of 10X Reverse Transcription Buffer (Applied Biosystems), 4 µL of 25X dNTPs (Applied Biosystems), 10 µL of 10X random primers (Applied Biosystems), 5 µL of MultiScribe^{TM} Reverse Transcriptase (50 U/µL) (Applied Biosystems), and 21 µL of nuclease free water

(Applied Biosystems). These volumes were pipetted into a 10 mL tube and placed on ice.

The cDNA archive reaction plate (Applied Biosystems) was prepared by adding 50 µL of 2X RT master mix into each well on the plate as well as 50 µL of RNA sample into the wells. This was titrated with a pipette 2 times to mix and the plates were covered with caps. The plate was briefly centrifuged to spin down the contents and to eliminate any air bubbles. It was then placed on ice until the thermal cycler was ready to be loaded.

The following conditions were programmed into the thermal cycler: step 1 temperature 25˚C for 10 min and step 2 temperature 37˚C for 120 min. The reaction volume was set to 100 µL and the plates were loaded into the thermal cycler to start the reverse transcription run.

The PCR reaction mix was prepared as follows. The reaction mix for four 20 µL reactions contained, 5 µL of TaqMan® Gene Expression Assay mix (20X) (Applied Biosystems), and 50 µL of TaqMan® Fast Universal PCR Master Mix (2X) (Applied Biosystems) were combined. The TaqMan® Gene Expression Assay mix (Applied Biosystems) needs to be protected from direct exposure to light as this may affect the fluorescent probes. The tubes were capped and mixed by gentle inversion. They were then centrifuged briefly to spin down the contents and to eliminate any air bubbles. A 20 µL aliquot of the reaction mix

was transferred to the wells of an Optical 96-Well Fast Plate (Applied Biosystems). The arrangement of the reactions was double checked to make sure it matched the arrangement of the plate document used for the run. A 2.5 µL aliquot of appropriate cDNA was added to each well. The plate was sealed with an optical adhesive cover (Applied Biosystems) and centrifuged briefly to spin down the contents and eliminate any air bubbles. The plate was run by placing it in the 7500 Fast Real Time PCR System (Applied Biosystems). The fast thermal cycling conditions were set to 95˚C for 20 seconds then 40 cycles of 95˚C for 3 seconds followed by 60˚C for 30 seconds.

The data was analyzed by viewing the amplification plots. The software was programmed to automatically set the baseline and threshold values. The gene-expression values were normalized to the calibration control and the endogenous control (GAPDH), they were then log transformed (on a base 2 scale) and changed into fold change differences. The fold changes were plotted and compared to data generated from the microarray experiments.

Results

3.1 Virus quantification and classification

3.1.1 Plaque Assay

To determine the titre of the virus stock, plaque assays were undertaken. The double overlay (DO) and CMC methods were used. The DO was stained with neutral red while the CMC plates were stained with crystal violet. Cytopathic effects in infected Vero cells appear as white plaques after both neutral red and crystal violet staining. Plaque size is determined by the extent of virus spreading in the infected monolayer. Each plaque represents an infection from a single viral particle. At a dilution of 10^{-5} the concentration of viral particles was too great to count the individual plaques (figure 7). The 10^{-6} dilution of the CMC plates had 76 and 60 plaques respectively while the DO plates had 104 and 67 plaques respectively. The 10^{-7} dilution had 5 and 9 plaques respectively in the CMC plates. This same dilution had 6 and 12 plaques in the DO method. The final dilution of 10^{-8} had 1 and 2 plaques respectively in the CMC plates while the DO plates had 1 and 0 plaques respectively. This assay determined the viral titre of HSV-1 strain F to be 3.92×10^{7} pfu/mL.

3.1.2 Electron Microscopy

To further establish that the plaques formed in the plaque assays were in fact caused by HSV-1 infection electron microscopy of the virus was undertaken. The virus that was grown up in cell culture was examined. Nucleocapsids taken

Figure 7. HSV-1 virus plaque assay results on green African monkey kidney cells (Vero) at 2 days. Serial dilutions of virus were plated. A: Cells stained with crystal violet. B: Cells stained with neutral red.

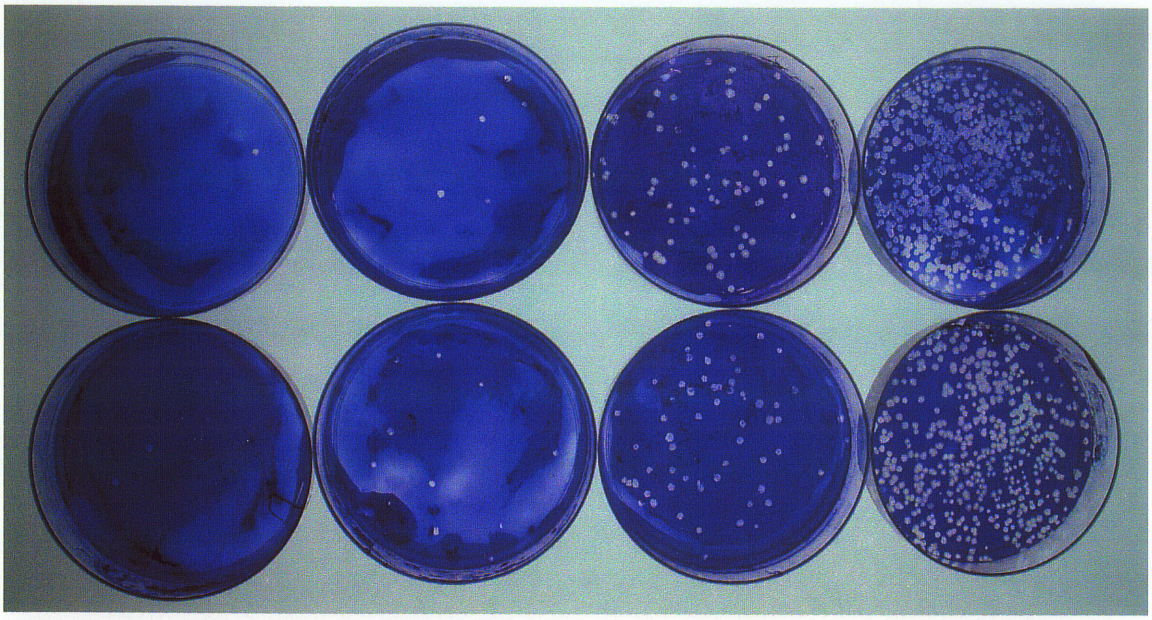

A

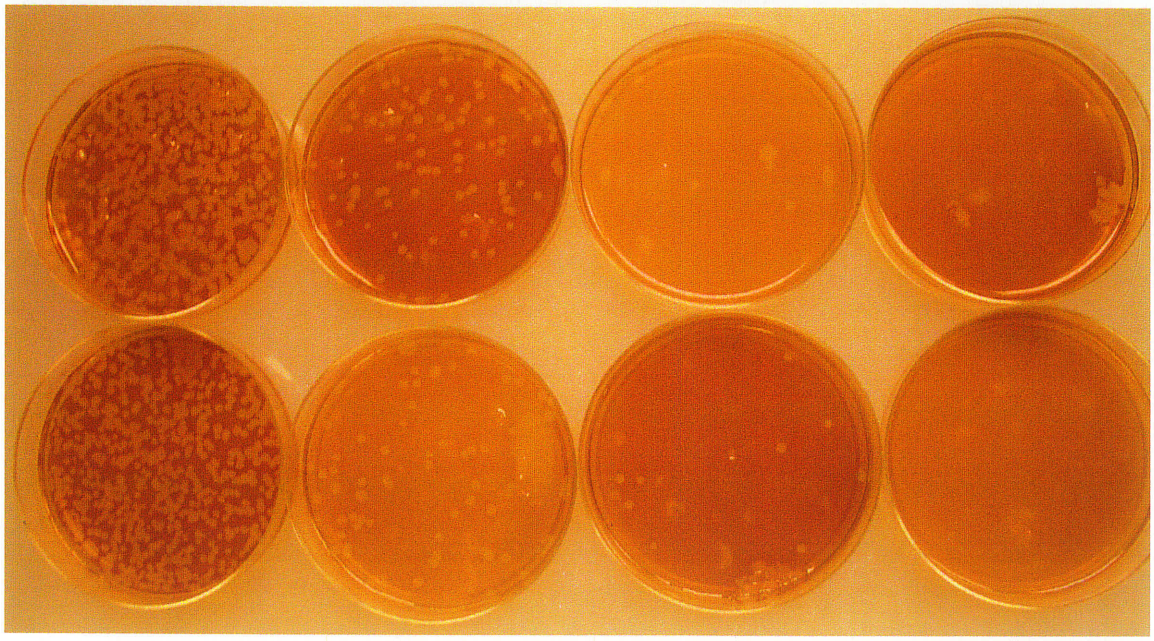

B

from inside infected cells (figure 8) revealed regular sized particles that measured approximately 120 nm. This corresponds with the known size of HSV-1 nucleocapsids. The viral particles show icosahedral symmetry and individual nucleocapsid proteins are visible. The viral envelopes are not visible in these images. The tegument is also not seen since it would have resided between the nucleocapsid and the lipid bilayer of the envelope. An electron microscope image of HSV-1 complete with tegument and envelope intact is shown in Figure 1.

3.2 Animal Infection

None of the female adult SJL mice (52 control and 64 HSV-1 infected) that were inoculated with HSV-1 showed outward signs of disease. Ruffled coat, hunched posture, weight gain or loss, laboured respiration, hyper-excitability or depression, seizures or circling were the signs that were expected of HSV-1 encephalitis infected mice (Hudson, Dix et al., 1991;Lamade, Lamade et al., 1996;Thomas, Kapadia et al., 2001). It was observed that the infected mice bled and twitched more upon decapitation than the control mice did. The brains that were extracted from the infected mice showed no gross signs of encephalitis. They were the same size and weight compared to the control brains. The control group had an average weight of 20g, which was the same average weight of the HSV-1 infected mice.

Figure 8. HSV-1 nucleocapsids as seen under an electron microscope.

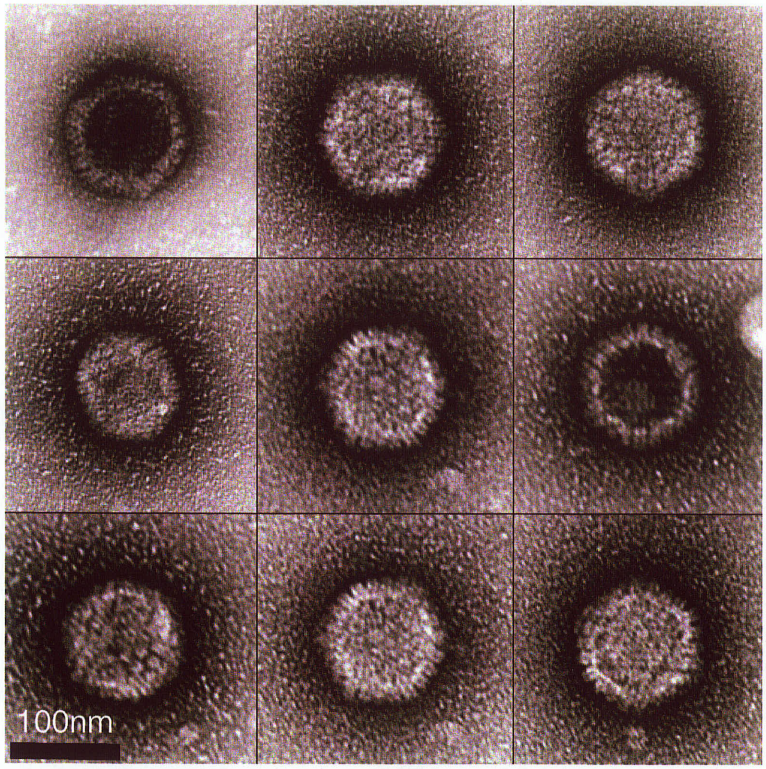

3.3 PCR

3.3.1 PCR

The "gold standard" of HSV-1 isolation and detection in HSE has become PCR. This technique was used to ensure that HSV-1 had in fact infected the mouse brains. After HSV-1 inoculation DNA was extracted from frozen mouse brains to verify that an infection had occurred (figure 9). The negative control was a mock-infected brain and the positive control was a brain obtained from Dr. Alberto Severini known to be infected with HSV-1. Every time point showed the correct band at 532 bp. The band at 14 dpi was very faint. This is common to the fact that HSV-1 is hard to detect in the CSF after 2 weeks of infection (Sauerbrei, Eichhorn et al., 2000).

3.3.2 Virus titre PCR

In order to confirm HSV-1 infection quantitative PCR was undertaken to find out how many copies of the virus was in the brain. PCR showed the presence of HSV-1 in the brain of infected animals. Extraction of DNA was undertaken from whole mouse brain tissue at 3, 7, 14 and 21 dpi. Viral load peaked at 7 dpi with $2.8x10^3$ copies/μL thereafter it declined to a low baseline value of less than 10 copies/μL (table 2).

Figure 9. PCR pattern for HSV-1 DNA found in mouse brains at 3, 7, 14 and 21 dpi.

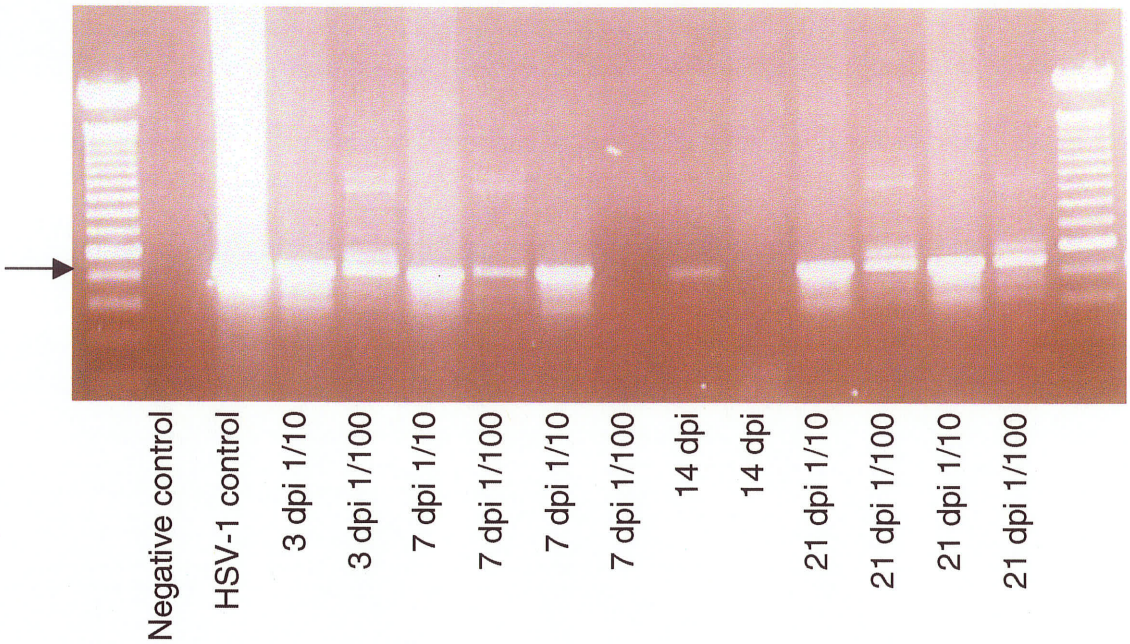

Table 2. Quantification of HSV-1 virus titer using real time PCR.

Sample	Viral Titer (copies/μL)
3 dpi	< 10
7dpi	$2.8x10^3$
14 dpi	< 10
21 dpi	< 10

3.4 Histology

3.4.1 Histology

Pathological differences between the infected and mock-infected brains of SJL mice were assessed by histology. Samples were examined histologically for differences in perivascular cuffing and marginalization of chromatin. Perivascular cuffing was observed in all time points and was most noticeable from 7 dpi and on (figure 10).

3.4.2 Electron microscopy

Electron microscopy was undertaken in an attempt to identify virus particles in the brain tissue of infected mice. A particle of the correct size and shape that corresponds to those of an HSV-1 virion is shown in figure 11. However, it was not possible to confirm whether these particles were indeed HSV-1 by electron microscopy.

3.5 Immunohistochemistry

Immunohistochemistry was performed but since there was too much background on the slides no conclusive result could be drawn. Another laboratory was asked to perform the immunohistochemistry. To date, their results show some brain cells identified as positive for HSV-1 but no images are available.

Figure 10. Histology of control and HSV-1 infected mouse brains. Images A, C, E and G are control mouse brain histopathology from 3, 7, 14 and 21 dpi respectively. Images B, D, F and H are HSV-1 infected mouse brains from 3, 7, 14 and 21 dpi respectively. The HSV-1 infected brains show an infiltration of monocytes in the temporal lobe which is an indication of perivascular cuffing which is characteristic of HSE.

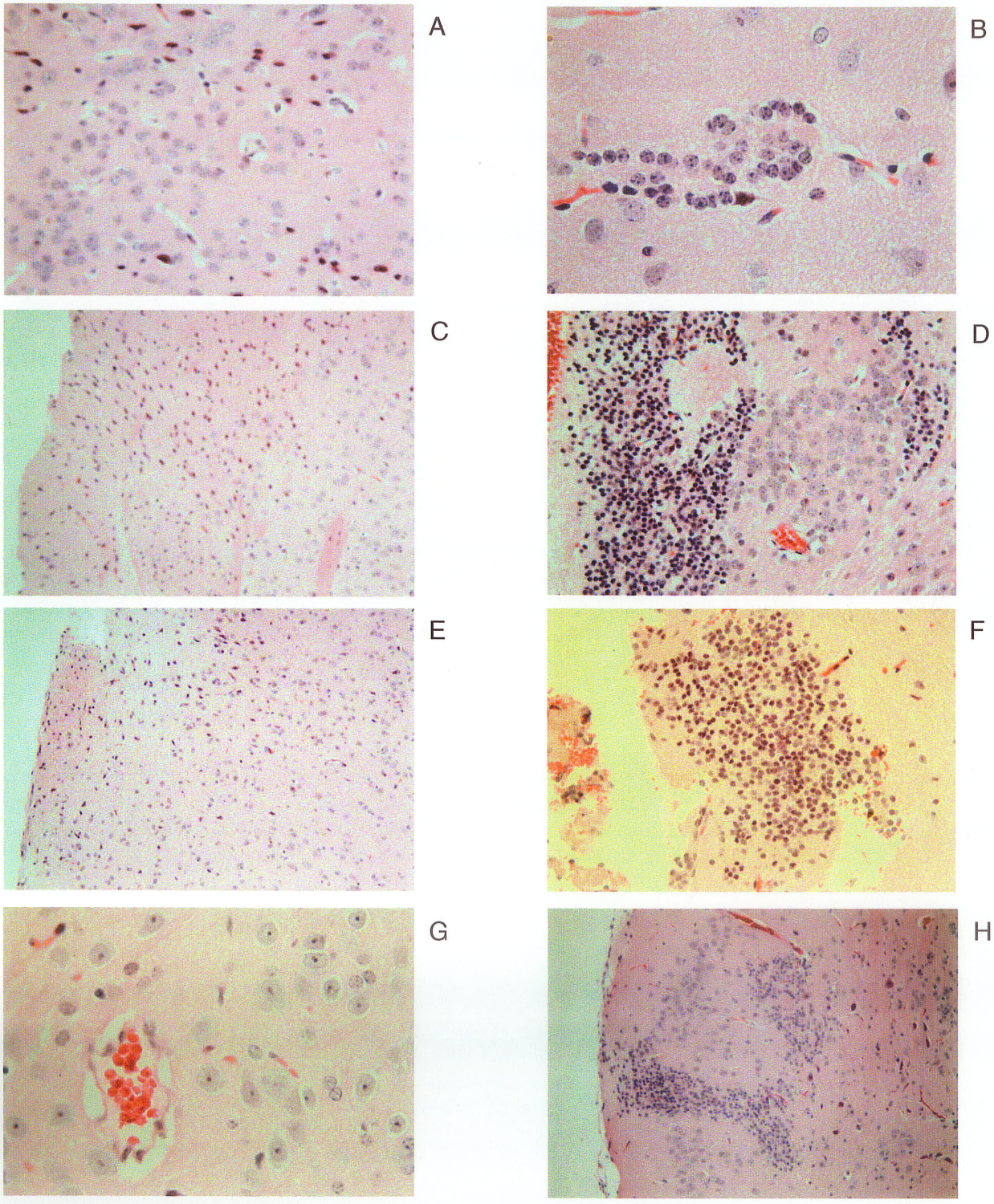

Figure 11. Electron microscope images of infected mouse brains. Arrow indicates potential HSV-1 particle

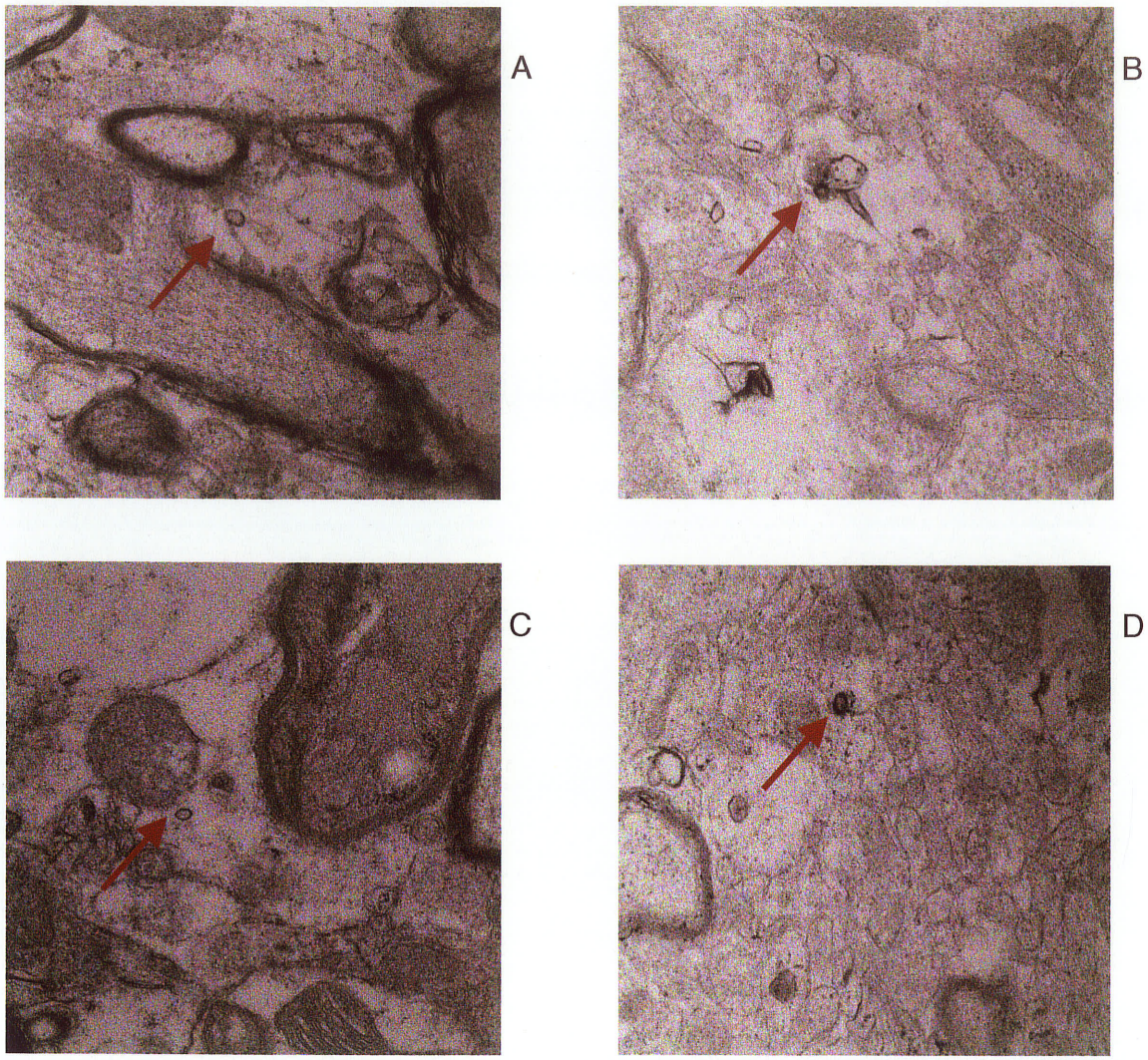

3.6 Microarrays

3.6.1 Experimental Design

There were 36 SJL mice inoculated by intranasal injection of HSV-1 to identify differences in expression of host genes during infection compared to mock infected mice. Microarray experiments were undertaken to determine genes that are significantly up or down regulated in mouse brain tissue reflecting the host response to HSV-1 infection.

Microarrays were preformed in four groups based on the time points used in the animal infection experiment. Gene expression levels in samples of total mouse brain RNA isolated 3, 7, 14 and 21 dpi were compared with those in mock-infected controls. Eight mice were included for infected and mock-infected groups at each time point. This number of mice was used to induce the statistical power of the experiment to garner statistically significant results.

Expression of mouse genes was analyzed using a standard two-colour microarray experimental format. Labeled total RNA isolated from infected and mock-infected mouse brains were compared directly by mixing equivalent amounts of labeled RNA samples and hybridizing to DNA microarrays. The cDNA microarrays used contained a large number of transcripts specific to the CNS along with a large number of ESTs. The DNA Core at the NML prepared an 11136-element cDNA microarray. Each element on the array was a PCR product that was generated from a mouse CNS-derived EST library. This

allowed for transcripts from the CNS to be specifically targeted. Both known genes and ESTs were included to allow for future gene discovery. The resulting data from the microarray experiments were filtered using various software and analyzed to identify genes of interest. All four sets of microarray experiments were examined together as a time course experiment looking at infection as the single variable. Data was analyzed using the following three programs; EDGE (Extraction of Differential Gene Expression), SAM (Significance Analysis of Microarrays) and a quadratic regression analysis for gene discovery and pattern recognition. Each of the above mentioned methods of data analysis yielded a list of significant genes. These methodologies generated these very similar lists due to some difference in the statistical analysis used.

3.6.2 EDGE Analysis

The Extraction of Differential Gene Expression (EDGE) software is based on the Optimal Discovery Procedure (ODP). ODP uses all relevant information from all genes in order to test each one for differential expression. In temporal studies, the statistical significance is calculated while accounting for sources of dependence over time.

Two methods of EDGE were used to scrutinize the data. One looked at the data as a temporal experiment while the other examined the data as a static experiment. In the temporal analysis, a control time point of zero days post infection was included. The control mice were used as zero dpi mice. The

temporal analysis studied the dynamic behaviour of gene expression while the static analysis examined the arrays irrespective of time. There were 341 genes found to have differences in expression that were statistically significant by the temporal method and 128 by the static method.

The fold changes of the 341 genes over the course of each microarray experiment are shown in figure 12. The significant fold changes are coloured based on an increase or decrease in expression. Upregulated genes are coloured red and downregulated genes are green. There are very few upregulated genes compared to downregulated genes by the 21 dpi time point. Each row represents one gene while every column represents one array. The dendogram on the left hand side of the image shows the relationship of how similar the significant genes are to one another.

The heat map generated by the static method of analysis is shown in figure 13. The dendogram on the left hand side of the image shows the relationship of the significant genes. Upregulated genes are red and downregulated genes are coloured blue. The intensity of the colour reveals how up or downregulated a gene is. Each row represents one gene while every column represents one array. There are more genes significantly downregulated at 21 dpi compared to 3 and 7 dpi. The 9 most significant genes have a Q-value of 8.75×10^{-4} and are the following genes: heterogeneous nuclear ribonucleoprotein U-like 2, splicing factor 3b subunit 1, LUC-7 like 2, EST highly similar to Smt3A,

Figure 12. A cluster analysis of genes with expression levels that changed over the course of HSV-1 infection. Total RNA was assessed at 3, 7, 14 and 21 days post infection by microarray analysis. A total of 341 genes whose intensities varied at least 2-fold over at least one time point during the infection were subjected to hierarchical clustering analysis. Time points are represented by columns and genes in rows. Red, yellow and green represent the higher, equal or lower expression levels relative to a control mouse brain. These 341 genes were clustered using GeneMaths software.

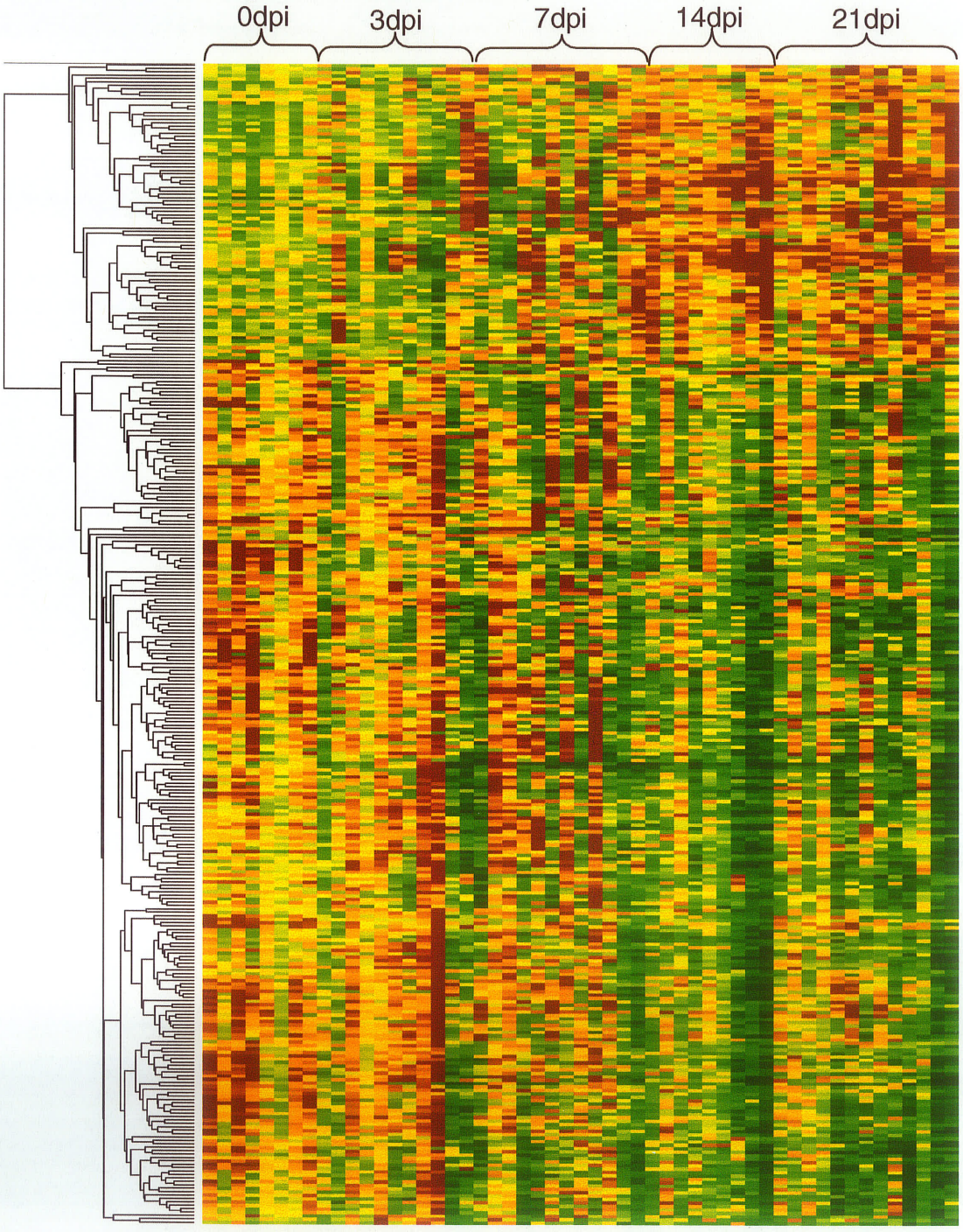

Figure 13. A heat map analysis of genes with expression levels that changed during an HSV-1 infection. All time points were analysed as a static experiment. Time points are represented by columns and genes in rows. Colour intensity corresponds to the degree of overexpression or underexpression with brighter colours indicating a more significant level of expression. Upregulated genes are blue and downregulated ones are red. These 127 genes were clustered using EDGE
software

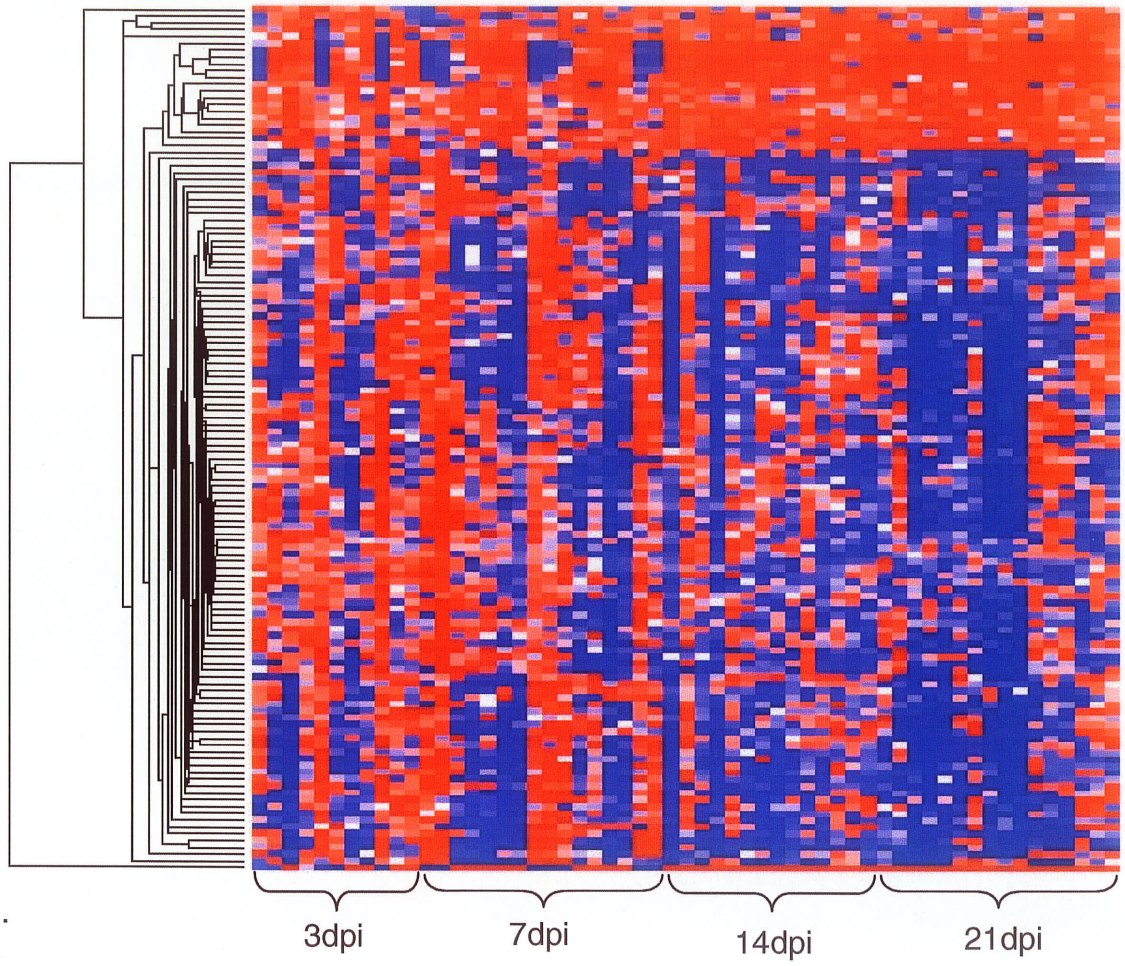

dihydropyrimidinase-like 2, ATPase class VI, surfeit gene 4 and 2 ESTs. The Q-value is similar to the false discovery rate (FDR) used in the SAM analysis.

3.6.3 SAM Analysis

The statistical method employed by SAM is the modified t-statistic. SAM can recognize genes with a statistically significant change in expression by incorporating a set of gene-specific t-tests. Each gene is allocated a score on the basis of its change in gene expression relative to the standard deviation of repeated measurements for that gene. This measures the strength of the relationship between gene expression and the response variable. Genes that have a score higher than the baseline are considered possibly significant. The FDR is the percentage of significant genes that could be identified by chance. Recognizing nonsense genes and inspecting the permutations of the measurements calculate the FDR. Statistics are calculated on the basis that the differences between groups in the dataset are larger than the differences within the group. This means that genes with a very small fold change between the two groups can have very high SAM score and be predicted as significant.

A one-class response analysis was performed using SAM. This assumes that each array in the dataset is equivalent and then determines the significant differences in regulation in comparison with a control. The $\log_2$ ratios for infected mice versus mock-infected, age-matched control mice were used. The resulting plot for a one-class SAM analysis is shown in figure 14. A delta value of 0.44

Figure 14. SAM plot with a delta value of 0.44 in a one class response analysis. 6 genes were found to be upregulated and 161 were downregulated.

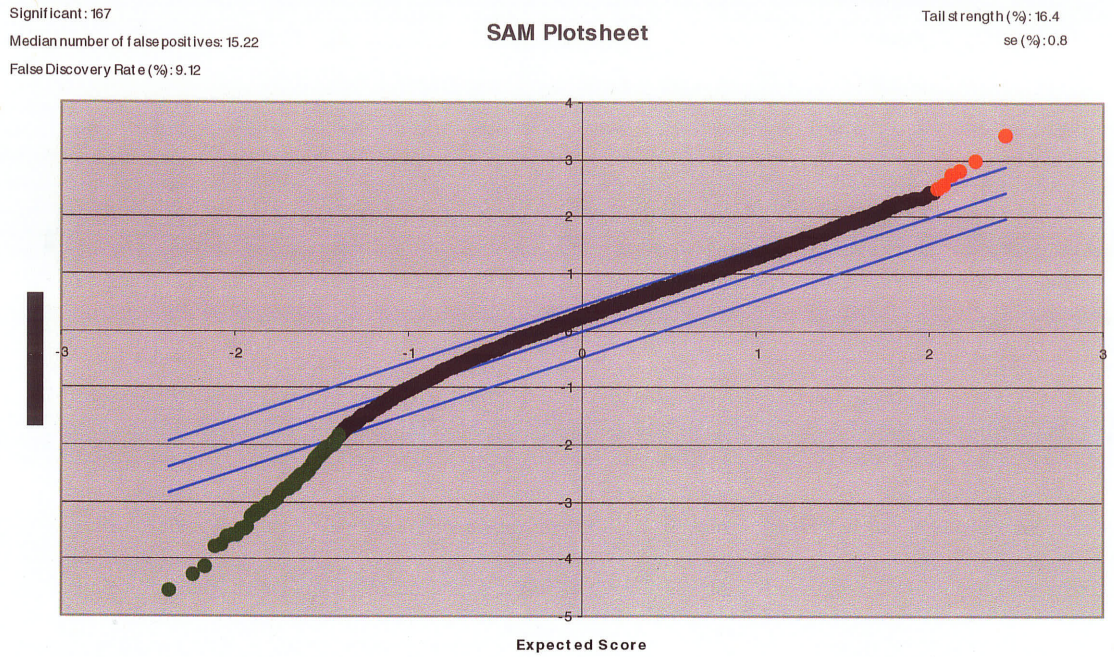

was selected that resulted in less than 10% FDR for a set of 167 genes. The delta value is a numeric vector specifying a set of values for the threshold *Delta* that should be used. The following genes were predicted to be significantly differentially represented in the infected mice versus the mock-infected mice. There were six deemed to be upregulated and 161 genes shown to be downregulated. The following genes were upregulated UDP-glucose ceramide glucosyltransferase-like 1, cullin associated and neddylation disassociated 1, WW domain binding protein 11, leucine rich repeat and fibronectin type III domain containing 5 and 2 ESTs. The 6 most down regulated genes were LUC7-like 2, EST highly similar to Smt3A, dihydropyrimidinase-like 2, ATPase class VI, surfeit gene 4 and 1 EST.

3.6.4 Quadratic Regression Analysis

The quadratic regression analysis uses a model based approach using a step down quadratic regression. It can be used for non-cyclic short time-course microarray data. Time is treated as a continuous variable. Each gene is fitted with a quadratic regression model. If the gene has no statistically significant relationship with time it is fitted with a linear regression model. Significant genes are determined using F-statistics and least squares estimates. Genes are identified based on their temporal expression profiles.

The quadratic regression analysis yielded 244 significant genes. They were divided up into the following categories as seen in figure 15; 30 linear up, 145

Figure 15. Quadratic regression analysis of microarray data generated 244 significant genes. LU: Linear Up, LD: Linear Down, QC: Quadratic Concave, QV: Quadratic Convex, QLCU: Quadratic Linear Concave Up, QLCD: Quadratic Linear Concave Down, QLVU: Quadratic Linear Convex Up, QLVD: Quadratic Linear Convex Down.

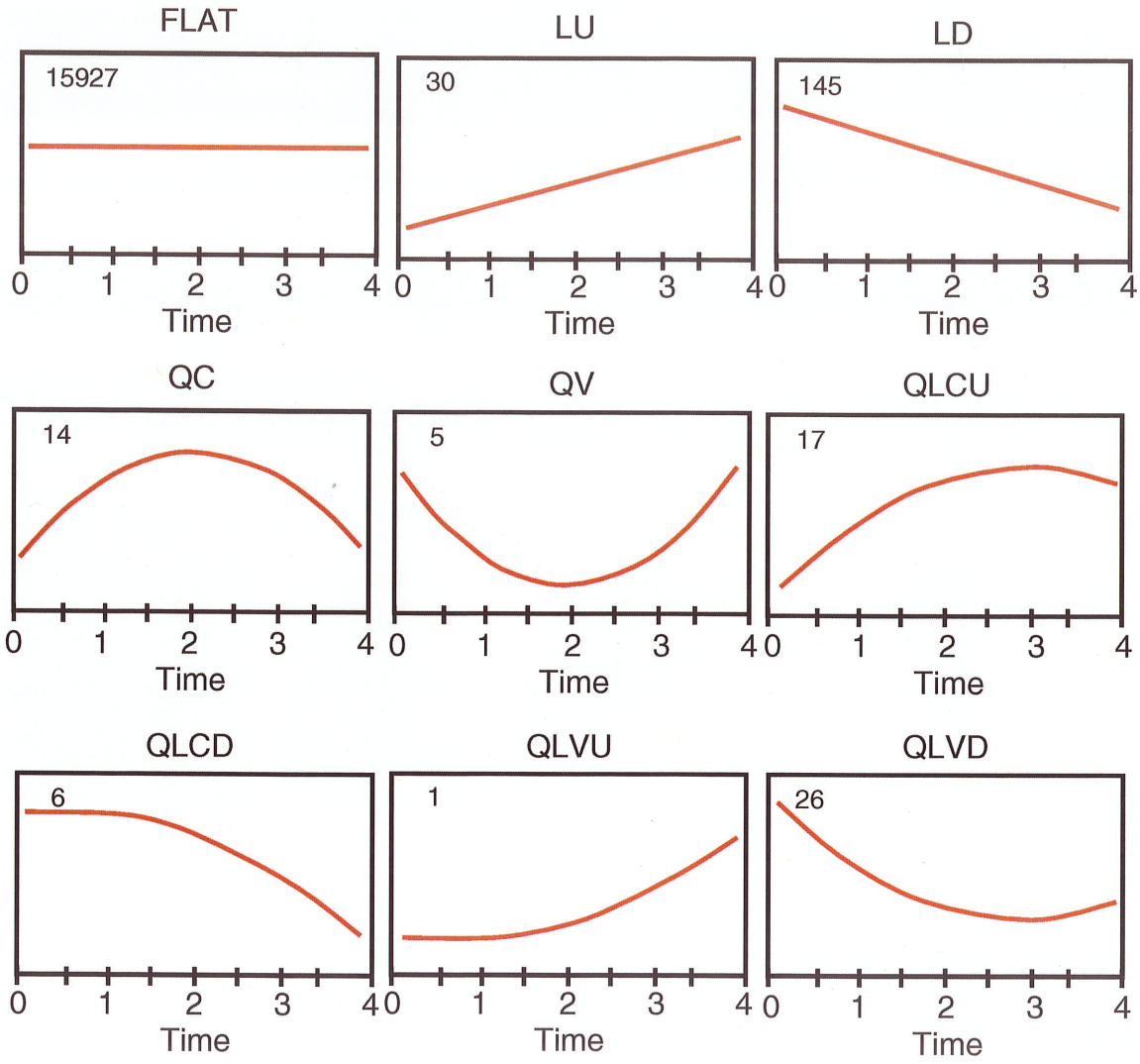

linear down, 14 quadratic concave, 5 quadratic convex, 17 quadratic linear concave up, 6 quadratic linear concave down, 1 quadratic linear convex up and 26 quadratic linear convex down. All of the genes listed as flat were not significant. The ten most linear upregulated genes correspond with those found in SAM and the other methods of analysis while only three of the ten most linear downregulated genes are found on other lists. None of the other categories of analysis had any genes matching in any other list.

3.6.5 Comparison of Analyses

Genes from all methods of analysis were compared (table 3). In total seven different methods were matched up to each other. Data from a reference pool of RNA that was tested against experimental infected RNA was used in this comparison. The rest of the data comes from the above mentioned examinations. The following seven genes were found to be significant by all methods of analyses: UDP-glucose ceramide glucosyltransferase-like 1, muscleblind-like 2, SWI/SNF related matrix associated actin dependent regulator of chromatin subfamily a member 2 transcript variant 2, MKIAA1189 protein, cullin associated and neddylation disassociated 1, and RAR-related orphan receptor alpha. There were 187 genes found to be significant when only the experimental data set was used.

Table 3. List of genes found to be significant by several forms of analysis. Column A represents genes found to be significant from the reference data set using EDGE. Column B and column C represent genes found to be significant from the reference data set using SAM at day 14 and 21 respectively. Column D represents significant genes from the experimental data set using EDGE set to static. Column E represents significant genes using the quadratic regression model. Column F represents genes found to be significant from the experimental data set using SAM. Genes in the column titled "Gene Name" were found to be significant using EDGE set to temporal. Columns 1, 2, 3, 4 and 5 represent the various time points used (control, 3, 7, 14 and 21 dpi respectively).

A	B	C	D	E	F	GenBank	Gene Name
						AI414429	UDP-glucose ceramide glucosyltransferase-like 1
						AI837865	muscleblind-like 2
						AI839352	SWI/SNF related, actin dependent regulator of chromatin
						AI840969	MKIAA1189 protein
						AI840993	cullin associated and neddylation disassociated 1
						AI854159	RAR-related orphan receptor alpha
						AI448172	Glycerol-3-phosphate dehydrogenase 1-like
						AI448819	Armadillo repeat containing 1
						AI452233	Suppression inducing transmembrane adaptor 1
						AI837717	Trinucleotide repeat containing 6a
						AI839190	
						AI839289	Smg-6 homolog, nonsense mediated mRNA decay factor
						AI840407	RIKEN cDNA 1110064P04 gene
						AI840873	Kinesin family member 5B
						AI841344	Heat shock protein 90kDa alpha, class A member 1
						AI841883	
						AI841884	N-acetylgalactosaminyltransferase 2
						AI843592	Adult male testis cDNA
						AI844215	BAT2 domain containing 1
						AI845643	DNA segment, Chr 4, Wayne State University 53, expressed
						AI845657	Kruppel-like factor 9
						AI846745	MKIAA1244 protein
						AI848239	Serine/arginine-rich protein specific kinase 2
						AI848462	Zinc finger protein 148
						AI849369	Poly(A) binding protein, nuclear 1
						AI849459	Myeloid/lymphoid or mixed-lineage leukemia 5
						AI849635	Metadherin
						AI850651	
						AI851745	SPARC-like 1
						AI853086	Methionine adenosyltransferase II, alpha
						AI853636	Cyclic AMP-regulated phosphoprotein, 21
						AI323455	Peptidylglycine alpha-amidating monooxygenase

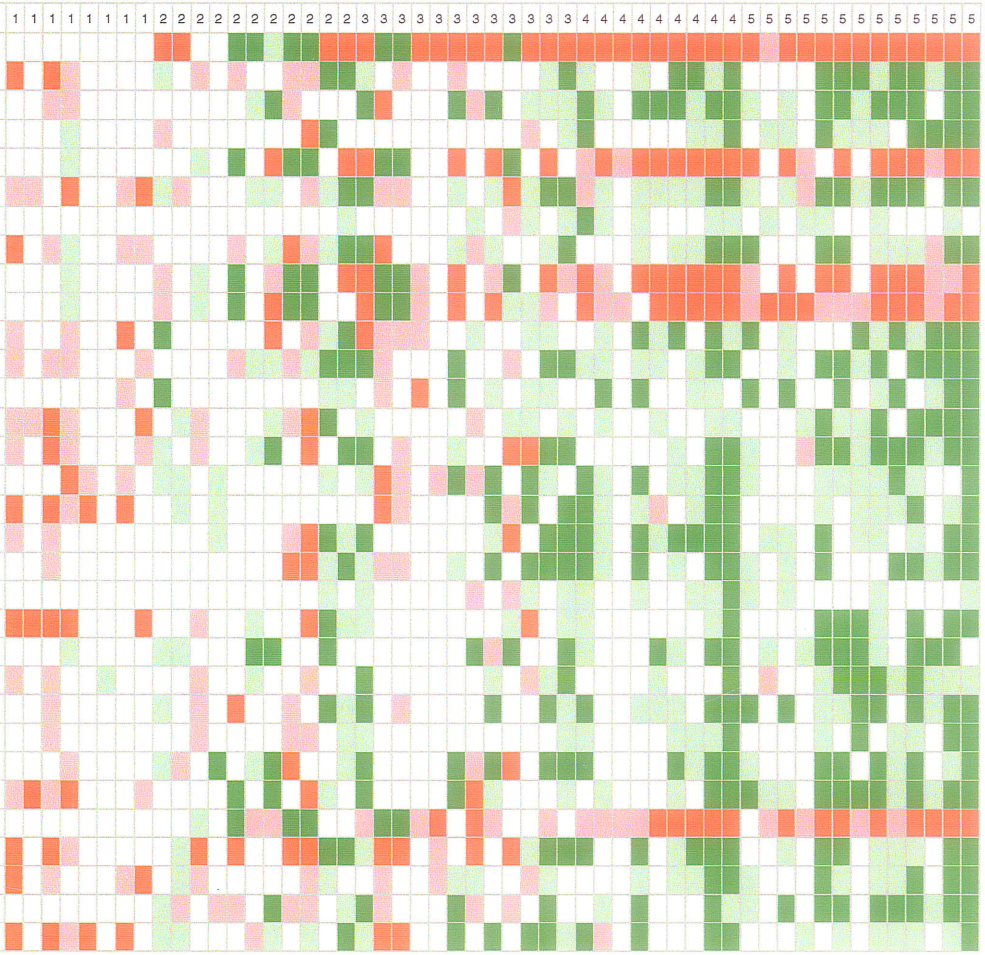

AI448344	Active BCR-related gene
AI450315	Diaphanous homolog 2 (Drosophila)
AI465155	heterogeneous nuclear ribonucleoprotein U-like 2
AI662302	LUC7-like 2 (S. cerevisiae)
AI666563	Splicing factor 3b, subunit 1
AI836351	Acid phosphatase 1, soluble
AI837503	Chimerin (chimaerin) 1
AI838689	Protein tyrosine phosphatase 4a2
AI839589	3-monooxygenase/tryptophan 5-monooxygenase, gamma
AI839703	sodium channel, type IV, beta
AI839754	Glycoprotein m6b
AI840009	
AI840074	RNA-binding protein isoform G3BP-2a
AI840578	Nuclear receptor interacting protein 1
AI841338	RAB6, member RAS oncogene family
AI841876	
AI842320	Neurofibromatosis 2
AI846004	Pleiotrophin
AI846954	alkylation repair homolog 5 (E. coli)
AI847745	Phosphatase and tensin homolog
AI847999	RIKEN cDNA E130013N09 gene
AI849003	
AI849259	Cellular nucleic acid binding protein 1
AI850103	
AI850132	Metaxin 1
AI850922	Purine rich element binding protein B
AI851286	Transcribed locus
AI851517	Nucleosome assembly protein 1-like 5
AI852762	Ubiquitin protein ligase E3A
AI854214	Inositol monophosphatase domain containing 1
AI854679	Tumor differentially expressed 2
AI323897	Tropomodulin 2
AI323904	Peroxisomal membrane protein 4
AI325494	Destrin
AI325913	Nitrogen fixation gene 1 (S. cerevisiae)
AI325979	Transmembrane protein 30A
AI413505	RAB6, member RAS oncogene family
AI413721	Hypermethylated in cancer 2 protein
AI414590	Serine/arginine-rich protein specific kinase 2
AI426310	Mannan-binding serine peptidase 1
AI426983	Transcribed locus
AI428022	Nipped-B homolog (Drosophila)
AI429157	RIKEN cDNA 8430427H17 gene

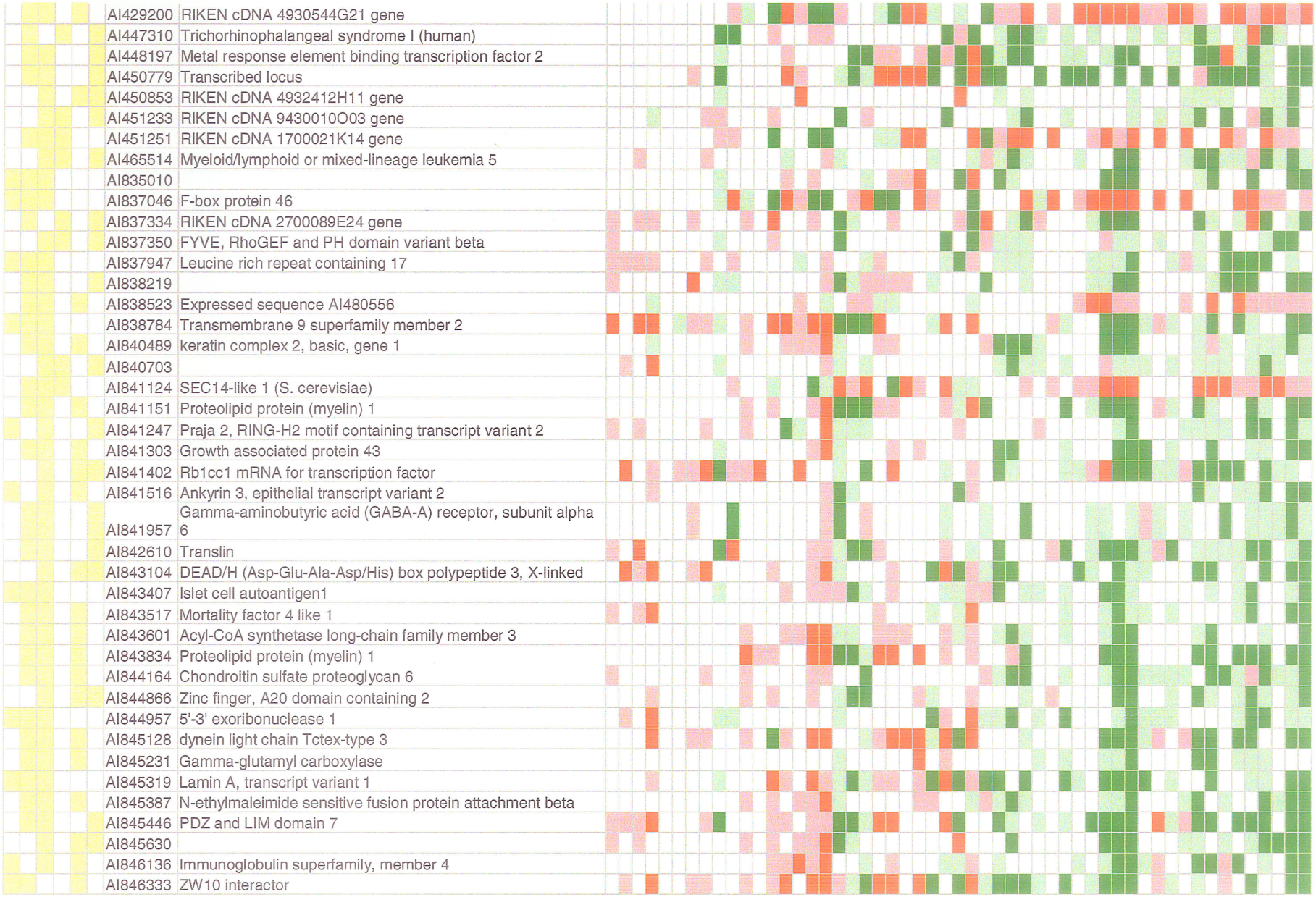

AI429200	RIKEN cDNA 4930544G21 gene
AI447310	Trichorhinophalangeal syndrome I (human)
AI448197	Metal response element binding transcription factor 2
AI450779	Transcribed locus
AI450853	RIKEN cDNA 4932412H11 gene
AI451233	RIKEN cDNA 9430010O03 gene
AI451251	RIKEN cDNA 1700021K14 gene
AI465514	Myeloid/lymphoid or mixed-lineage leukemia 5
AI835010	
AI837046	F-box protein 46
AI837334	RIKEN cDNA 2700089E24 gene
AI837350	FYVE, RhoGEF and PH domain variant beta
AI837947	Leucine rich repeat containing 17
AI838219	
AI838523	Expressed sequence AI480556
AI838784	Transmembrane 9 superfamily member 2
AI840489	keratin complex 2, basic, gene 1
AI840703	
AI841124	SEC14-like 1 (S. cerevisiae)
AI841151	Proteolipid protein (myelin) 1
AI841247	Praja 2, RING-H2 motif containing transcript variant 2
AI841303	Growth associated protein 43
AI841402	Rb1cc1 mRNA for transcription factor
AI841516	Ankyrin 3, epithelial transcript variant 2
AI841957	Gamma-aminobutyric acid (GABA-A) receptor, subunit alpha 6
AI842610	Translin
AI843104	DEAD/H (Asp-Glu-Ala-Asp/His) box polypeptide 3, X-linked
AI843407	Islet cell autoantigen1
AI843517	Mortality factor 4 like 1
AI843601	Acyl-CoA synthetase long-chain family member 3
AI843834	Proteolipid protein (myelin) 1
AI844164	Chondroitin sulfate proteoglycan 6
AI844866	Zinc finger, A20 domain containing 2
AI844957	5'-3' exoribonuclease 1
AI845128	dynein light chain Tctex-type 3
AI845231	Gamma-glutamyl carboxylase
AI845319	Lamin A, transcript variant 1
AI845387	N-ethylmaleimide sensitive fusion protein attachment beta
AI845446	PDZ and LIM domain 7
AI845630	
AI846136	Immunoglobulin superfamily, member 4
AI846333	ZW10 interactor

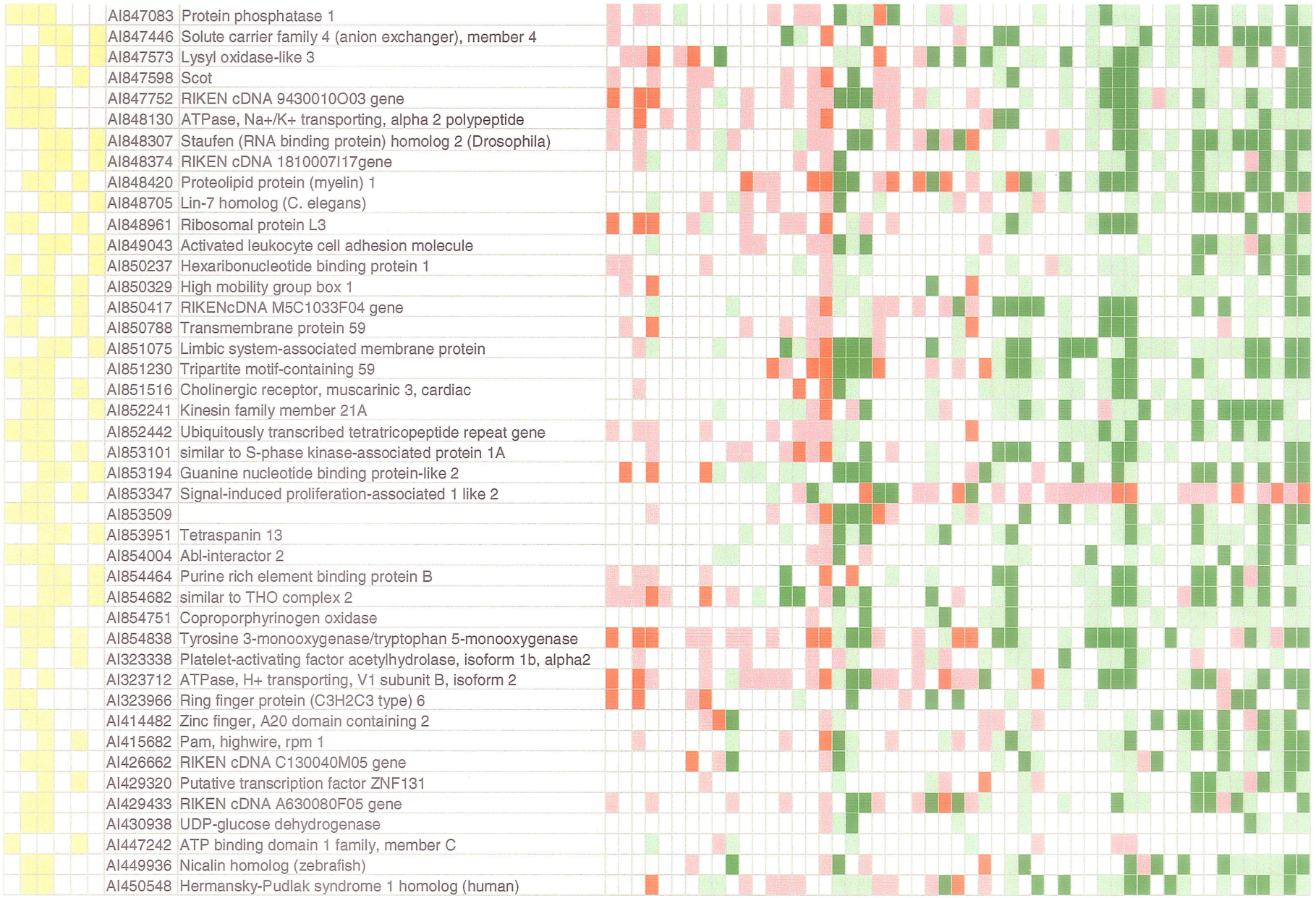

AI847083	Protein phosphatase 1
AI847446	Solute carrier family 4 (anion exchanger), member 4
AI847573	Lysyl oxidase-like 3
AI847598	Scot
AI847752	RIKEN cDNA 9430010O03 gene
AI848130	ATPase, Na+/K+ transporting, alpha 2 polypeptide
AI848307	Staufen (RNA binding protein) homolog 2 (Drosophila)
AI848374	RIKEN cDNA 1810007I17gene
AI848420	Proteolipid protein (myelin) 1
AI848705	Lin-7 homolog (C. elegans)
AI848961	Ribosomal protein L3
AI849043	Activated leukocyte cell adhesion molecule
AI850237	Hexaribonucleotide binding protein 1
AI850329	High mobility group box 1
AI850417	RIKENcDNA M5C1033F04 gene
AI850788	Transmembrane protein 59
AI851075	Limbic system-associated membrane protein
AI851230	Tripartite motif-containing 59
AI851516	Cholinergic receptor, muscarinic 3, cardiac
AI852241	Kinesin family member 21A
AI852442	Ubiquitously transcribed tetratricopeptide repeat gene
AI853101	similar to S-phase kinase-associated protein 1A
AI853194	Guanine nucleotide binding protein-like 2
AI853347	Signal-induced proliferation-associated 1 like 2
AI853509	
AI853951	Tetraspanin 13
AI854004	Abl-interactor 2
AI854464	Purine rich element binding protein B
AI854682	similar to THO complex 2
AI854751	Coproporphyrinogen oxidase
AI854838	Tyrosine 3-monooxygenase/tryptophan 5-monooxygenase
AI323338	Platelet-activating factor acetylhydrolase, isoform 1b, alpha2
AI323712	ATPase, H+ transporting, V1 subunit B, isoform 2
AI323966	Ring finger protein (C3H2C3 type) 6
AI414482	Zinc finger, A20 domain containing 2
AI415682	Pam, highwire, rpm 1
AI426662	RIKEN cDNA C130040M05 gene
AI429320	Putative transcription factor ZNF131
AI429433	RIKEN cDNA A630080F05 gene
AI430938	UDP-glucose dehydrogenase
AI447242	ATP binding domain 1 family, member C
AI449936	Nicalin homolog (zebrafish)
AI450548	Hermansky-Pudlak syndrome 1 homolog (human)

AI451417	Nemo like kinase
AI452022	Forkhead/winged-helix transcription factor 2
AI465262	Four jointed box 1 (Drosophila)
AI465279	DNA segment, Chr 10, Wayne State Uni 102, expressed
AI661042	Receptor interacting protein kinase 5
AI662428	teashirt zinc finger family member 1
AI834985	RIKEN cDNA 1810007I17 gene
AI835419	Phosphatidic acid phosphatase type 2B
AI836312	Peroxiredoxin 3
AI836414	Protease, serine, 32
AI836546	Voltage-dependent anion channel 2
AI836854	Spinocerebellar ataxia 10 homolog (human)
AI837233	RIKEN cDNA 1110049F12 gene
AI837528	Janus kinase 1
AI837621	Tetraspanin 13
AI837858	Acid phosphatase 1, soluble
AI837903	RAB guanine nucleotide exchange factor (GEF) 1
AI838117	General transcription factor II H, polypeptide 1
AI838257	Wiskott-Aldrich syndrome-like (human)
AI838957	S-phase kinase-associated protein 1A
AI839071	RNA binding motif protein 5
AI839343	Phytanoyl-CoA hydroxylase
AI839561	ATPase, H+ transporting, V1 subunit C, isoform 1
AI839745	Proteolipid protein (myelin) 1
AI839821	ADP-ribosylation factor 2
AI839865	Gamma-aminobutyric acid (GABA-A) receptor, subunit alpha 6
AI839932	Heat shock Protein 90kDa alpha, class A member 1
AI840046	whn-dependent transcript 3
AI840089	similar to Splicing factor, arginine/serine-rich 3
AI840225	Proteasome 26S subunit, non-ATPase, 11
AI840598	DNA segment, Chr 10, ERATO Doi 641, expressed
AI840661	MRNA fragment for elongation factor TU (N-terminus)
AI841298	RIKEN cDNA 1500031H04 gene
AI841419	Growth associated protein 43
AI841427	CDNA sequence BC003885
AI841927	UBX domain containing 2
AI842095	S-adenosylhomocysteine hydrolase-like 1
AI842279	Integral membrane protein 2A
AI842293	Palmitoylated membrane anchor R7BP
AI842479	NECAP endocytosis associated 1
AI842623	Nuclear receptor interacting protein 3
AI842964	Protein phosphatase 2a, catalytic subunit, alpha isoform

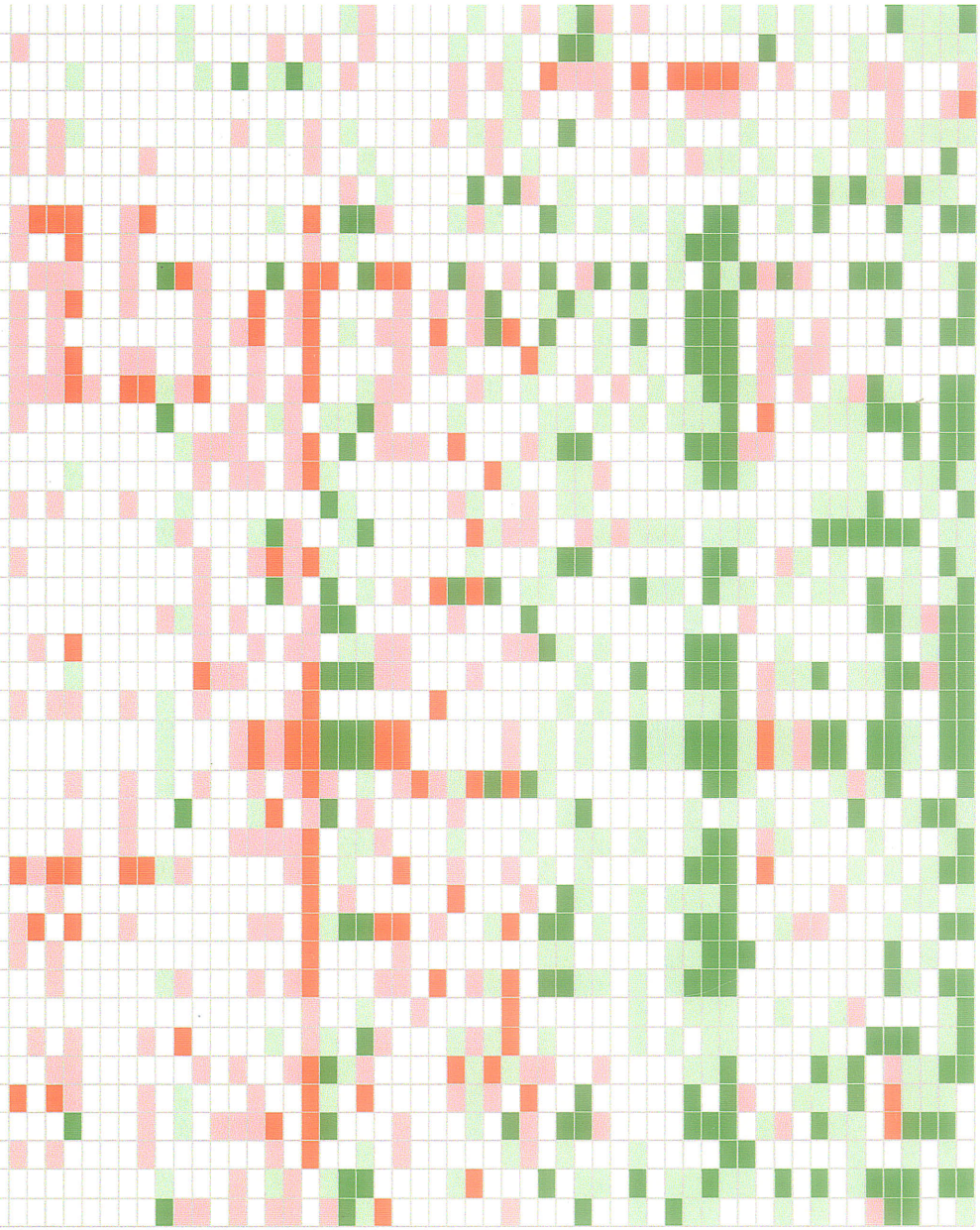

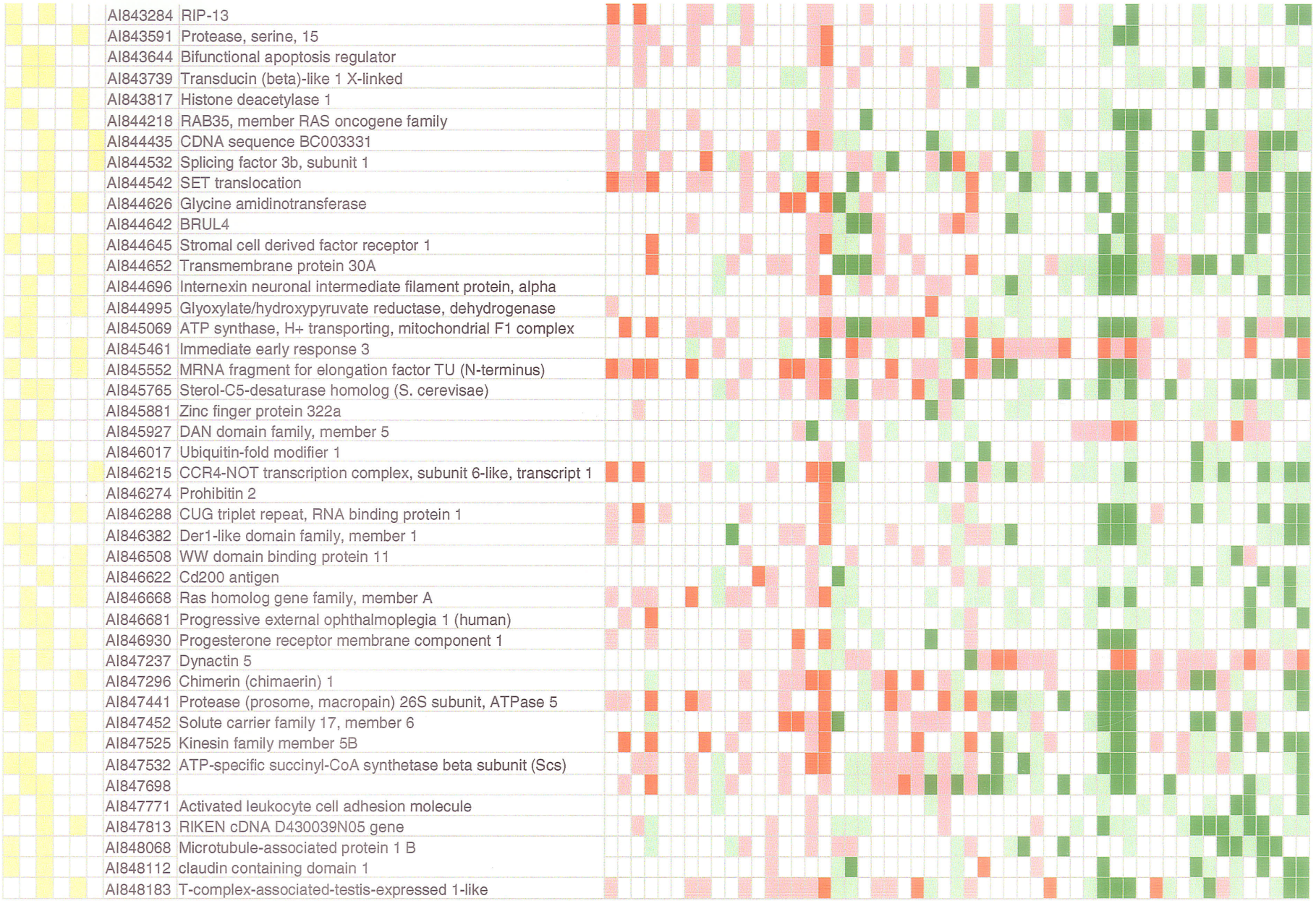

AI843284	RIP-13
AI843591	Protease, serine, 15
AI843644	Bifunctional apoptosis regulator
AI843739	Transducin (beta)-like 1 X-linked
AI843817	Histone deacetylase 1
AI844218	RAB35, member RAS oncogene family
AI844435	CDNA sequence BC003331
AI844532	Splicing factor 3b, subunit 1
AI844542	SET translocation
AI844626	Glycine amidinotransferase
AI844642	BRUL4
AI844645	Stromal cell derived factor receptor 1
AI844652	Transmembrane protein 30A
AI844696	Internexin neuronal intermediate filament protein, alpha
AI844995	Glyoxylate/hydroxypyruvate reductase, dehydrogenase
AI845069	ATP synthase, H+ transporting, mitochondrial F1 complex
AI845461	Immediate early response 3
AI845552	MRNA fragment for elongation factor TU (N-terminus)
AI845765	Sterol-C5-desaturase homolog (S. cerevisae)
AI845881	Zinc finger protein 322a
AI845927	DAN domain family, member 5
AI846017	Ubiquitin-fold modifier 1
AI846215	CCR4-NOT transcription complex, subunit 6-like, transcript 1
AI846274	Prohibitin 2
AI846288	CUG triplet repeat, RNA binding protein 1
AI846382	Der1-like domain family, member 1
AI846508	WW domain binding protein 11
AI846622	Cd200 antigen
AI846668	Ras homolog gene family, member A
AI846681	Progressive external ophthalmoplegia 1 (human)
AI846930	Progesterone receptor membrane component 1
AI847237	Dynactin 5
AI847296	Chimerin (chimaerin) 1
AI847441	Protease (prosome, macropain) 26S subunit, ATPase 5
AI847452	Solute carrier family 17, member 6
AI847525	Kinesin family member 5B
AI847532	ATP-specific succinyl-CoA synthetase beta subunit (Scs)
AI847698	
AI847771	Activated leukocyte cell adhesion molecule
AI847813	RIKEN cDNA D430039N05 gene
AI848068	Microtubule-associated protein 1 B
AI848112	claudin containing domain 1
AI848183	T-complex-associated-testis-expressed 1-like

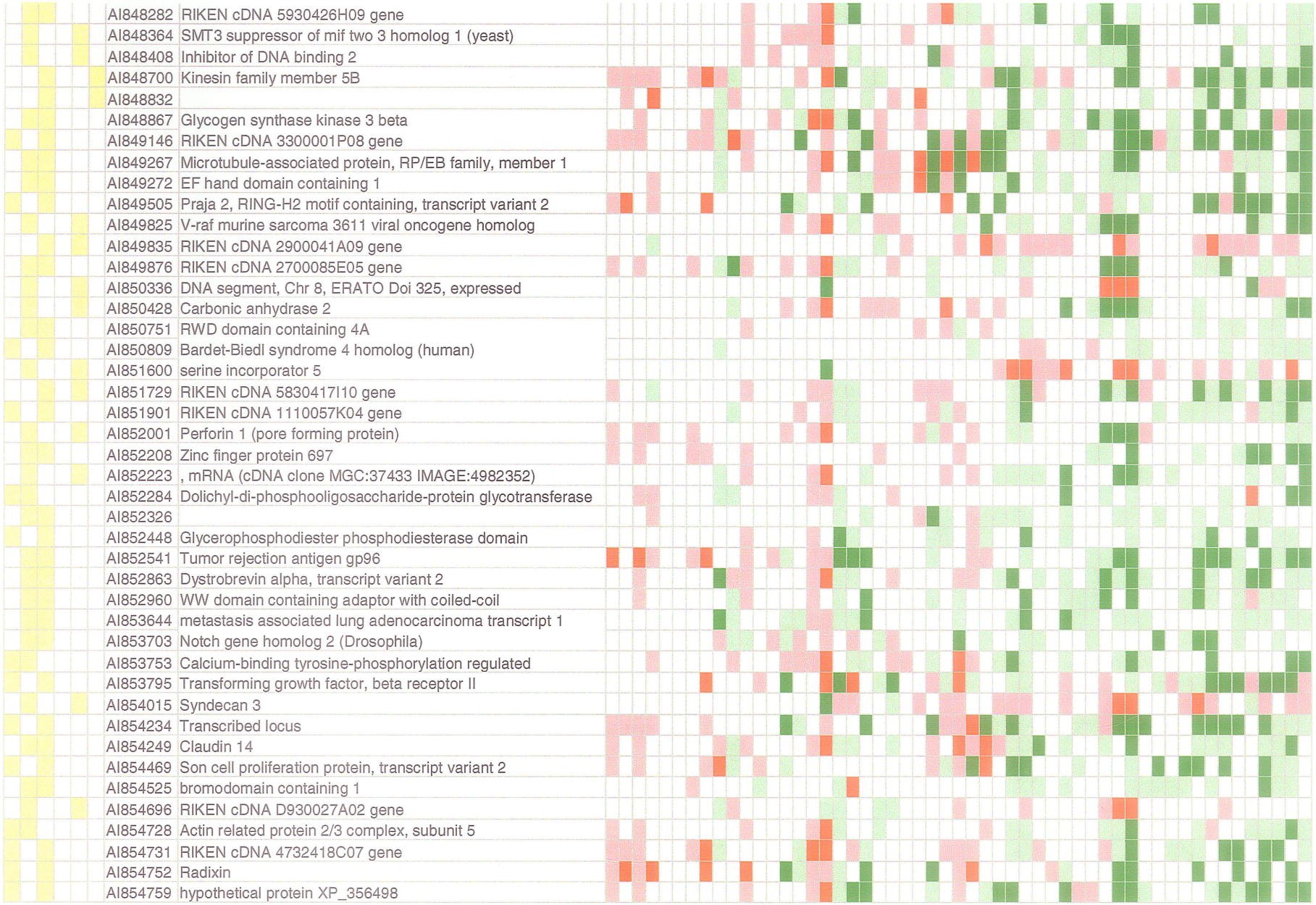

AI848282	RIKEN cDNA 5930426H09 gene
AI848364	SMT3 suppressor of mif two 3 homolog 1 (yeast)
AI848408	Inhibitor of DNA binding 2
AI848700	Kinesin family member 5B
AI848832	
AI848867	Glycogen synthase kinase 3 beta
AI849146	RIKEN cDNA 3300001P08 gene
AI849267	Microtubule-associated protein, RP/EB family, member 1
AI849272	EF hand domain containing 1
AI849505	Praja 2, RING-H2 motif containing, transcript variant 2
AI849825	V-raf murine sarcoma 3611 viral oncogene homolog
AI849835	RIKEN cDNA 2900041A09 gene
AI849876	RIKEN cDNA 2700085E05 gene
AI850336	DNA segment, Chr 8, ERATO Doi 325, expressed
AI850428	Carbonic anhydrase 2
AI850751	RWD domain containing 4A
AI850809	Bardet-Biedl syndrome 4 homolog (human)
AI851600	serine incorporator 5
AI851729	RIKEN cDNA 5830417I10 gene
AI851901	RIKEN cDNA 1110057K04 gene
AI852001	Perforin 1 (pore forming protein)
AI852208	Zinc finger protein 697
AI852223	, mRNA (cDNA clone MGC:37433 IMAGE:4982352)
AI852284	Dolichyl-di-phosphooligosaccharide-protein glycotransferase
AI852326	
AI852448	Glycerophosphodiester phosphodiesterase domain
AI852541	Tumor rejection antigen gp96
AI852863	Dystrobrevin alpha, transcript variant 2
AI852960	WW domain containing adaptor with coiled-coil
AI853644	metastasis associated lung adenocarcinoma transcript 1
AI853703	Notch gene homolog 2 (Drosophila)
AI853753	Calcium-binding tyrosine-phosphorylation regulated
AI853795	Transforming growth factor, beta receptor II
AI854015	Syndecan 3
AI854234	Transcribed locus
AI854249	Claudin 14
AI854469	Son cell proliferation protein, transcript variant 2
AI854525	bromodomain containing 1
AI854696	RIKEN cDNA D930027A02 gene
AI854728	Actin related protein 2/3 complex, subunit 5
AI854731	RIKEN cDNA 4732418C07 gene
AI854752	Radixin
AI854759	hypothetical protein XP_356498

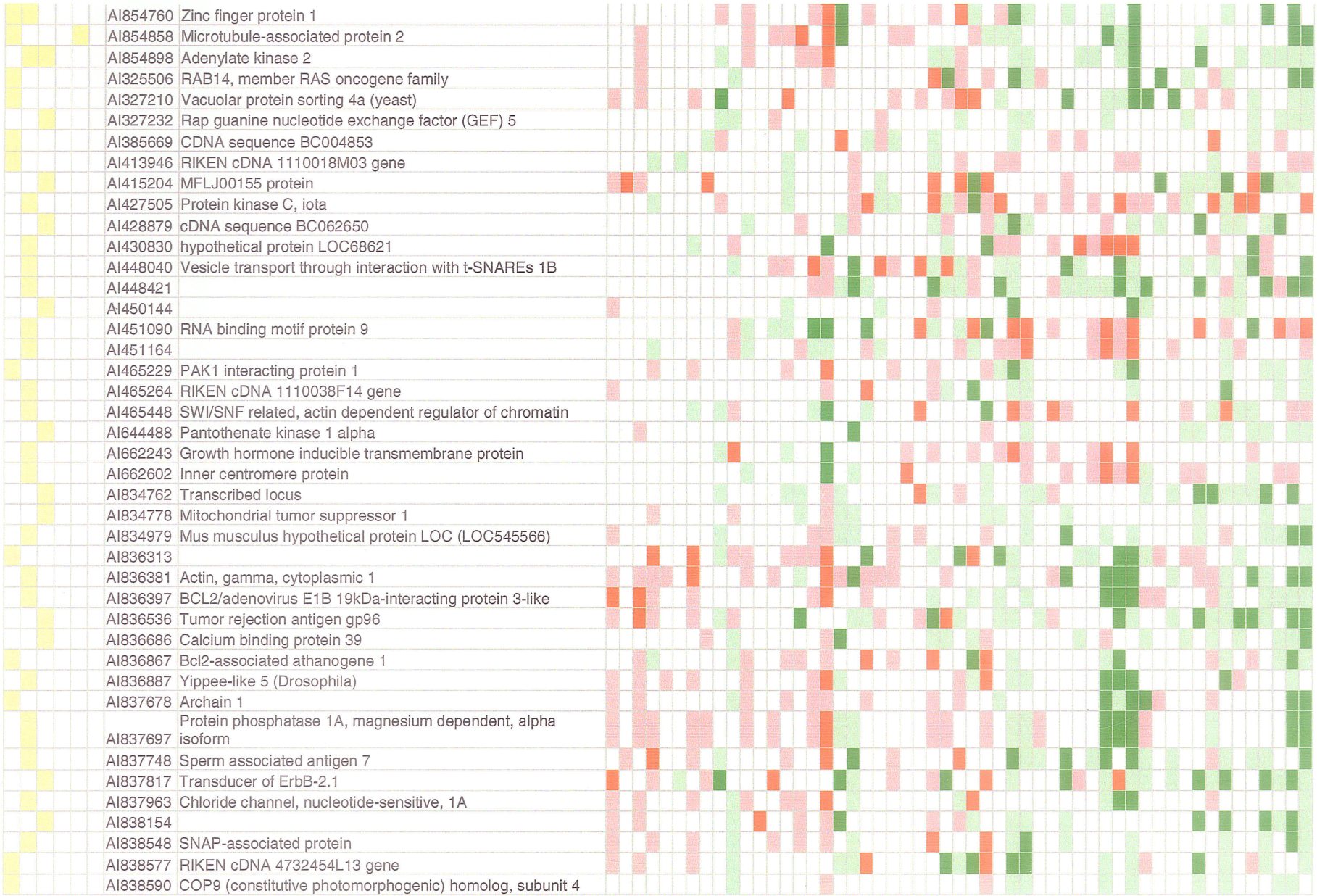

AI854760	Zinc finger protein 1
AI854858	Microtubule-associated protein 2
AI854898	Adenylate kinase 2
AI325506	RAB14, member RAS oncogene family
AI327210	Vacuolar protein sorting 4a (yeast)
AI327232	Rap guanine nucleotide exchange factor (GEF) 5
AI385669	CDNA sequence BC004853
AI413946	RIKEN cDNA 1110018M03 gene
AI415204	MFLJ00155 protein
AI427505	Protein kinase C, iota
AI428879	cDNA sequence BC062650
AI430830	hypothetical protein LOC68621
AI448040	Vesicle transport through interaction with t-SNAREs 1B
AI448421	
AI450144	
AI451090	RNA binding motif protein 9
AI451164	
AI465229	PAK1 interacting protein 1
AI465264	RIKEN cDNA 1110038F14 gene
AI465448	SWI/SNF related, actin dependent regulator of chromatin
AI644488	Pantothenate kinase 1 alpha
AI662243	Growth hormone inducible transmembrane protein
AI662602	Inner centromere protein
AI834762	Transcribed locus
AI834778	Mitochondrial tumor suppressor 1
AI834979	Mus musculus hypothetical protein LOC (LOC545566)
AI836313	
AI836381	Actin, gamma, cytoplasmic 1
AI836397	BCL2/adenovirus E1B 19kDa-interacting protein 3-like
AI836536	Tumor rejection antigen gp96
AI836686	Calcium binding protein 39
AI836867	Bcl2-associated athanogene 1
AI836887	Yippee-like 5 (Drosophila)
AI837678	Archain 1
AI837697	Protein phosphatase 1A, magnesium dependent, alpha isoform
AI837748	Sperm associated antigen 7
AI837817	Transducer of ErbB-2.1
AI837963	Chloride channel, nucleotide-sensitive, 1A
AI838154	
AI838548	SNAP-associated protein
AI838577	RIKEN cDNA 4732454L13 gene
AI838590	COP9 (constitutive photomorphogenic) homolog, subunit 4

AI838596	CDNA, clone:Y2G0146G10, strand:unspecified
AI838676	Mus musculus similar to zeta proteasome chain (LOC545687)
AI838762	Hemoglobin, beta adult major chain
AI839281	
AI839319	U2AF homology motif (UHM) kinase 1
AI839355	PCTAIRE-motif protein kinase 1
AI839722	Enolase 1, alpha non-neuron
AI839729	Bromodomain containing 2, transcript variant 1
AI839975	Makorin, ring finger protein, 2
AI840023	strongly similar to NP_036732.1 malic enzyme 1
AI840088	Replication protein A2
AI840155	Calcium activated nucleotidase 1
AI840227	similar to mCDC47
AI840232	Secreted acidic cysteine rich glycoprotein
AI840266	Hypothetical protein E130311K13 (E130311K13)
AI840347	
AI840523	
AI840647	Oxysterol binding protein-like 1A
AI840802	5'-3' exoribonuclease 2
AI841105	Nucleophosmin 1
AI841345	Tyrosine 3-monooxygenase/tryptophan 5-monooxygenase
AI841346	Glutathione S-transferase, mu 1
AI841349	Selenoprotein
AI841440	RIKEN cDNA 3300001P08 gene
AI841469	Protein-L-isoaspartate (D-aspartate) O-methyltransferase 1
AI841577	Heat shock protein 9A
AI841759	Matrin 3
AI841804	Expressed in non-metastatic cells 1, protein
AI842167	RIKEN cDNA 9430036N22 gene
AI842169	Adenylate kinase 3
AI842307	Rho GTPase activating protein 23
AI842699	SM-11044 binding protein, transcript variant 1
AI842875	Glycogen synthase kinase 3 beta
AI842933	Acid phosphatase 2, lysosomal
AI843125	
AI843133	SFT2 domain containing 3
AI843378	Dynein cytoplasmic 1 intermediate chain 2
AI843451	Eukaryotic translation elongation factor 1 alpha 1
AI843578	Splicing factor, arginine/serine-rich 11
AI843621	
AI843699	Islet cell autoantigen1
AI843750	Tumor protein D52-like 1
AI843768	Amyloid beta (A4) precursor protein

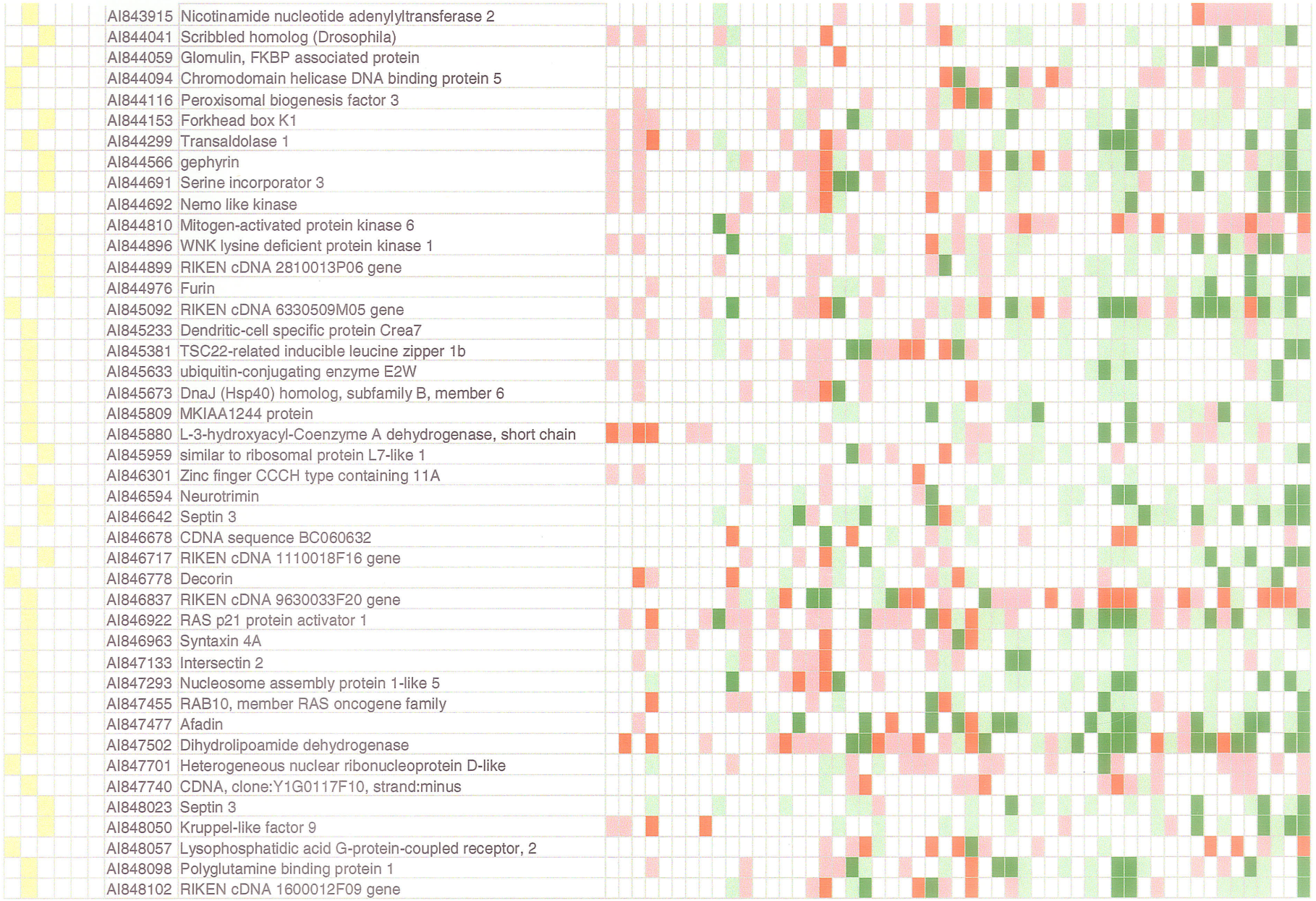

AI843915	Nicotinamide nucleotide adenylyltransferase 2
AI844041	Scribbled homolog (Drosophila)
AI844059	Glomulin, FKBP associated protein
AI844094	Chromodomain helicase DNA binding protein 5
AI844116	Peroxisomal biogenesis factor 3
AI844153	Forkhead box K1
AI844299	Transaldolase 1
AI844566	gephyrin
AI844691	Serine incorporator 3
AI844692	Nemo like kinase
AI844810	Mitogen-activated protein kinase 6
AI844896	WNK lysine deficient protein kinase 1
AI844899	RIKEN cDNA 2810013P06 gene
AI844976	Furin
AI845092	RIKEN cDNA 6330509M05 gene
AI845233	Dendritic-cell specific protein Crea7
AI845381	TSC22-related inducible leucine zipper 1b
AI845633	ubiquitin-conjugating enzyme E2W
AI845673	DnaJ (Hsp40) homolog, subfamily B, member 6
AI845809	MKIAA1244 protein
AI845880	L-3-hydroxyacyl-Coenzyme A dehydrogenase, short chain
AI845959	similar to ribosomal protein L7-like 1
AI846301	Zinc finger CCCH type containing 11A
AI846594	Neurotrimin
AI846642	Septin 3
AI846678	CDNA sequence BC060632
AI846717	RIKEN cDNA 1110018F16 gene
AI846778	Decorin
AI846837	RIKEN cDNA 9630033F20 gene
AI846922	RAS p21 protein activator 1
AI846963	Syntaxin 4A
AI847133	Intersectin 2
AI847293	Nucleosome assembly protein 1-like 5
AI847455	RAB10, member RAS oncogene family
AI847477	Afadin
AI847502	Dihydrolipoamide dehydrogenase
AI847701	Heterogeneous nuclear ribonucleoprotein D-like
AI847740	CDNA, clone:Y1G0117F10, strand:minus
AI848023	Septin 3
AI848050	Kruppel-like factor 9
AI848057	Lysophosphatidic acid G-protein-coupled receptor, 2
AI848098	Polyglutamine binding protein 1
AI848102	RIKEN cDNA 1600012F09 gene

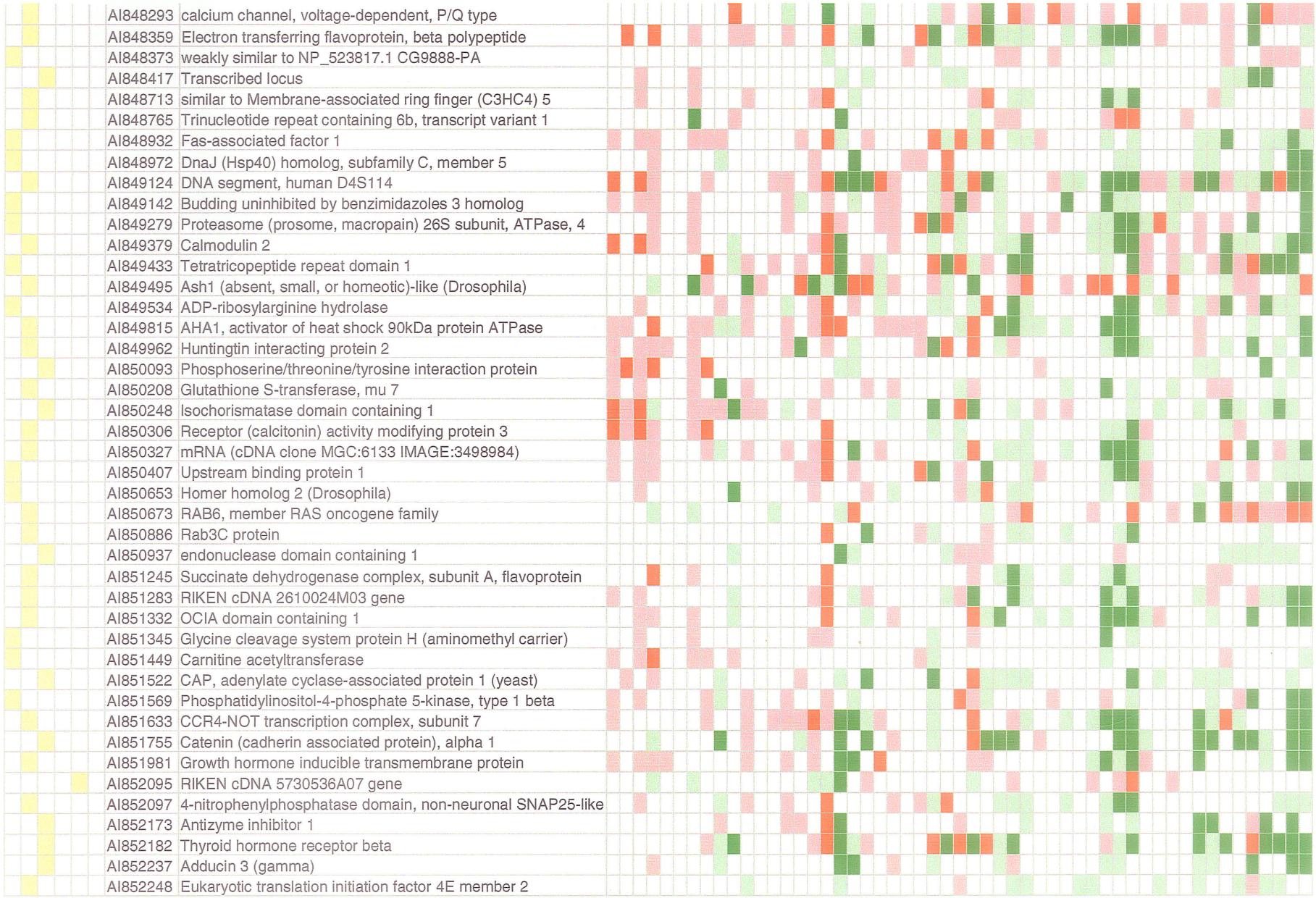

AI848293	calcium channel, voltage-dependent, P/Q type
AI848359	Electron transferring flavoprotein, beta polypeptide
AI848373	weakly similar to NP_523817.1 CG9888-PA
AI848417	Transcribed locus
AI848713	similar to Membrane-associated ring finger (C3HC4) 5
AI848765	Trinucleotide repeat containing 6b, transcript variant 1
AI848932	Fas-associated factor 1
AI848972	DnaJ (Hsp40) homolog, subfamily C, member 5
AI849124	DNA segment, human D4S114
AI849142	Budding uninhibited by benzimidazoles 3 homolog
AI849279	Proteasome (prosome, macropain) 26S subunit, ATPase, 4
AI849379	Calmodulin 2
AI849433	Tetratricopeptide repeat domain 1
AI849495	Ash1 (absent, small, or homeotic)-like (Drosophila)
AI849534	ADP-ribosylarginine hydrolase
AI849815	AHA1, activator of heat shock 90kDa protein ATPase
AI849962	Huntingtin interacting protein 2
AI850093	Phosphoserine/threonine/tyrosine interaction protein
AI850208	Glutathione S-transferase, mu 7
AI850248	Isochorismatase domain containing 1
AI850306	Receptor (calcitonin) activity modifying protein 3
AI850327	mRNA (cDNA clone MGC:6133 IMAGE:3498984)
AI850407	Upstream binding protein 1
AI850653	Homer homolog 2 (Drosophila)
AI850673	RAB6, member RAS oncogene family
AI850886	Rab3C protein
AI850937	endonuclease domain containing 1
AI851245	Succinate dehydrogenase complex, subunit A, flavoprotein
AI851283	RIKEN cDNA 2610024M03 gene
AI851332	OCIA domain containing 1
AI851345	Glycine cleavage system protein H (aminomethyl carrier)
AI851449	Carnitine acetyltransferase
AI851522	CAP, adenylate cyclase-associated protein 1 (yeast)
AI851569	Phosphatidylinositol-4-phosphate 5-kinase, type 1 beta
AI851633	CCR4-NOT transcription complex, subunit 7
AI851755	Catenin (cadherin associated protein), alpha 1
AI851981	Growth hormone inducible transmembrane protein
AI852095	RIKEN cDNA 5730536A07 gene
AI852097	4-nitrophenylphosphatase domain, non-neuronal SNAP25-like
AI852173	Antizyme inhibitor 1
AI852182	Thyroid hormone receptor beta
AI852237	Adducin 3 (gamma)
AI852248	Eukaryotic translation initiation factor 4E member 2

AI852447	RIKEN cDNA 2310011J03 gene
AI852538	Glycogenin 1
AI852638	Spastic paraplegia 3A homolog (human)
AI852812	Metastasis suppressor 1
AI852907	CCAAT/enhancer binding protein (C/EBP), gamma
AI853150	D-dopachrome tautomerase
AI853192	ATP synthase, H+ transporting, mitochondrial F1 complex
AI853232	RIKEN cDNA 2900026A02 gene
AI853420	Ring finger protein 146
AI853439	Archain 1
AI853538	Survival motor neuron domain containing 1
AI853599	Groucho-related protein 4
AI853672	AT rich interactive domain 1B (Swi1 like)
AI853685	RIKEN cDNA D330037H05 gene
AI853686	Glutamate receptor, ionotropic, AMPA3 (alpha 3)
AI853698	LUC7-like 2 (S. cerevisiae)
AI853755	RIKEN cDNA 4933431E20 gene
AI854269	RIKEN cDNA 5730419I09 gene
AI854524	Solute carrier family 15, member 3
AI854567	Smu-1 suppressor of mec-8 and unc-52 homolog (C. elegans)
AI854630	Eph receptor A5
AI854632	Angel homolog 2 (Drosophila)
AI854701	Sterile alpha motif domain containing 4
AI854743	Adenylate kinase 3
AI854765	PDZ domain containing 11
AI854804	FSHD region gene 1
AI854835	Tripartite motif-containing 59
AI854866	RIKEN cDNA 1700019D03 gene
AI854874	ATPase, Ca++ transporting, plasma membrane 2
AI893653	Chromobox homolog 5 (Drosophila HP1a)
AI840147	AT rich interactive domain 4B (Rbp1 like)
AI843116	3-hydroxy-3-methylglutaryl-Coenzyme A synthase 1
AI848255	RIKEN cDNA 5730403B10 gene
AI850004	Dynactin 3
AI850505	RIKEN cDNA 4931428D14 gene
AI850733	RIKEN cDNA D530033C11 gene

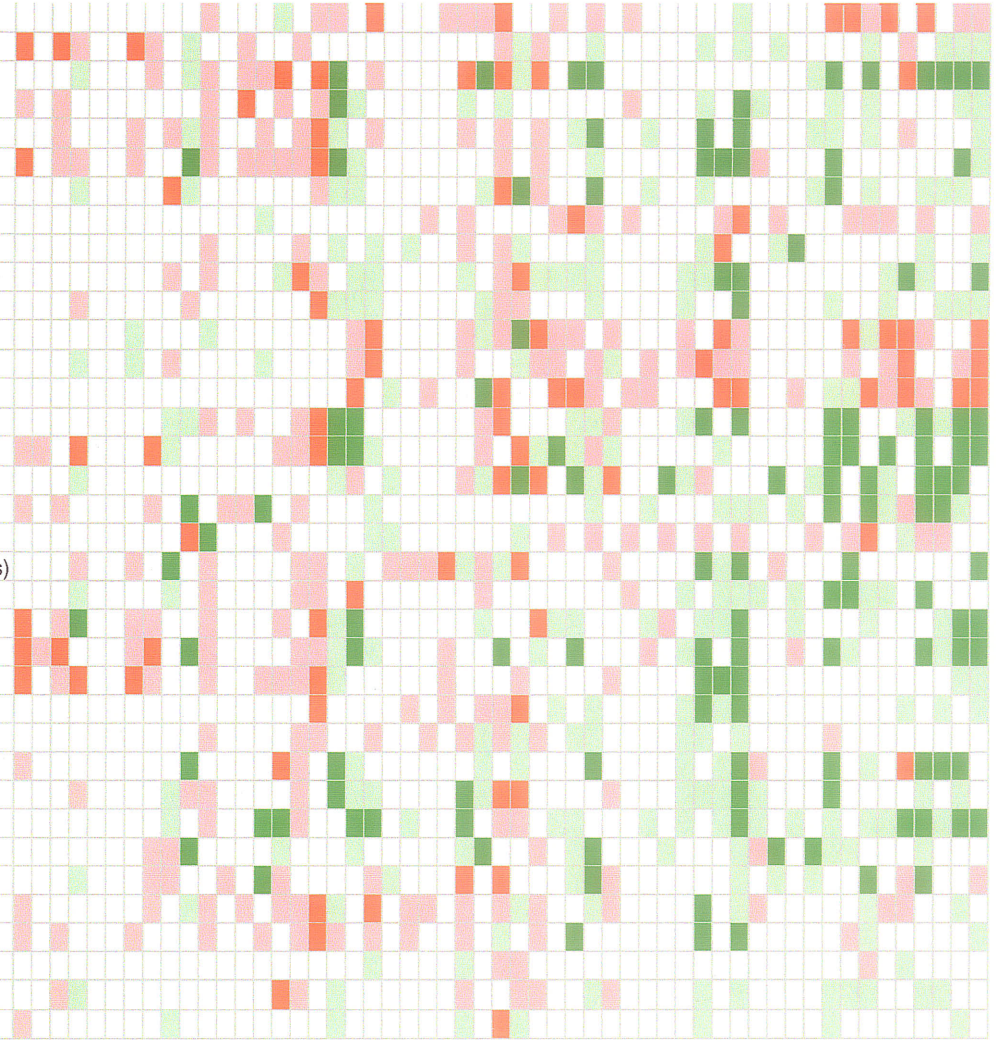

3.6.6 Functional Analysis

The 187 significant genes from experimental data set were inputted into the Expression Analysis Systematic Explorer (EASE). EASE is a program that processes a list of genes into biologically themed groups. It functions by looking at over-representation analysis of functional gene categories. EASE first maps the gene identifiers to a standardized gene accession system and then maps the genes to biological categories. Removing one gene within the given category from the list and calculating the resulting Fisher exact probability for that category calculated the EASE score. The EASE score favours more robust categories than the Fisher exact probability because it represents the lower bound of all possible jackknife probabilities. It also has advantages in terms of penalizing the significance of categories supported by few genes. Table 4 shows the EASE table for selected biological themes.

All 497 genes listed in table 3 were analyzed using the Database for Annotation, Visualization and Integrated Discovery 2.1 (DAVID) software. The functional classification tool was used. This method groups genes based on their functional similarity. It was used to enhance the biological interpretation of the list of genes.

It uses cluster algorithms to classify similar genes into functionally related groups. A heat map visualization of gene-to-term relationships (figure 16) is used to demonstrate the global view of the cluster associations. From this analysis five functional groups were chosen that best represented the changes

Table 4. List of EASE functional gene categories that were found by over-representation analysis.

Gene Category	List Hits	List Total	Population Hits	Population Total	EASE score
cellular process	37	67	45	97	1.58E-02
nucleotide binding	18	72	20	106	4.60E-02
purine nucleotide binding	18	72	20	106	4.60E-02
cytoplasm	30	67	38	99	8.14E-02
ATP binding	15	72	17	106	1.15E-01
adenyl nucleotide binding	15	72	17	106	1.15E-01
intracellular transport	9	67	9	97	1.50E-01
transport	17	67	20	97	1.54E-01
protein metabolism	19	67	23	97	1.72E-01
cell growth and/or maintenance	28	67	36	97	1.84E-01
catalytic activity	28	72	37	106	2.30E-01
cell	63	67	91	99	2.51E-01
transferase activity	12	72	14	106	2.52E-01
transporter activity	12	72	14	106	2.52E-01
cell communication	17	67	21	97	2.65E-01
physiological process	57	67	80	97	2.66E-01
intracellular protein transport	7	67	7	97	2.80E-01
protein transport	7	67	7	97	2.80E-01

Figure 16. Functional analysis heat map using DAVID software. This heat map visualization shows a global view of cluster-to-cluster relationships.

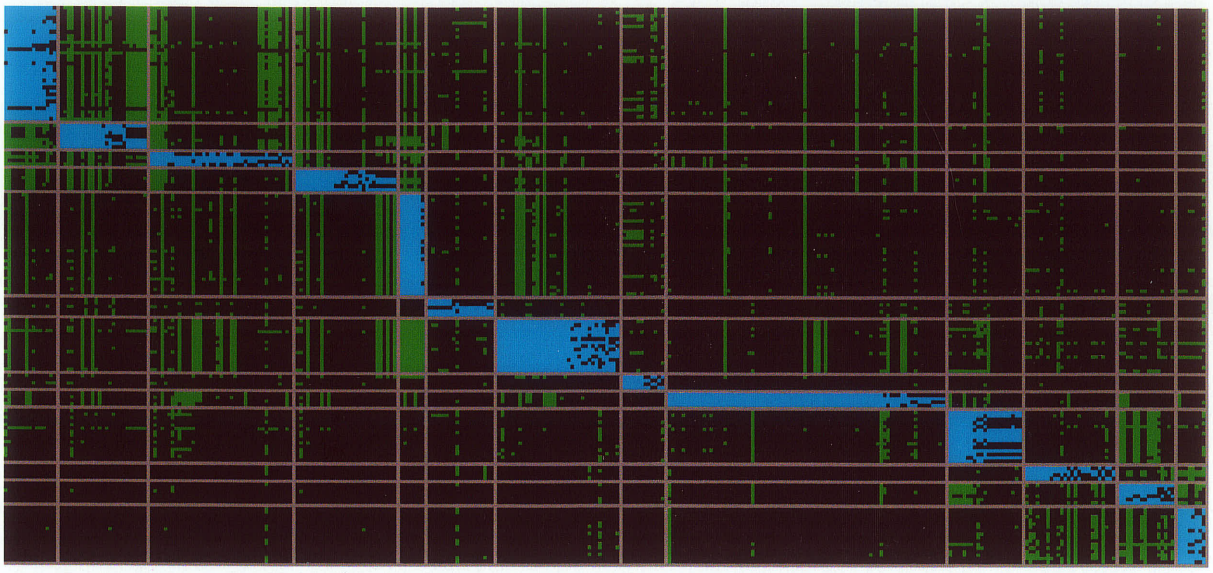

seen during the course of HSE (immune response, apoptosis, CNS specific, actin/microtubule and cellular protein metabolism). A truncated version of the expression of genes in these groups is in Table 5.

3.7 Antibody Arrays

Antibody arrays were analyzed in the same manner as the above-mentioned microarray experiments. SAM (figure 17) and the quadratic regression model (figure 18) were the only two programs to yield significant proteins. These experiments were used to corroborate microarray findings. It was difficult to compare the findings from the antibody array and microarray data since very few immune response genes were on the microarray slide and a much larger percentage were found on the antibody arrays. The proteins listed in Table 6 and Table 7 were found to be significant by SAM analysis and quadratic regression analysis respectively.

3.8 Real Time PCR

Real time PCR was used to confirm the microarray gene expression patterns for a selection of genes. Genes were selected due to a significant increase or decrease in gene expression based on microarray data (Table 8). The fold changes seen in the microarray analysis was compared to the fold changes observed in the relative quantification of the real time PCR data. The relative quantification is the normalized gene expression value on a base 2 scale ($2^{-\Delta\Delta Ct}$).

Table 5. Significant genes divided into functional groupings.

			Immune Response
AI426310	17174	Masp 1	Mannan-binding serine peptidase 1
AI452233	54390	Sit1	Suppression inducing transmembrane adaptor 1
AI838257	73178	Wasl	Wiskott-Aldrich syndrome-like (human)
AI839932	15519	Hsp90aa1	Heat shock Protein 90kDa alpha (cytosolic), class A member 1
AI844059	170823	Glmn	Glomulin, FKBP associated protein
AI852638	73991	Spg3a	Spastic paraplegia 3A homolog (human)
			Apoptosis
AI849146	67684		
AI836867	12017	Bag1	Bcl2-associated athanogene 1
AI839589	22628	Ywhag	3-monooxygenase/tryptophan 5-monooxygenase activation protein, gamma polypeptide
AI841440	67684		
AI843644	67118	Bfar	Bifunctional apoptosis regulator
AI843768	11820	App	Amyloid beta (A4) precursor protein
AI844691	26943	Serinc3	Serine incorporator 3
AI847745	19211	Pten	Phosphatase and tensin homolog
AI848364	22218	Sumo1	SMT3 suppressor of mif two 3 homolog 1 (yeast)
AI848867	56637	Gsk3b	Glycogen synthase kinase 3 beta
AI848932	14084	Faf1	Fas-associated factor 1
AI852001	18646	Prf1	Perforin 1 (pore forming protein)
AI853538	76479	Smndc1	Survival motor neuron domain containing 1
AI853703	18129	Notch2	Notch gene homolog 2 (Drosophila)
			CNS Specific
AI323897	50876	Tmod2	Tropomodulin 2
AI327232	217944	Rapgef5	Rap guanine nucleotide exchange factor (GEF) 5
AI448344	109934	Abr	Active BCR-related gene
AI838548	20615	Snapap	SNAP-associated protein
AI839589	22628	Ywhag	3-monooxygenase/tryptophan 5-monooxygenase activation protein, gamma polypeptide
AI839745	18823	Plp1	Proteolipid protein (myelin) 1
AI839865	14399	Gabra6	Gamma-aminobutyric acid (GABA-A) receptor, subunit alpha 6
AI841151	18823	Plp1	Proteolipid protein (myelin) 1
AI841303	14432	Gap43	Growth associated protein 43
AI841419	14432	Gap43	Growth associated protein 43
AI841957	14399	Gabra6	Gamma-aminobutyric acid (GABA-A) receptor, subunit alpha 6
AI843407	15893	Ica1	Islet cell autoantigen1
AI843699	15893	Ica1	Islet cell autoantigen1
AI843834	18823	Plp1	Proteolipid protein (myelin) 1
AI844696	226180	Ina	Internexin neuronal intermediate filament protein, alpha
AI846963	20909	Stx4a	Syntaxin 4A (placental)
AI847452	140919	Slc17a6	Solute carrier family 17 (sodium-dependent inorganic phosphate co transporter), member 6
AI847745	19211	Pten	Phosphatase and tensin homolog

AI848068	17755	Mtap1b	Microtubule-associated protein 1 B
AI848130	98660	Atp1a2	ATPase, Na+/K+ transporting, alpha 2 polypeptide
AI848420	18823	Plp1	Proteolipid protein (myelin) 1
AI848705	108030	Lin7a	Lin-7 homolog (C. elegans)
AI850809	102774	Bbs4	Bardet-Biedl syndrome 4 homolog (human)
AI851516	12671	Chrm3	Cholinergic receptor, muscarinic 3, cardiac
AI852812	211401	Mtss	Metastasis suppressor 1
AI853686	53623	Gria	Glutamate receptor, ionotropic, AMPA3 (alpha 3)
AI853703	18129	Notch2	Notch gene homolog 2 (Drosophila)
AI854858	17756	Mtap2	Microtubule-associated protein 2
			Actin/Microtubule
AI323897	50876	Tmod2	Tropomodulin 2
AI427505	18759	Prkci	Protein kinase C, iota
AI450315	54004	Diap2	Diaphanous homolog 2 (Drosophila)
AI838257	73178	Wasl	Wiskott-Aldrich syndrome-like (human)
AI840802	24128	Xrn2	5'-3' exoribonuclease 2
AI841105	18148	Npm1	Nucleophosmin 1
AI843378	13427	Dync1i2	Dynein cytoplasmic 1 intermediate chain 2
AI844094	269610	Chd5	Chromodomain helicase DNA binding protein 5
AI844164	13006	Cspg6	Chondroitin sulfate proteoglycan 6
AI846668	11848	Rhoa	Ras homolog gene family, member A
AI847525	16573	Kif5b	Kinesin family member 5B
AI848068	17755	Mtap1b	Microtubule-associated protein 1 B
AI848700	16573	Kif5b	Kinesin family member 5B
AI850004	53598	Dctn3	Dynactin 3
AI850809	102774	Bbs4	Bardet-Biedl syndrome 4 homolog (human)
AI852241	16564	Kif21a	Kinesin family member 21A
AI852812	211401	Mtss1	Metastasis suppressor 1
AI854728	67771	Arpc5	Actin related protein 2/3 complex, subunit 5
AI854858	17756	Mtap2	Microtubule-associated protein 2
			Cellular Protein Metabolism
AI323897	50876	Tmod2	Tropomodulin 2
AI414429	320011	Ugcgl1	UDP-glucose ceramide glucosyltransferase-like 1
AI414590	20817	Srpk2	Serine/arginine-rich protein specific kinase 2
AI415682	105689	Phr1	Pam, highwire, rpm 1
AI426310	17174	Masp 1	Mannan-binding serine peptidase 1
AI427505	18759	Prkci	Protein kinase C, iota
AI451417	18099	Nlk	Nemo like kinase
AI661042	213452	Ripk5	Receptor interacting protein kinase 5
AI836414	69814	Prss32	Protease, serine, 32
AI836536	22027	Hsp90b1	Heat shock protein 90kDa beta (Grp94), member 1
AI836867	12017	Bag1	Bcl2-associated athanogene 1
AI837528	16451	Jak1	Janus kinase 1
AI837697	19042	Ppm1a	Protein phosphatase 1A, magnesium dependent, alpha isoform
AI837858	11431	Acp1	Acid phosphatase 1, soluble
AI838689	19244	Ptp4a2	Protein tyrosine phosphatasee 4a2

AI838957	21402	Skp1a	S-phase kinase-associated protein 1A
AI839352	67155	Smarca2	SWI/SNF related, matrix associated, actin dependent regulator of chromatin, subfamily a, member 2
AI839355	18555	Pctk1	PCTAIRE-motif protein kinase 1
AI839932	15519	Hsp90aa1	Heat shock protein 90kDa alpha (cytosolic), class A member 1
AI839975	67027	Mkrn2	Makorin, ring finger protein, 2
AI840023	19896	Rpl10a	Ribosomal protein L10A
AI840661	13627	Eef1a1	Eukaryotic translation elongation factor 1 alpha 1
AI840993	71902	Cand1	Cullin associated and neddylation disassociated 1
AI841344	15519	Hsp90aa1	Heat shock protein 90kDa alpha (cytosolic), class A member 1
AI841427	18537	Pcmt1	Protein-L-isoapartate (D-aspartate) O-methytransferase 1
AI841469	18537	Pcmt1	Protein-L-isoapartate (D-aspartate) O-methytransferase 1
AI841577	15526	Hspa9a	Heat shock protein 9A
AI841884	108148	Galnt2	UDP-N-acetyl-alpha-D-galactosamine: polypeptide N-acetylgalactosaminyltransferase 2
AI843451	13627	Eef1a1	Eukaryotic translation elongation factor 1 alpha 1
AI843644	67118	Bfar	Bifunctional apoptosis regulator
AI843739	21372	Tb11x	Transducin (beta)-like 1 X-linked
AI843817	433759	Hdac1	Histone deacetylase 1
AI844059	170823	Glmn	Glomulin, FKBP associated protein
AI844094	269610	Chd5	Chromodomain helicase DNA binding protein 5
AI844642	108013	Bruno14	Bruno-like 4, RNA binding protein
AI844692	18099	Nlk	Nemo like kinase
AI844810	50772	Mapk6	Mitogen-activated protein kinase 6
AI844896	232341	Wnk1	WNK lysine deficient protein kinase 1
AI844976	18550	Furin	Furin (paired basic amino acid cleaving enzyme)
AI845633	66799	Ube2w	Ubiquitin-conjugating enzyme E2W (putative)
AI845673	23950	Dnajb6	DnaJ (Hsp 40) homolog, subfamily B, member 6
AI845959	66229	Rpl7l1	Ribosomal protein L7-like 1
AI846288	13046	Cugbp1	CUG triplet repeat, RNA binding protein 1
AI846382	67819	Derl1	Der1-like domain family, member 1
AI847083	19046	Ppp1cb	Protein phosphatase 1, catalytic subunit, beta isoform
AI847745	19211	Pten	Phosphatase and tensin homolog
AI848239	20817	Srpk2	Serine/arginine-rich protein specific kinase 2
AI848364	22218	Sumo1	SMT3 suppressor of mif two 3 homolog 1 (yeast)
AI848373	75669	Pik3r4	Phosphatydylinositol 3 kinase, regulatory subunit, polypeptide 4, p150
AI848867	56637	Gsk3b	Glycogen synthase kinase 3 beta
AI848972	13002	Dnajc5	DnaJ (Hsp 40) homolog, subfamily C, member 5
AI849815	217737	Ahsa1	AHA, activator of heat shock protein ATPase homolog 1 (yeast)
AI849825	11836	Araf	V-raf murine sarcoma 3611 viral oncogene homolog
AI851230	66949	Trim59	Tripartite motif-containing 59
AI851286	74105	Gga2	Golgi associated, gamma adaptin ear containing, ARF binding protein 2
AI851517	58243	Nap1l5	Nucleosome assembly protein 1-like 5
AI851522	12331	Cap1	CAP, adenylate cyclase-associated protein 1 (yeast)
AI852248	26987	Eif4e2	Eukaryotic translation elongation factor 4E member 2
AI852284	13200	Ddost	Dolichyl-di-phosphooligosaccharide-protein glycotransferase

AI852541	22027	Hsp90b1	Heat shock protein 90kDa beta (Grp94), member 1
AI852762	22215	Ube3a	Ubiquitin protein ligase E3A
AI852812	211401	Mtss1	Metastasis suppressor 1
AI853420	68031	Rnf146	Ring finger protein 146
AI853538	76479	Smndc1	Survival motor neuron domain containing 1
AI853795	21813	Tgfbr2	Transforming growth factor, beta receptor II
AI854234	228005	Ppig	Peptidyl-prolyl isomerase G (cyclophilin G)
AI854630	13839	Epha5	Eph receptor A5
AI854835	66949	Trim59	Tripartite motif-containing 59
AI854858	17756	Mtap2	Microtubule-associated protein 2

Figure 17. SAM plot with a delta value of 0.3 in a one class response analysis. 18 genes were found to be upregulated and 4 were downregulated.

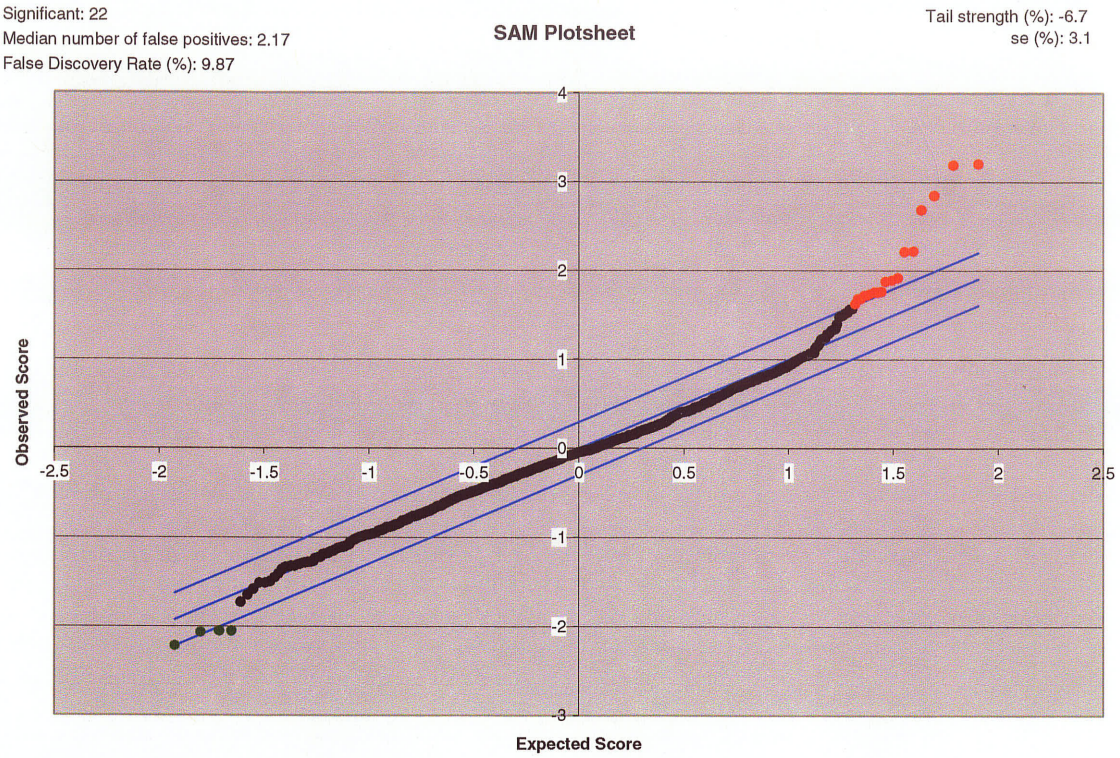

Figure 18. Quadratic regression analysis of antibody array data generated 59 significant proteins. LU: Linear Up, LD: Linear Down, QC: Quadratic Concave, QV: Quadratic Convex, QLCU: Quadratic Linear Concave Up, QLCD: Quadratic Linear Concave Down, QLVU: Quadratic Linear Convex Up, QLVD: Quadratic Linear Convex Down.

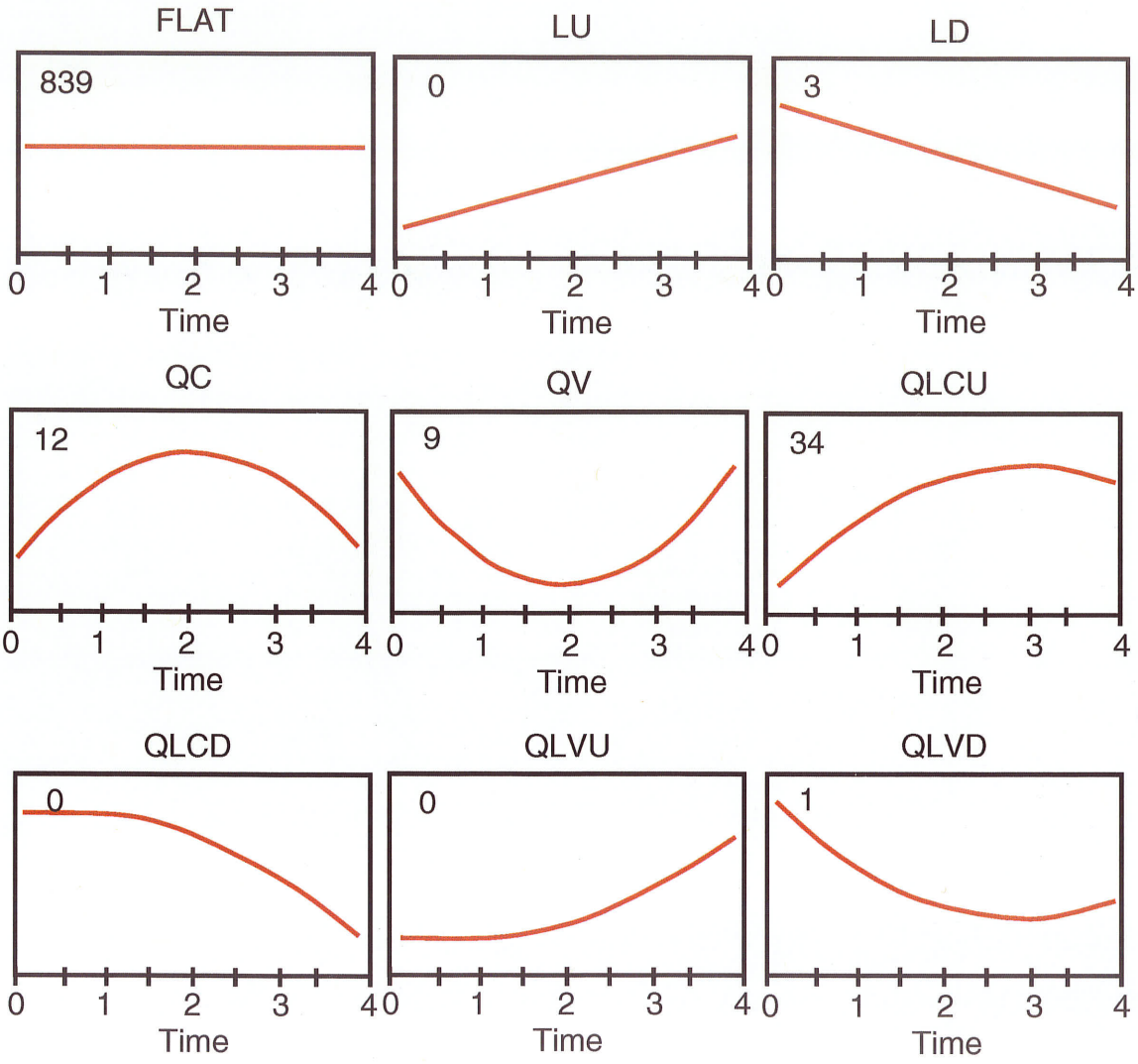

Table 6. Proteins found to be significantly up or down regulated by SAM analysis.

Upregulated Genes

AB ID	Locus Link	Gene ID	Gene Name	q-value(%)
AB_000637	9368	EBP50	solute carrier family 9 (sodium/hydrogen exchanger), isoform 3 regulatory factor 1	0
AB_000669	2932	GSK-3b	glycogen synthase kinase 3 beta	0
AB_001169	11140	CDC37	CDC37 cell division cycle 37 homolog (S. cerevisiae)	0
AB_001302	1397	CRP2	cysteine-rich protein 2	0
AB_000800	5897	Rag-2	recombination activating gene 2	0
AB_001175	84152	DARPP-32	protein phosphatase 1, regulatory (inhibitor) subunit 1B (dopamine and cAMP regulated phosphoprotein, DARPP-32)	0
AB_001175	84152	DARPP-32	protein phosphatase 1, regulatory (inhibitor) subunit 1B (dopamine and cAMP regulated phosphoprotein, DARPP-32)	9.87
AB_000380	4089	Smad 4 / DPC4	MAD, mothers against decapentaplegic homolog 4 (Drosophila)	9.87
AB_001169	11140	CDC37	CDC37 cell division cycle 37 homolog (S. cerevisiae)	9.87
AB_000800	5897	Rag-2	recombination activating gene 2	9.87
AB_000725	5504	Inhibitor 2	protein phosphatase 1, regulatory (inhibitor) subunit 2	9.87
AB_000387	50511	SCP3	synaptonemal complex protein 3	9.87

Downregulated Genes

AB ID	Locus Link	Gene ID	Gene Name	q-value(%)
AB_001287	7353	Ufd1L	ubiquitin fusion degradation 1-like	0
AB_000410	9352	TRP32	thioredoxin-like, 32kDa	0

Table 7. Proteins found to be significant by quadratic regression analysis.

	AB ID	Locus Link	Gene Name	Overall P-Value
LD	AB_001012	995	CDC25C	0.0019425
	AB_001012	995	CDC25C	0.0035565
	AB_000288	1500	pp120 src substrate	0.0092451
QC	AB_000395	7145	Tensin	0.0027648
	AB_000413	7155	DNA Topoisomerase II b	0.0042683
	AB_001266	6354	MCP-3	0.0048878
	AB_000227	4436	MSH2	0.0055244
	AB_000765	5595	ERK1	0.0064978
	AB_000765	5595	ERK1	0.0076153
	AB_000334	5909	Rap 1	0.0078683
	AB_000960	5551	Perforin	0.0082393
	AB_000395	7145	Tensin	0.0083747
	AB_000960	5551	Perforin	0.0087209
	AB_000334	5909	Rap 1	0.0094092
	AB_000413	7155	DNA Topoisomerase II b	0.0095335
QV	AB_000637	9368	EBP50	0.0007467
	AB_000637	9368	EBP50	0.0008416
	AB_000554	857	Caveolin 1	0.0008527
	AB_000415	7329	Ubc9	0.0019336
	AB_000415	7329	Ubc9	0.0021623
	AB_000554	857	Caveolin 1	0.0044224
	AB_000387	50511	SCP3	0.0052678
	AB_001249	121512	Frabin	0.0089637
	AB_001198	9546	Mint3	0.0097291
QLCU	AB_001268	3569	IL-6	4.816E-05
	AB_001268	3569	IL-6	4.834E-05
	AB_000398	6878	TAF II 70	0.000386
	AB_000607	1676	DFF 45 (ICAD)	0.0003965
	AB_000398	6878	TAF II 70	0.000397
	AB_000987	842	Caspase-9 / ICE-LAP6 / Apaf-3	0.0008149
	AB_000782	3164	Nur77	0.000916
	AB_000987	842	Caspase-9 / ICE-LAP6 / Apaf-3	0.0010419
	AB_000422	1845	VHR	0.0010916
	AB_000503	8604	Aralar	0.0010984
	AB_001154	6311	Ataxin 2	0.0011449
	AB_000782	3164	Nur77	0.0013126
	AB_000503	8604	Aralar	0.0015393
	AB_000422	1845	VHR	0.0017154
	AB_001312	56616	Smac/DIABLO	0.0021445
	AB_001162	1114	CHGB	0.0024047
	AB_001162	1114	CHGB	0.0026502
	AB_001154	6311	Ataxin 2	0.0028499

	AB_001174	9046	p56dok2	0.003707
	AB_001217	5824	PEX19	0.0043713
	AB_000820	890 8900	Cyclin A	0.0049305
	AB_001217	5824	PEX19	0.0049657
	AB_000820	890 8900	Cyclin A	0.0049958
	AB_001174	9046	p56dok2	0.0052768
	AB_001312	56616	Smac/DIABLO	0.0053065
	AB_001097	9564	p130 Cas	0.0053151
	AB_000724	4792	IkBa/MAD-3	0.0057251
	AB_001017	4255	MGMT	0.0061262
	AB_000355	3437	RIG-G	0.0062228
	AB_000355	3437	RIG-G	0.0066958
	AB_000805	4654	MyoD	0.0072627
	AB_000758	3903	LAIR-1	0.0084868
	AB_000805	4654	MyoD	0.0088543
	AB_001209	5970	NF-kB	0.009025
QLVD	AB_001178	7514	Exportin-1/CRM1	0.008291

Table 8. Genes selected for real time PCR due to an increase or decrease in expression based on microarray data.

Downregulated Genes

GenBank	Name
AI840009	EST
AI839289	Smg-6 homolog, nonsense mediated mRNA decay factor
AI413721	hypermethylated in cancer 2
AI849635	Metadherin
AI849146	EST
AI849259	cellular nucleic acid binding protein 1
AI848700	kinesin family member 5B
AI846745	EST
AI847446	solute carrier family 4 (anion exchanger), member 4
AI840074	EST

Upregulated Genes

GenBank	Name
AI414429	UDP-glucose ceramide glucosyltransferase-like 1
AI840993	cullin associated and neddylation disassociated 1
AI837717	trinucleotide repeat containing 6a
AI448344	active BCR-related gene
AI429200	EST
AI429157	EST
AI849905	neurofilament 3, medium
AI850673	RAB6, member RAS oncogene family
AI846837	EST
AI841124	SEC14-like 1

The results shown in figure 19 validate the patterns of several gene as observed in the microarray gene expression data. Several upregulated genes have similar slopes such as AI429200, trinucleotide repeat containing 6a and SEC14-like 1. All of the ten genes which were up-regulated as measured by the microarray results, were also up-regulated as measured by real-time PCR, or in one case remained constant (figure 19). For the genes that were down-regulated, the correlation between microarray and real-time PCR was weak. This has been observed in previous studies, where the down-regulated genes showed a poor correlation compared to up-regulated genes (Booth, Bowman et al., 2004).

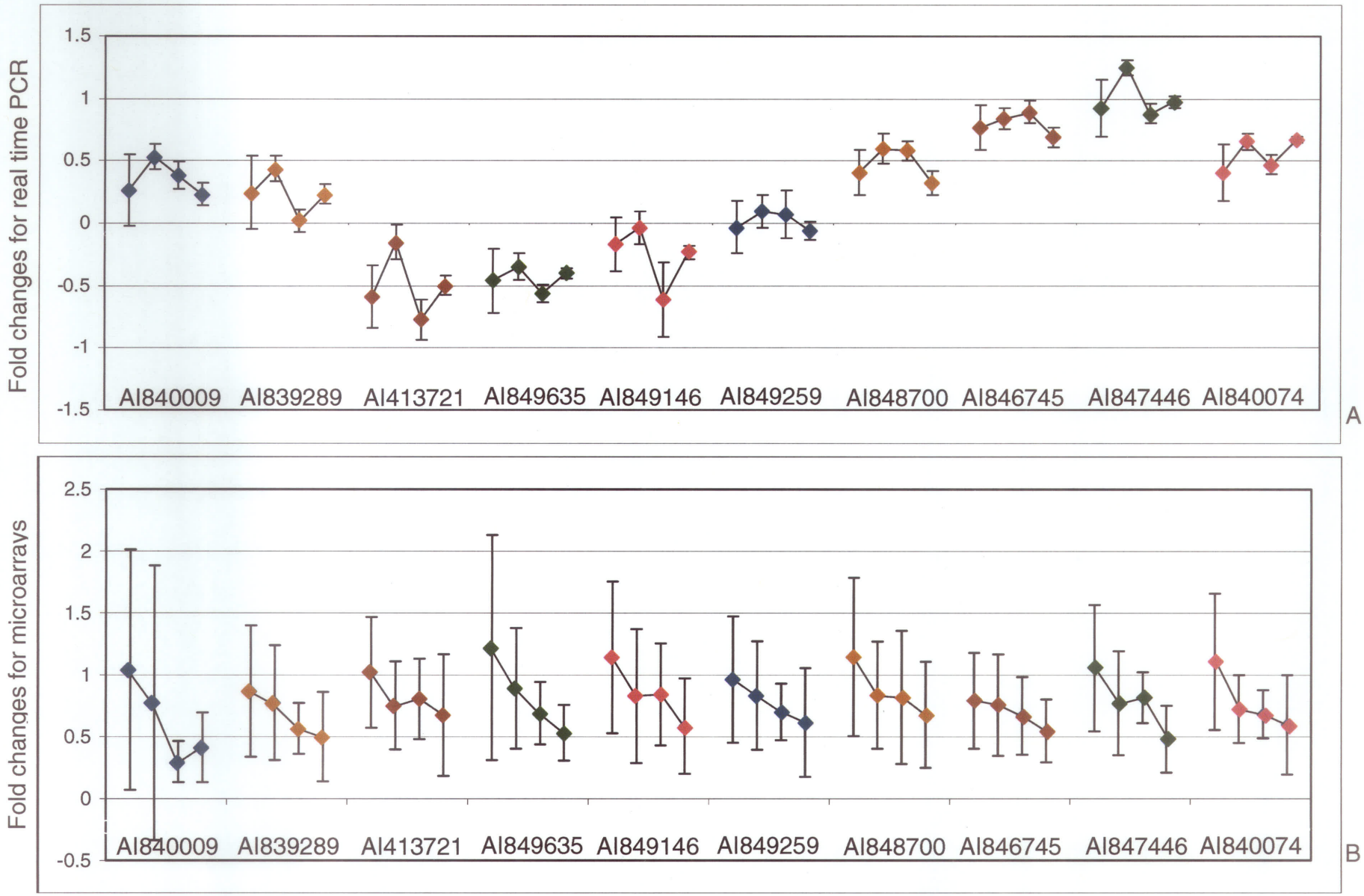

Figure 19. Real time PCR data compared with microarray data for the same genes. A and B correspond to downregulated genes while C and D represent upregulated genes. A and C are the fold changes of relative quantification ($2^{-\Delta\Delta Ct}$). B and D are the average fold changes observed during the microarray experiments. Each gene has 4 points that represent 3, 7, 14 and 21 dpi respectively.

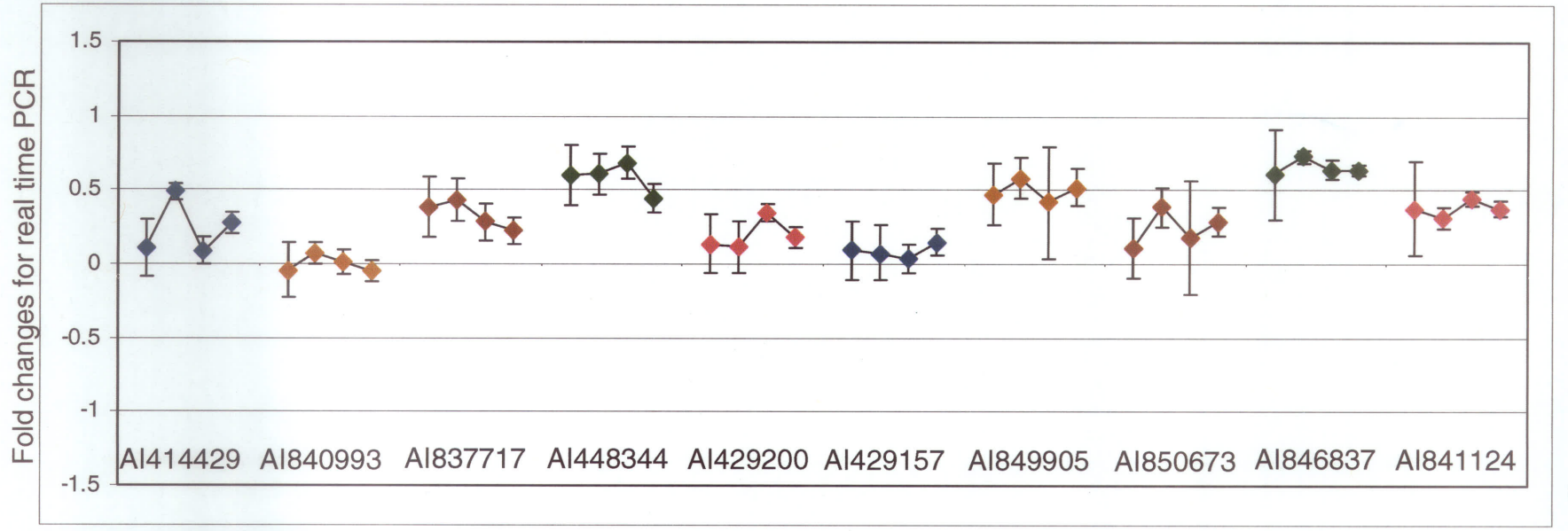
Fold changes for real time PCR
1.5
1
0.5
0
-0.5
-1
-1.5
AI414429
AI840993
AI837717
AI448344
AI429200
AI429157
AI849905
AI850673
AI846837
AI841124

C

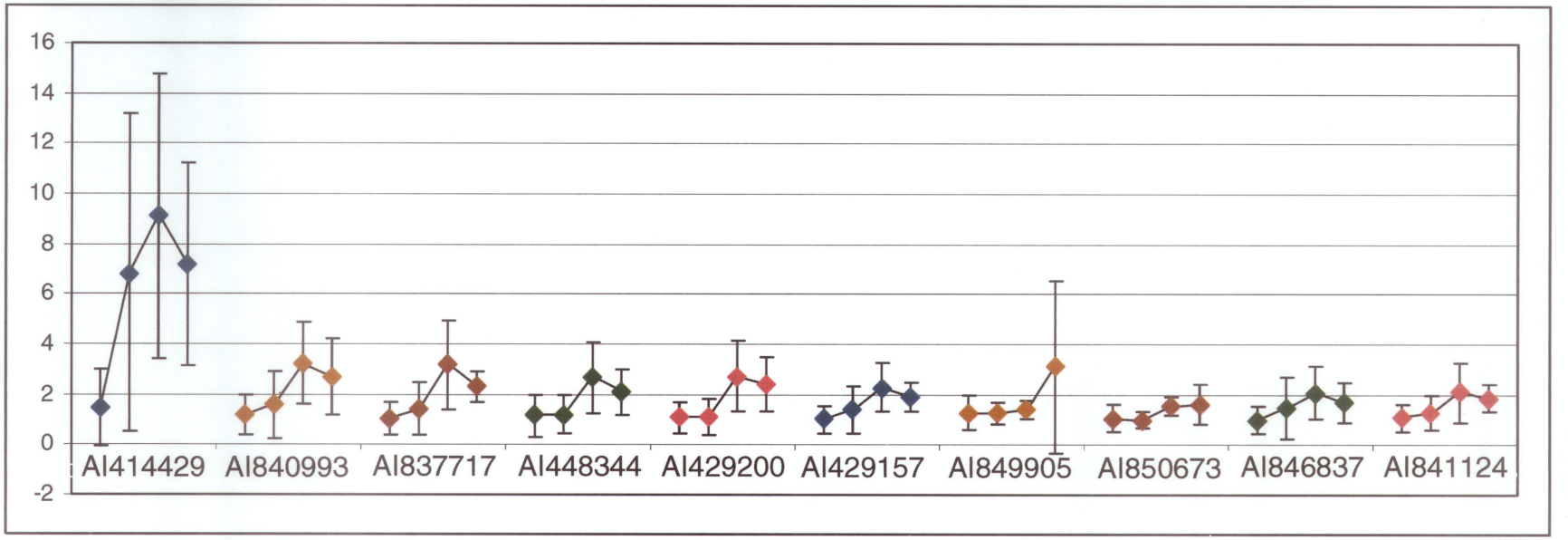
Fold changes for microarrays
16
14
12
10
8
6
4
2
0
-2
AI414429
AI840993
AI837717
AI448344
AI429200
AI429157
AI849905
AI850673
AI846837
AI841124

D

Discussion

The scope of this project was to determine which, if any, genes were regulated differently in mouse brain tissue in response to HSV-1 infection. This was carried out by intranasally infecting mice with a neurovirulent strain of HSV-1. This method of infection was used because it most closely resembles HSE infection in humans (Hudson and Streilein 1994;Lamade et al. 1996). At specified time points the mice were sacrificed. Separate groups of mice were used to determine the course of HSV-1 infection, or used in microarray experiments. HSV-1 infection was determined using such techniques as histology, real time PCR and electron microscopy. The mice designated for the microarray experiments had RNA extracted from the brain. There were 16 mice (8 control and 8 infected) sacrificed at each time point (3, 7, 14 and 21 dpi). Microarrays were carried out and verified by antibody arrays and semi-quantitative real time PCR.

4.1 Determination of HSV-1 infection

Although there were no outward signs or symptoms that the mice infected with HSV-1 were sick, there was evidence found by both histology and virus titration by real time PCR concluding that they were in fact infected. Clinical signs of encephalitis in mice are difficult to observe since the mice were not monitored continuously during the time of infection and most of the symptoms associated with HSE might occur only rarely in infected animals (such as circling) (Hudson et al. 1991). When given a sub-lethal dose (as in these experiments) mice will

recover from the infection. Different strains of mice react differently to HSE. SJL mice are able to survive longer than other strains before becoming moribund (Hudson et al. 1991) and this could be one of the reasons that the mice in this experiment did not exhibit outward signs of HSE. SJL mice were chosen since it has been shown that the mode of HSE infection very closely parallels what is seen during a human HSE infection (Hudson and Streilein 1994).

Histopathological findings showed perivascular cuffing in the temporal lobe of HSV-1 infected mice. Perivascular cuffing occurs when there is a penetration of monocytes into blood vessels. This is akin to a ring of nuclei around the blood vessels. Perivascular cuffing demonstrates that an area may be infected. Marginalization of chromatin is very hard to see and looks like a granular ring of chromatin on the outside of the nucleus while the center appears empty. Dendrites and axons become degenerated when the chromatin is marginalized and look compacted and bubbly. The only histological evidence that was observed was perivascular cuffing. Immune cells were present in large numbers in sections of the infected brains compared to the control brains as seen in figure 10.

Although the virus titer real time PCR did not recover many copies of HSV-1 viral DNA in mouse brains, it did show a significant count at 7 dpi. Two other studies of HSE showed that there was a decline in viral load between days 7 and 14 post infection (Meyding-Lamade et al. 1998;Meyding-Lamade et al. 2003). Since a

non-lethal dose of HSV-1 was given to the mice it is not surprising that the viral load would not be as high as when mice challenged with a lethal dose would see. It has also been shown that there is no correlation between viral burden and clinical symptoms (Meyding-Lamade et al. 1998).

Electron microscopy is not a sensitive tool for the detection of HSV-1 since more than 10^8 particles are needed in a sample. A high concentration of viral particles would not be expected in HSE. At least 10^8 particles in total would be needed to have enough to really identify HSV-1 visually on each field of view. Unfortunately there was no conclusive evidence of HSE provided by electron microscopy. There was very little preservation of cell structures and the cell organelles were fairly disintegrated. The nuclei were also hard to make out possibly due to the extended period that tissues resided in gluteraldehyde. Since the mice didn't exhibit signs or symptoms of HSE there might not have been a large number of viral particles present in the brain. This would make the task of finding HSV-1 viral particles even more difficult. It would have been better to immunogold label the tissue so that HSV-1 viral particles would have been more recognizable.

4.2 Microarray

The Qiazol method of RNA extraction worked significantly better compared to the Trizol extraction method. The quantity and quality of the RNA was superior using the Qiazol method. Although trizol has a strong lysis capability, Qiazol achieved the most effective homogenization. One reason for this could be the high fatty

acid content of brain tissue. Qiazol is designed to give a high yield of RNA out of fatty tissues. In addition, Qiazol RNA extraction does not require formation of a pellet of RNA before continuing on to the clean-up method. Less RNA appeared to have been lost due to omission of this step. Moreover, the elution step was carried out twice for each sample using the Qiazol method, further improving the quantity of RNA extracted.

Most previous published research that examined host response to pathogens looked at one specific cell type in a very controlled experiment (Jenner and Young 2005). Moreover, the research presented here used an *in vivo* model whilst most previous studies have used *in vitro* models. The *in vivo* model includes all of the specific cell types present in the brain tissue rather than just concentrating on a neuronal or astrocytes cell line for example. These earlier studies looked at the antiviral response in mammalian cells (Mossman et al. 2001), the infection of sensory neurons (Kramer et al. 2003) and the transcriptional response of rat embryonic fibroblasts (Ray and Enquist 2004). Mossman *et al* found many genes regulated by interferon were significantly upregulated (Mossman et al. 2001). Sensory neurons in Kramer *et al*'s work showed an upregulation of genes involved in immune response, gene expression, neurotransmission signalling and axonal remodelling (Kramer et al. 2003). The transcriptional response examined by Ray and Enquist showed genes involved in apoptosis, notch signalling, interferon related, heat shock and oxidative stress (Ray and Enquist 2004).

The data from the present study shows that most statistically significant genes fall under the immune and stress response. Other categories in which genes tend to be found to be significant are cell adhesion/structure, neuronal, signal transduction, and cell cycle/apoptosis. The most significant categories were found to be: immune response, apoptosis, CNS specific, actin/microtubule and cellular protein metabolism, which is in accordance with earlier research findings.

Host responses to pathogens have been studied from a wide variety of sources. Many different animal and cell models have been used in conjunction with many diverse pathogens. It would seem that upon comparison the host response has many similarities. Genes involving interferon, mitogenesis and inflammation all share a common expression pattern in infected cells. Using these categories as a guide, the present study looked at genes involved in the immune response, apoptosis, CNS specific, actin and microtubule organization and cellular protein metabolism.

One interesting detail about HSV-1 infection is that unlike other pathogens HSV-1 seems to block the expression of IFN-stimulated genes (Jenner and Young 2005;Kramer et al. 2003). This could be a form of immunoevasion developed by the virus. Other research has shown that in order for the host cell to induce an antiviral response several key HSV-1 genes must be rendered ineffective (Mossman et al. 2001). Very few upregulated genes were found in the host

response to HSV-1 infection. This could occur because HSV-1 takes control of the host cell machinery and shuts down host cell protein synthesis (Smiley 2004).

The microarrays used in these experiments did not have a high proportion of genes representing interferon, the immune system or cytokines pathways. Even though these genes were under represented in the array, those that were present showed significant changes in activity. All arms of the immune system were represented from innate immunity to B and T cell immunity.

The BMAP library that was selected for use on the microarrays was chosen because it was constructed from genes located in mouse brain and associated tissues. Since HSE is a neurological disease, it was thought that the potential for novel gene discovery would be greatest if genes expressed in the CNS were targeted. The library also contained a significant number of ESTs with no known biological function, this again could lead to novel gene discovery. Novel gene discovery is beyond the scope of this project. The ESTs that were shown to have had a change in gene expression in this study might help in better understanding HSE when they become characterized in the future.

There are several factors that could potentially limit the confidence with which one can interpret microarray results. The first is that only a small fraction of cells within the entire mouse brain are infected by HSV-1, while the second is the intrinsic variability of microarray measurements. Those cells that are not infected

might mask the large differences in gene expression that might occur in individual infected cells. This might give rise to a very small difference in expression on a whole brain basis. There are three forms of intrinsic microarray variability. Those are biological, technical and measurement error. To reduce this variability replicates at each time point were used. Increasing the number of mice studied would insure that a statistically significant difference could be detected or that no difference could be determined. Doing all RNA extractions within a short period of time using the same protocols as well as doing a dye swap to eliminate labeling bias of the samples was also utilized to minimize these events. Finally, using the same scanner to make sure that the lasers used would be of the same quality and also to normalize the data received minimized measurement error problems as well. Due to time restrictions it was not possible to carry out more than one set of mice infections. It would have lent strength to this study if that had been possible.

4.2.1 Immune Response

The following genes that were identified could be linked to innate immunity such as Masp1, Hsp90aa1, and Gsk3b. Masp1 is a complement-dependent factor that can activate C3 and C2 in the complement cascade (Matsushita et al. 2000). Hsp90aa1 plays a critical role in type I and II interferon pathways. It has a central role in IL-1 receptor associated kinase dependent signaling by toll-like receptors and can activate Wasl for podosome formation and neurite extension (Shang and Tomasi 2006). Gsk3b modulates the inflammatory response and

toll-like receptor cytokine production (Martin et al. 2005). Masp1 was highly upregulated compared to controls late in infection. This might be expected, since an HSv-1 infection was present in mouse brain cells. Both Hsp90aa1 and Gsk3b were downregulated during the course of infection. This makes sense because both are important factors in the interferon and inflammatory responses. Dysregulation of these pathways would allow the virus a greater chance to go unchecked by the host immune system.

Sit1 was another highly upregulated gene. It is involved in negative regulation of T-cell receptor-mediated signaling (Simeoni et al. 2005). Since HSV-1 shuts off and tends to control most cell functions it would make sense to upregulate an immune repressor gene. In order to mask the infection T-cells would need to be inactivated. HSV-1 has found a way to remain hidden from host immune systems and this could be one way in which this is achieved.

Pten can regulate both B and T cells. It regulates the proliferation of developing T cells in the thymus (Hagenbeek et al. 2004) and plays a role in the developmental fate of B cells along with being important for their homeostasis (Suzuki et al. 2003;Suzuki et al. 2004). In this study it was found that Pten was downregulated during the course of HSV-1 infection. The downregulation of this gene has the potential to significantly hamper the immune system of the host. Without it T cells would have trouble proliferating and B cells might not be regulated. Pten also has the ability to down-regulated macrophage Fc gamma

receptor-mediated signaling while promoting the macrophage inflammatory response to TLR4 signaling (Cao et al. 2004). The down regulation of this gene would affect every arm of the host immune response to infection.

4.2.2 Apoptosis

Apoptosis (programmed cell death) occurs for many different reasons. One such reason is infection. Activation of apoptosis in response to infectious processes can be considered to be a self-defense mechanism to prevent the infection from spreading to nearby susceptible cells. The main form of cell death in HSE is by apoptosis.

Only one anti-apoptotic gene was identified, Ywhag, in the list of significant genes. Ywhag regulates cell division and apoptosis mainly in the brain. It can be found in both neurons and astrocytes and is usually upregulated under decreased blood supply to the brain (Chen and Yu 2002). Even though Ywhag is an anti-apoptotic gene, it may have been upregulated since HSE leads to a decrease in blood supply to the brain and that is what caused its upregulation.

Bfar is an anti-apoptotic regulator that was found to be slightly downregulated during the course of HSV-1 infection. It contains a DED-like domain that is capable of limiting apoptosis by signaling Fas and can also interact with Bcl-2 family proteins (Chen and Yu 2002;Roth et al. 2003). It is thought to play a regulatory role between the extrinsic (death receptor) and intrinsic (Bax)

apoptotic pathways (Roth et al. 2003;Zhang et al. 2000) by acting as a scaffolding protein that can bridge components of both pathways. It does this by mediating Caspase-8 binding (Roth et al. 2003). Upregulation of this gene can provide some protection from cell death but downregulation, as seen in this experiment, can lead to sensitization to apoptosis (Roth et al. 2003).

The rest of the genes found to be significant (Table 5) all show pro-apoptotic properties (Cheng et al. 2003;Choy et al. 2004;Dahia et al. 1999;Maggirwar et al. 1999;Ryu et al. 1999). They seem to be upregulated slightly early during infection but by 14dpi start to become downregulated. This could be explained by the fact that the mice started to recover from HSE since a non-lethal dose of HSV-1 was administered. During recovery less cells would be undergoing apoptosis.

4.2.3 CNS Specific

A group of CNS specific genes was also found (Table 5). Some of these genes can be further subdivided into the following categories, behaviour, synapse specific and myelin. Gap43, Tmod2 and Atp1a2 are all downregulated and play a role in behaviour. Gap 43 is involved in learning and memory processes (Metz and Schwab 2004;Rekart et al. 2005). It is required for information processing and storage. It plays a crucial role in the hippocampus where it regulates memory processing (Rekart et al. 2005). When mice are deficient in Tmod2 they have been found to suffer deficits in fear conditioning and learning. Tmod2 has a role in learning, memory and synaptic plasticity (Cox et al. 2003). Atp1a2 is

mainly expressed in the brain. Decreased expression of Atp1a2 in mice caused more fear and anxiety behaviours and increased neuronal activity after conditioning with fear stimuli (Ikeda et al. 2003).

The genes found to play a role at the synaptic level of neurons are Snapap, Gabra6 and Atp1a2. Snapap is located on the synaptic vesicle and inhibits neurotransmitter release and vesicle docking (Ilardi et al. 1999). It regulates the exocytosis of neurotransmitter. Gabra6 inhibits synaptic transmission (Wisden et al. 2002) while Atp1a2 protects neurons from continued activity by clearning neurotransmitter (Ikeda et al. 2003). A decrease in these 3 genes would lead to more synaptic activity and more neurotransmitter present in the neuronal synapse. The continued activity of neurons could eventually lead to cell death and could also affect behaviours such as learning and memory.

Myelin is very important for the CNS. It protects neurons and allows signals to be transmitted quickly from one point to the next. Plp1 and Pten are genes associated with myelin and were both downregulated. Plp1 encodes a major myelin protein (Al Saktawi et al. 2003;McLaughlin et al. 2002). Without this protein the myelin sheath that surrounds neurons would not be maintained. This would lead to decreased communication in the brain. Pten controls Bergmann glia differentiation and scaffold organization (Yue et al. 2005). Bergmann glia are cerebellar astroglial cells that wrap dendrites and Purkinje cell dendrites and

synapses. A decrease in myelin and Bergmann proteins would lead to havoc in the brain of diseased mice.

4.2.4 Actin/Microtubule

Mitotic processes can be viewed by looking at genes involved in actin and microtubule organization. These two proteins are activated during mitosis. The following downregulated genes were identified as having a role in actin or microtuble formation, stabilization or assembly; Tmod2, Diap2, Wasl, Rhoa, Bbs4, Mtss1 and Arpc5. Two genes were found to have more significant roles in mitosis; Npm1 and Dctn3. Npm1 is localized to unduplicated centrosomes, it dissociates prior to duplication upon phosphorylation (Tarapore et al. 2002). It can also form complexes involved in DNA duplication, pre-ribosomal RNA processing and nucleocytoplasmic protein trafficking (Shinmura et al. 2005). Dctn3 is involved in the movement of lysosomes and endosomes, spindle formation, chromosome movement and nuclear positioning (Karki et al. 1998). These functions are necessary for cell division to occur.

4.2.5 Cellular Protein Metabolism

Cellular Protein Metabolism deals with the chemical reactions and protein modification involving a specific protein, rather than of proteins in general, occurring at the level of an individual cell. Several proteins identified in this group were of interest, specifically Ugcgl1 and Ier3. Ugcgl1 was found to be significant by all methods of statistical analysis and was upregulated during the

course of HSV-1 infection. A previous study by Suzuki and Blough showed that upon HSV infection cells stimulated the expression of glucosyltransferase in microsomes (Suzuki and Blough 1982). This is thought to play a role in virion assembly. Another gene of interest is Ier3. Taddeo et al showed that Ier3 was upregulated following HSV-1 infection (Taddeo et al. 2002). A subsequent study showed that HSV-1 infection stabilized Ier3 mRNA and that viral gene expression was necessary for full induction of Ier3 transcripts during infection (Hsu et al. 2005).

4.3 Antibody Arrays

Antibody arrays were used to find out if changes in gene expression were correlated to changes in protein expression. The advantage of this experiment was that it compared gene and protein expression using similar technology. Another advantage of using the antibody array is that a large number of proteins can be compared in the same experiment. The major disadvantage was that the range of antibodies on the arrays did not correlate well with the genes located on the microarrays. There are ESTs located on the microarrays which have not been well characterized nor the genes associated with them characterized. This made it difficult to compare the two experiments directly. The other disadvantage of this experiment is that it is primarily a screening tool and cannot be used to quantitatively measure exact amounts of protein. These arrays were designed to provide information on the relative protein abundance, which depends on the binding affinity, which varies for different antibody-protein combinations.

This particular antibody array was chosen because it contained a lot of antibodies that correspond to factors found in the CNS. Since this study has shown that most changes occurred in aspects involved in the immune response it would have enhanced the experiment to select an antibody array that had a majority of immune response antibodies.

4.4 Real Time PCR

The results seen in figure 19 demonstrate that several gene expression patterns were confirmed by real time PCR analysis. The ones that showed gene expression patterns that differed could be perhaps because amplification was necessary and to the fact that the probes used in the real time PCR experiment were obtained from a different source than those used in the microarray experiments. Also some genes may have been poorly annotated and the correct ones may not have been chosen to compare directly with the probes used on the microarray slides.

4.5 Future Directions

In this work data was obtained that indicated that HSV-1 infection of mouse brains altered the overall gene expression. There were 497 genes that were identified to be up or downregulated. Further work should address the points described below.

Determining the effect of a lethal infectious dose of virus would be useful to see the minimum dose needed to initiate an infection and the dose response in terms of survival time, or time to initiate symptoms. It has been shown that certain strains of mice are refractory to HSV-1 infection if the infective dose is too high (Altavilla et al. 2002). This is called interference. It would have been helpful to see the dose response required for mortality to set in.

Testing different strains of mice to see if they all produced the same expression patterns would also have been practical as well as seeing if different modes of infection garnered the same results. Intranasal infection is considered to be the route in which humans acquire HSE. Although most adults are infected with HSV-1, very few actually develop with HSE. It would be interesting to see if different modes of infection in mice led to more lethality, more changes in gene expression, or affected the severity symptoms to occur. It has been shown that mice can get HSE by intraperitoneal, intracranial and intramuscular injections. It would also have been constructive to see if the course of disease progression was altered, or if the incubation period is affected by route of infection such as to hind footpad.

A zero dpi time point approximately six hours post infection would have been beneficial. This would have been an immediate early time point and could have set the bar to see if the mice reacted more to the fact that there was an infection or to the type of infection itself. Since the virus would not have had time to infect

the CNS of the infected mice it would be interesting to see what changes would have occurred (if any) at this immediate early time point.

Ascertaining if different HSV-1 infected cell lines generate the same gene expression pattern as seen in the whole mouse brain would be interesting. It is known that HSE occurs in many different types of cells, in addition to neurons. It would be interesting to see how different cell types react to an HSV-1 infection in tissue culture by using cell types that can be cultured. Most brain tissue cannot grow *in vitro*, but there are cell lines such as neuroblastoma and glioblastoma.

Laser capture microdissection could also be used to determine if uninfected cells are masking differences of expression, since non-infected cells are in the majority in the whole infected brain. In this case you would need to determine which cells are actually infected and to do this you could use a GFP-tagged virus. This would allow infected cells to fluoresce and therefore be able to be selected for over non-infected cells. This would also mean that non-infected cells could serve as another form of control since these cells would be from the same brain and therefore lessen any genetic variability. It would still of course be necessary to use control mice that have been mock-infected just in case there are some whole brain and inflammatory signals that are causing the non-infected cells to behave differently from the controls.

Instead of using the entire mouse brain for total RNA extraction it might be better to simply use the temporal lobes of the mice since this is where most of the HSE occurs. This would help in limiting the amount of non-infected cells that might mask the overall gene expression patterns for infected cells.

Seeing how the anti-viral drug, acyclovir, affects the genetic profile of the infected mice would generate a good comparison to data obtained in the present study. Giving acyclovir at specific time points could aid in determining if there are several or certain pathways that are inhibited by this drug. This might lead to new pathways that have yet to be targeted to become visible and hence another or new drug could be used to inhibit these pathways and therefore lower even more significantly the mortality and damage caused by HSE.

Comparing various forms of encephalitis caused by other viruses and bacteria would yield results useful in future drug development. This would show if identified pathways are common to all encephalitis or if there are specific ones for each disease. This could lead to more specific drugs and hence better care for infected individuals.

HSV-1 specific probes could be added to the microarray to simultaneously detect viral and host gene expression. This would be important since it is hard to determine any signs or symptoms of disease from the mice. This is because neurological signs might only occur for approximately 30 seconds in one day and

if the mice are not monitored twenty-four hours a day then the signs may be missed. Another option would be to set up a video monitor so that the actions of the mice can be reviewed to determine if any such signs are apparent.

Future work could also include probing the genes found to be significant in more detail. There are many that are still ESTs (uncharacterized genes) with that number decreasing daily as new genes are figured out.

The microarrays used had very few genes from the immune system represented on them. A few chemokines, interleukins, complement and interferon factors were represented on the microarray. To have so few genes from the immune system represented, but nonetheless to have several of them found to be significantly expressed shows that changes to the immune system were occurring during the course of HSV-1 infection.

4.6 Conclusions

The conclusions from my research revealed that 497 genes in the mouse brain responded during the course of an HSV-1 infection by significant up or downregulation of their expression levels. Of these, 96 were significantly upregulated and 401 were significantly downregulated. Prior studies focused on few genes and used *in vitro* models. A more comprehensive approach was undertaken in this project that included an *in vivo* mouse model and microarray analysis. Previously HSV-1 infection was thought to shut down host cell protein

synthesis by totally shutting down many genes (Smiley 2004). In contrast, results from my study show that a number of genes were significantly upregulated, while confirming that many genes were also downregulated.

My research has contributed to further scientific knowledge by being the first to study the whole host brain response to Herpes simplex encephalitis by measuring gene expression in 16 000 genes simultaneously using DNA microarrays. The results identified several new groups of significant genes including: immune response, cell death, neurotropism, cell structure/cytoskeletal and cellular protein metabolism and demonstrate that these genes play a role in pathogenesis.

My study discovered many new genes that responded to HSV-1, demonstrating additional mechanisms and genetic pathways whereby HSV-1 can manipulate the host response to infection. This study will help to elucidate the intricate relationship between HSV-1 and the host cell during HSE, specifically the regulation of immune response, apoptosis, CNS specific, actin/microtubule and cellular protein metabolism. Genes discovered here could act as a target for future novel drug discovery to decrease the incident of HSE morbidity and mortality.

Reference List

Al Saktawi K., McLaughlin M., Klugmann M., Schneider A., Barrie J. A., McCulloch M. C., Montague P., Kirkham D., Nave K. A., and Griffiths I. R. (2003) Genetic background determines phenotypic severity of the Plp rumpshaker mutation. *J Neurosci Res* **72,** 12-24.

Anglen C. S., Truckenmiller M. E., Schell T. D., and Bonneau R. H. (2003) The dual role of CD8+ T lymphocytes in the development of stress-induced herpes simplex encephalitis. *J Neuroimmunol* **140,** 13-27.

Augustinova H., Hoeller D., and Yao F. (2004) The dominant-negative herpes simplex virus type 1 (HSV-1) recombinant CJ83193 can serve as an effective vaccine against wild-type HSV-1 infection in mice. *J Virol* **78,** 5756-5765.

Baringer J. R. (2000) *Infectious diseases of the nervous system*, Butterworth-Heinemann, Oxford.

Ben Hur T., Rosenthal J., Itzik A., and Weidenfeld J. (1996) Rescue of HSV-1 neurovirulence is associated with induction of brain interleukin-1 expression, prostaglandin synthesis and neuroendocrine responses. *J Neurovirol* **2,** 279-288.

Ben Hur T., Cialic R., Itzik A., Barak O., Yirmiya R., and Weidenfeld J. (2001) A novel permissive role for glucocorticoids in induction of febrile and behavioral signs of experimental herpes simplex virus encephalitis. *Neuroscience* **108,** 119-127.

Ben Hur T., Cialic R., and Weidenfeld J. (2003) Virus and host factors that mediate the clinical and behavioral signs of experimental herpetic encephalitis. A short auto-review. *Acta Microbiol Immunol Hung* **50,** 443-451.

Bidanset D. J., Placidi L., Rybak R., Palmer J., Sommadossi J. P., and Kern E. R. (2001) Intravenous infusion of cereport increases uptake and efficacy of acyclovir in herpes simplex virus-infected rat brains. *Antimicrob Agents Chemother* **45,** 2316-2323.

Bishop S. A. and Hill T. J. (1991) Herpes simplex virus infection and damage in the central nervous system: immunomodulation with adjuvant, cyclophosphamide and cyclosporin A. *Arch Virol* **116,** 57-68.

Bloom D. C. (2004) HSV LAT and neuronal survival. *Int Rev Immunol* **23,** 187-198.

Booth S., Bowman C., Baumgartner R., Sorensen G., Robertson C., Coulthart M., Phillipson C., and Somorjai R. L. (2004) Identification of central nervous system genes involved in the host response to the scrapie agent during preclinical and clinical infection. *J Gen Virol* **85,** 3459-3471.

Browne E. P., Wing B., Coleman D., and Shenk T. (2001) Altered cellular mRNA levels in human cytomegalovirus-infected fibroblasts: viral block to the accumulation of antiviral mRNAs. *J Virol* **75,** 12319-12330.

Cao X., Wei G., Fang H., Guo J., Weinstein M., Marsh C. B., Ostrowski M. C., and Tridandapani S. (2004) The inositol 3-phosphatase PTEN negatively regulates Fc gamma receptor signaling, but supports Toll-like receptor 4 signaling in murine peritoneal macrophages. *J Immunol* **172,** 4851-4857.

Chaudhuri A. and Kennedy P. G. (2002) Diagnosis and treatment of viral encephalitis. *Postgrad Med J* **78,** 575-583.

Chen X. Q. and Yu A. C. (2002) The association of 14-3-3gamma and actin plays a role in cell division and apoptosis in astrocytes. *Biochem Biophys Res Commun* **296,** 657-663.

Cheng P., Nefedova Y., Miele L., Osborne B. A., and Gabrilovich D. (2003) Notch signaling is necessary but not sufficient for differentiation of dendritic cells. *Blood* **102,** 3980-3988.

Chou J., Kern E. R., Whitley R. J., and Roizman B. (1990) Mapping of herpes simplex virus-1 neurovirulence to gamma 134.5, a gene nonessential for growth in culture. *Science* **250,** 1262-1266.

Chou J. and Roizman B. (1992) The gamma 1(34.5) gene of herpes simplex virus 1 precludes neuroblastoma cells from triggering total shutoff of protein synthesis characteristic of programed cell death in neuronal cells. *Proc Natl Acad Sci U S A* **89,** 3266-3270.

Choy J. C., Kerjner A., Wong B. W., McManus B. M., and Granville D. J. (2004) Perforin mediates endothelial cell death and resultant transplant vascular disease in cardiac allografts. *Am J Pathol* **165,** 127-133.

Cox P. R., Fowler V., Xu B., Sweatt J. D., Paylor R., and Zoghbi H. Y. (2003) Mice lacking Tropomodulin-2 show enhanced long-term potentiation, hyperactivity, and deficits in learning and memory. *Mol Cell Neurosci* **23,** 1-12.

Cui F. D., Asada H., Kishida T., Itokawa Y., Nakaya T., Ueda Y., Yamagishi H., Gojo S., Kita M., Imanishi J., and Mazda O. (2003) Intravascular naked DNA vaccine encoding glycoprotein B induces protective humoral and cellular immunity against herpes simplex virus type 1 infection in mice. *Gene Ther* **10,** 2059-2066.

Dahia P. L., Aguiar R. C., Alberta J., Kum J. B., Caron S., Sill H., Marsh D. J., Ritz J., Freedman A., Stiles C., and Eng C. (1999) PTEN is inversely correlated with the cell survival factor Akt/PKB and is inactivated via multiple mechanismsin haematological malignancies. *Hum Mol Genet* **8,** 185-193.

Davis L. E. and Johnson R. T. (1979) An explanation for the localization of herpes simplex encephalitis? *Ann Neurol* **5,** 2-5.

DeRisi J., Penland L., Brown P. O., Bittner M. L., Meltzer P. S., Ray M., Chen Y., Su Y. A., and Trent J. M. (1996) Use of a cDNA microarray to analyse gene expression patterns in human cancer. *Nat Genet* **14,** 457-460.

Duggan D. J., Bittner M., Chen Y., Meltzer P., and Trent J. M. (1999) Expression profiling using cDNA microarrays. *Nat Genet* **21,** 10-14.

Erturk M., Hill T. J., Shimeld C., and Jennings R. (1992) Acute and latent infection of mice immunised with HSV-1 ISCOM vaccine. *Arch Virol* **125,** 87-101.

Esiri M. M. (2001) Potential for HSV-1 vaccination to reduce risk of HSV-1 encephalitis and/or Alzheimer's disease? *Neurobiol Aging* **22,** 711-713.

Goel N., Rong Q., Zimmerman D., and Rosenthal K. S. (2003) A L.E.A.P.S. heteroconjugate vaccine containing a T cell epitope from HSV-1 glycoprotein D elicits Th1 responses and protection. *Vaccine* **21,** 4410-4420.

Goldsmith K., Chen W., Johnson D. C., and Hendricks R. L. (1998) Infected cell protein (ICP)47 enhances herpes simplex virus neurovirulence by blocking the CD8+ T cell response. *J Exp Med* **187,** 341-348.

Hagenbeek T. J., Naspetti M., Malergue F., Garcon F., Nunes J. A., Cleutjens K. B., Trapman J., Krimpenfort P., and Spits H. (2004) The loss of PTEN allows TCR alphabeta lineage thymocytes to bypass IL-7 and Pre-TCR-mediated signaling. *J Exp Med* **200,** 883-894.

Hsu W. L., Saffran H. A., and Smiley J. R. (2005) Herpes simplex virus infection stabilizes cellular IEX-1 mRNA. *J Virol* **79,** 4090-4098.

Hudson S. J., Dix R. D., and Streilein J. W. (1991) Induction of encephalitis in SJL mice by intranasal infection with herpes simplex virus type 1: a possible model of herpes simplex encephalitis in humans. *J Infect Dis* **163,** 720-727.

Hudson S. J. and Streilein J. W. (1994) Functional cytotoxic T cells are associated with focal lesions in the brains of SJL mice with experimental herpes simplex encephalitis. *J Immunol* **152,** 5540-5547.

Ikeda K., Onaka T., Yamakado M., Nakai J., Ishikawa T. O., Taketo M. M., and Kawakami K. (2003) Degeneration of the amygdala/piriform cortex and enhanced fear/anxiety behaviors in sodium pump alpha2 subunit (Atp1a2)-deficient mice. *J Neurosci* **23,** 4667-4676.

Ilardi J. M., Mochida S., and Sheng Z. H. (1999) Snapin: a SNARE-associated protein implicated in synaptic transmission. *Nat Neurosci* **2,** 119-124.

Jenner R. G. and Young R. A. (2005) Insights into host responses against pathogens from transcriptional profiling. *Nat Rev Microbiol* **3,** 281-294.

Jing X. and He B. (2005) Characterization of the triplet repeats in the central domain of the gamma134.5 protein of herpes simplex virus 1. *J Gen Virol* **86,** 2411-2419.

Johnson R. T. (1998) *Viral infections of the nervous system*, Lippincott-Raven, Philadelphia.

Jones C. A. and Knipe D. (2003) Herpes simplex virus vaccines. *Pediatr Infect Dis J* **22,** 1003-1005.

Jones J. O. and Arvin A. M. (2003) Microarray analysis of host cell gene transcription in response to varicella-zoster virus infection of human T cells and fibroblasts in vitro and SCIDhu skin xenografts in vivo. *J Virol* **77,** 1268-1280.

Kang W., Mukerjee R., and Fraser N. W. (2003) Establishment and maintenance of HSV latent infection is mediated through correct splicing of the LAT primary transcript. *Virology* **312,** 233-244.

Karki S., LaMonte B., and Holzbaur E. L. (1998) Characterization of the p22 subunit of dynactin reveals the localization of cytoplasmic dynein and dynactin to the midbody of dividing cells. *J Cell Biol* **142,** 1023-1034.

Kennedy P. G. and Chaudhuri A. (2002) Herpes simplex encephalitis. *J Neurol Neurosurg Psychiatry* **73,** 237-238.

Kienzle T. E., Chen T. M., Mrak R. E., and Stroop W. G. (2001) A novel, cell-specific attenuation of a herpes simplex virus type 1 infection in vivo. *Acta Neuropathol (Berl)* **101,** 341-350.

Kobelt D., Lechmann M., and Steinkasserer A. (2003) The interaction between dendritic cells and herpes simplex virus-1. *Curr Top Microbiol Immunol* **276,** 145-161.

Kramer M. F., Cook W. J., Roth F. P., Zhu J., Holman H., Knipe D. M., and Coen D. M. (2003) Latent herpes simplex virus infection of sensory neurons alters neuronal gene expression. *J Virol* **77,** 9533-9541.

Lamade U. M., Lamade W., Hess T., Gosztonyi G., Kehm R., Sartor K., and Hacke W. (1996) A mouse model of herpes simplex virus encephalitis: diagnostic brain imaging by magnetic resonance imaging. *In Vivo* **10,** 563-568.

Lellouch-Tubiana A., Fohlen M., Robain O., and Rozenberg F. (2000) Immunocytochemical characterization of long-term persistent immune activation in human brain after herpes simplex encephalitis. *Neuropathol Appl Neurobiol* **26,** 285-294.

Lin W. R., Jennings R., Smith T. L., Wozniak M. A., and Itzhaki R. F. (2001) Vaccination prevents latent HSV1 infection of mouse brain. *Neurobiol Aging* **22,** 699-703.

Liu B. L., Robinson M., Han Z. Q., Branston R. H., English C., Reay P., McGrath Y., Thomas S. K., Thornton M., Bullock P., Love C. A., and Coffin R. S. (2003) ICP34.5 deleted herpes simplex virus with enhanced oncolytic, immune stimulating, and anti-tumour properties. *Gene Ther* **10,** 292-303.

Lockhart D. J., Dong H., Byrne M. C., Follettie M. T., Gallo M. V., Chee M. S., Mittmann M., Wang C., Kobayashi M., Horton H., and Brown E. L. (1996) Expression monitoring by hybridization to high-density oligonucleotide arrays. *Nat Biotechnol* **14,** 1675-1680.

Maggirwar S. B., Tong N., Ramirez S., Gelbard H. A., and Dewhurst S. (1999) HIV-1 Tat-mediated activation of glycogen synthase kinase-3beta contributes to Tat-mediated neurotoxicity. *J Neurochem* **73,** 578-586.

Mahajan M. and Duggal L. (2002) Herpes simplex encephalitis in acquired immune deficiency syndrome. *J Assoc Physicians India* **50,** 1314-1315.

Martin M., Rehani K., Jope R. S., and Michalek S. M. (2005) Toll-like receptor-mediated cytokine production is differentially regulated by glycogen synthase kinase 3. *Nat Immunol* **6,** 777-784.

Matsushita M., Thiel S., Jensenius J. C., Terai I., and Fujita T. (2000) Proteolytic activities of two types of mannose-binding lectin-associated serine protease. *J Immunol* **165,** 2637-2642.

Mayne M., Cheadle C., Soldan S. S., Cermelli C., Yamano Y., Akhyani N., Nagel J. E., Taub D. D., Becker K. G., and Jacobson S. (2001) Gene expression profile of herpesvirus-infected T cells obtained using immunomicroarrays: induction of proinflammatory mechanisms. *J Virol* **75,** 11641-11650.

McLaughlin M., Hunter D. J., Thomson C. E., Yool D., Kirkham D., Freer A. A., and Griffiths I. R. (2002) Evidence for possible interactions between PLP and DM20 within the myelin sheath. *Glia* **39,** 31-36.

Metz G. A. and Schwab M. E. (2004) Behavioral characterization in a comprehensive mouse test battery reveals motor and sensory impairments in growth-associated protein-43 null mutant mice. *Neuroscience* **129,** 563-574.

Meyding-Lamade U., Lamade W., Kehm R., Knopf K. W., Hess T., Gosztonyi G., Degen O., and Hacke W. (1998) Herpes simplex virus encephalitis: cranial magnetic resonance imaging and neuropathology in a mouse model. *Neurosci Lett* **248,** 13-16.

Meyding-Lamade U., Haas J., Lamade W., Stingele K., Kehm R., Fath A., Heinrich K., Storch H. B., and Wildemann B. (1998) Herpes simplex virus encephalitis: long-term comparative study of viral load and the expression of immunologic nitric oxide synthase in mouse brain tissue. *Neurosci Lett* **244,** 9-12.

Meyding-Lamade U. K., Oberlinner C., Rau P. R., Seyfer S., Heiland S., Sellner J., Wildemann B. T., and Lamade W. R. (2003) Experimental herpes simplex virus encephalitis: a combination therapy of acyclovir and glucocorticoids reduces long-term magnetic resonance imaging abnormalities. *J Neurovirol* **9,** 118-125.

Millhouse S. and Wigdahl B. (2000) Molecular circuitry regulating herpes simplex virus type 1 latency in neurons. *J Neurovirol* **6,** 6-24.

Mossman K. L., Macgregor P. F., Rozmus J. J., Goryachev A. B., Edwards A. M., and Smiley J. R. (2001) Herpes simplex virus triggers and then disarms a host antiviral response. *J Virol* **75,** 750-758.

Pearson A., Knipe D. M., and Coen D. M. (2004) ICP27 selectively regulates the cytoplasmic localization of a subset of viral transcripts in herpes simplex virus type 1-infected cells. *J Virol* **78,** 23-32.

Raschilas F., Wolff M., Delatour F., Chaffaut C., De Broucker T., Chevret S., Lebon P., Canton P., and Rozenberg F. (2002) Outcome of and prognostic factors for herpes simplex encephalitis in adult patients: results of a multicenter study. *Clin Infect Dis* **35,** 254-260.

Ray N. and Enquist L. W. (2004) Transcriptional response of a common permissive cell type to infection by two diverse alphaherpesviruses. *J Virol* **78,** 3489-3501.

Rekart J. L., Meiri K., and Routtenberg A. (2005) Hippocampal-dependent memory is impaired in heterozygous GAP-43 knockout mice. *Hippocampus* **15,** 1-7.

Roth W., Kermer P., Krajewska M., Welsh K., Davis S., Krajewski S., and Reed J. C. (2003) Bifunctional apoptosis inhibitor (BAR) protects neurons from diverse cell death pathways. *Cell Death Differ* **10,** 1178-1187.

Ryu S. W., Chae S. K., Lee K. J., and Kim E. (1999) Identification and characterization of human Fas associated factor 1, hFAF1. *Biochem Biophys Res Commun* **262,** 388-394.

Samaniego L. A., Neiderhiser L., and DeLuca N. A. (1998) Persistence and expression of the herpes simplex virus genome in the absence of immediate-early proteins. *J Virol* **72,** 3307-3320.

Sauerbrei A., Eichhorn U., Hottenrott G., and Wutzler P. (2000) Virological diagnosis of herpes simplex encephalitis. *J Clin Virol* **17,** 31-36.

Scanlan P. M., Tiwari V., Bommireddy S., and Shukla D. (2003) Cellular expression of gH confers resistance to herpes simplex virus type-1 entry. *Virology* **312,** 14-24.

Schmutzhard E. (2001) Viral infections of the CNS with special emphasis on herpes simplex infections. *J Neurol* **248,** 469-477.

Shang L. and Tomasi T. B. (2006) The heat shock protein 90-CDC37 chaperone complex is required for signaling by types I and II interferons. *J Biol Chem* **281,** 1876-1884.

Shinmura K., Tarapore P., Tokuyama Y., George K. R., and Fukasawa K. (2005) Characterization of centrosomal association of nucleophosmin/B23 linked to Crm1 activity. *FEBS Lett* **579,** 6621-6634.

Simeoni L., Posevitz V., Kolsch U., Meinert I., Bruyns E., Pfeffer K., Reinhold D., and Schraven B. (2005) The transmembrane adapter protein SIT regulates thymic development and peripheral T-cell functions. *Mol Cell Biol* **25,** 7557-7568.

Simmons A., Slobedman B., Speck P., Arthur J., and Efstathiou S. (1992) Two patterns of persistence of herpes simplex virus DNA sequences in the nervous systems of latently infected mice. *J Gen Virol* **73 (Pt 5),** 1287-1291.

Skoldenberg B. (1996) Herpes simplex encephalitis. *Scand J Infect Dis Suppl* **100,** 8-13.

Smiley J. R. (2004) Herpes simplex virus virion host shutoff protein: immune evasion mediated by a viral RNase? *J Virol* **78,** 1063-1068.

Suzuki A., Kaisho T., Ohishi M., Tsukio-Yamaguchi M., Tsubata T., Koni P. A., Sasaki T., Mak T. W., and Nakano T. (2003) Critical roles of Pten in B cell homeostasis and immunoglobulin class switch recombination. *J Exp Med* **197,** 657-667.

Suzuki A., Sasaki T., Mak T. W., and Nakano T. (2004) Functional analysis of the tumour suppressor gene PTEN in murine B cells and keratinocytes. *Biochem Soc Trans* **32,** 362-365.

Suzuki Y. and Blough H. A. (1982) Enzymatic deoxyglucosylation of ceramides by microsomes of BHK-21 cells. The effect of deoxyglucose treatment and herpesvirus infection. *Biochim Biophys Acta* **710,** 221-229.

Taddeo B., Esclatine A., and Roizman B. (2002) The patterns of accumulation of cellular RNAs in cells infected with a wild-type and a mutant herpes simplex virus 1 lacking the virion host shutoff gene. *Proc Natl Acad Sci U S A* **99,** 17031-17036.

Tarapore P., Okuda M., and Fukasawa K. (2002) A mammalian in vitro centriole duplication system: evidence for involvement of CDK2/cyclin E and nucleophosmin/B23 in centrosome duplication. *Cell Cycle* **1,** 75-81.

Taylor T. J., Brockman M. A., McNamee E. E., and Knipe D. M. (2002) Herpes simplex virus. *Front Biosci* **7,** d752-d764.

Thomas H. C., Kapadia R. D., Wells G. I., Gresham A. M., Sutton D., Solleveld H. A., Sarkar S. K., Dillon S. B., and Tal-Singer R. (2001) Differences in pathogenicity of herpes simplex virus serotypes 1 and 2 may be observed by histopathology and high-resolution magnetic resonance imaging in a murine encephalitis model. *J Neurovirol* **7,** 105-116.

Thompson R. L., Shieh M. T., and Sawtell N. M. (2003) Analysis of herpes simplex virus ICP0 promoter function in sensory neurons during acute infection, establishment of latency, and reactivation in vivo. *J Virol* **77,** 12319-12330.

Turner S. L. and Jenkins F. J. (1997) The roles of herpes simplex virus in neuroscience. *J Neurovirol* **3,** 110-125.

Whitley R. J., Soong S. J., Dolin R., Galasso G. J., Ch'ien L. T., and Alford C. A. (1977) Adenine arabinoside therapy of biopsy-proved herpes simplex encephalitis. National Institute of Allergy and Infectious Diseases collaborative antiviral study. *N Engl J Med* **297,** 289-294.

Whitley R. J. and Kimberlin D. W. (1999) Viral encephalitis. *Pediatr Rev* **20,** 192-198.

Wisden W., Cope D., Klausberger T., Hauer B., Sinkkonen S. T., Tretter V., Lujan R., Jones A., Korpi E. R., Mody I., Sieghart W., and Somogyi P. (2002) Ectopic expression of the GABA(A) receptor alpha6 subunit in hippocampal pyramidal neurons produces extrasynaptic receptors and an increased tonic inhibition. *Neuropharmacology* **43,** 530-549.

Yang C. T., Song J., Bu X., Cong Y. S., Bacchetti S., Rennie P., and Jia W. W. (2003) Herpes simplex virus type-1 infection upregulates cellular promoters and telomerase activity in both tumor and nontumor human cells. *Gene Ther* **10,** 1494-1502.

Yue H., Eastman P. S., Wang B. B., Minor J., Doctolero M. H., Nuttall R. L., Stack R., Becker J. W., Montgomery J. R., Vainer M., and Johnston R. (2001) An evaluation of the performance of cDNA microarrays for detecting changes in global mRNA expression. *Nucleic Acids Res* **29,** E41.

Zhang H., Xu Q., Krajewski S., Krajewska M., Xie Z., Fuess S., Kitada S., Pawlowski K., Godzik A., and Reed J. C. (2000) BAR: An apoptosis regulator at the intersection of caspases and Bcl-2 family proteins. *Proc Natl Acad Sci U S A* **97,** 2597-2602.

Zheng M., Qian H., Joshi R. M., Nechtman J., and Atherton S. S. (2003) DNA microarray analysis of the uninoculated eye following anterior chamber inoculation of HSV-1. *Ocul Immunol Inflamm* **11,** 187-195.